An investigation of the two-dimensional neutron noise field generated by a moving neutron absorber using the UTR-10 reactor

by

William Joseph Hennessy

A Thesis Submitted to the
Graduate Faculty in Partial Fulfillment of the
Requirements for the Degree of
MASTER OF SCIENCE

Major: Nuclear Engineering

Iowa State University
Ames, Iowa

1983

TABLE OF CONTENTS

LIST OF FIGURES

LIST OF TABLES

LIST OF ACRONYMS

APSD - Auto power spectral density

CIC - Compensated ion chamber

CPSD - Cross power spectral density

CVS - Central vertical stringer

E - East

FFT - Fast Fourier Transform

GFP-20 - Computer program which performs criticality calculations

GFP-24 - Computer program which calculates Green's functions

GFP-25 - Computer program which calculates the change in Green's functions

GFP-27 - Computer program which calculates the thermal fluxes

GFP-28 - Computer program which calculates the change in thermal fluxes

HP - Hewlett Packard

ISU - Iowa State University

LEOPARD - Computer code used to supply reactor parameters

LINV3F - Library subroutine which solves for the determinant of a matrix

LVDT - Linear variable differential transformer

N - North

PLOT - Graphics subroutine

PRBS - Pseudo-random binary signal

RMS - Root mean square

S - South

TF - Transfer function

W - West

I. INTRODUCTION

The response of a nuclear reactor to changes in the neutron absorption cross-section or other parameters in a localized area of the reactor core has been the object of much research [1-6]. Interest in this topic centers around a desire to be able to identify and locate the source of the changes. Fluctuations in the local neutron absorption cross sections are often caused by vibrations of the internal components of reactor cores. Vibrating internal components such as fuel elements or control rods generate neutron noise with specific characteristics. Research in neutron noise analysis is being performed in an attempt to understand these characteristics in more detail. A long term goal of the research described in this thesis is to be able to identify and locate moving reactor components in power reactor cores.

The neutron noise generated by vibrating neutron absorbers, usually referred to as the flux response, is observed using neutron detectors placed in the reactor core. The flux response is thus interpreted as a detector response. The response of several detectors located in different positions in the reactor core may then be used to derive information about the vibrating absorber. This information is found from frequency analysis of the detector signals.

The ability to locate moving or loose reactor components has both economic and safety related advantages. The economic advantages include the identification of loose control or fuel rods and reactor internal components. Locating these parts would enable their movements

to be monitored so that further deterioration of the parts could be corrected before extensive damage occurs. Safety implications relate to the ability to detect broken or loose internal parts before they can cause core damage by either direct mechanical damage or the blocking of a coolant channel. For example, a fuel rod which has come loose in a fuel assembly may, under the influence of coolant flow induced vibrations, impact upon the assembly support grids or other fuel rods. This could lead to damage to the fuel rod cladding with the possibility of the release of fission products. Obviously, a method which could detect and localize such a vibrating fuel rod is desirable.

The research which is the topic of this thesis is a continuation of the work being done at Iowa State University in the area of noise analysis of vibrating neutron absorbers in nuclear reactor cores, [5,6] and consists of analytical, computer, and experimental work. A review of the literature shows that a theoretical development very important to the present research was introduced by Van Dam [1]. In his work, Van Dam demonstrated that neutron noise consists of two independent effects. These effects are termed the local effect and the global effect. The local effect is space dependent and refers to the flux response of the reactor at locations very near the source of the neutron noise. The global response is space independent and is the overall flux response of the reactor to the neutron noise source.

Pazsit, using Van Dam's detector adjoint function, developed a two group model of a neutron noise source [2]. This work led Pazsit

to conclude that neutron noise generated by a vibrating neutron absorber is very space dependent. He also showed that the neutron noise generated by a vibrating neutron absorber is much different from the neutron noise which results from a stationary absorber of varying strength.

A two-dimensional Green's function analysis of the diffusion equations using one energy group of neutrons was done by Pazsit and Analytis [3]. In their work, they developed a two-dimensional Green's function model relating small stochastic cross-section fluctuations to neutron noise for a rectangular slab reactor using modified one-group diffusion theory. From this development, the neutron noise response to two-dimensional vibrating neutron absorbers was investigated. The two-dimensional model used in this research will follow closely the developments of Pazsit and Analytis [3]. Unlike their work, however, the model developed accounted for the different reactor regions (such as the fuel regions or graphite reflector regions of the UTR-10 reactor used in the study) and included two energy groups of neutrons.

Similar analytical work in this area was also done by Nodean [4]. The purpose of his work was to propose a method for determining the frequency response of a reactor. He did this by solving the one-dimensional, two-group diffusion equations using Green's function techniques. The present research expands on this work by doing the analysis in two dimensions and by applying the model to computer programs to predict the reactor response.

Previous experimental work at Iowa State University was done by Al-Ammar [5] and by Borland [6]. Al-Ammar designed and constructed a device which could place a vibrating neutron absorber into the Central Vertical Stringer (CVS) of the UTR-10 reactor core. Using this device, Al-Ammar obtained experimental data which confirmed the hypothesis put forth by Pazsit [2]. His device verified the presence of the local and global effects.

Al-Ammar's work was improved upon by Borland [6]. Borland constructed a vibrating absorber device which incorporated a better absorber position-measuring system and a sturdier vibrator, thus eliminating some of the problems inherent in Al-Ammar's design. Borland's device also had the capability to measure the flux response with different detector-vibrator configurations. His work verified Al-Ammar's results.

The experimental portion of the present research extends the work of Borland and Al-Ammar by investigating the flux response at detector locations farther away from the vibrating absorber. In previous experiments, the detectors were quite close to the vibrating absorber, where a large local effect is experienced. By moving the detectors farther away from the vibrating absorber, the spatial dependence of the local response can be investigated.

The objectives of the present research can be outlined as follows:

1. Construct an analytical model which describes the response of the neutron noise field and neutron detectors to a vibrating

neutron absorber located in the internal reflector region of the UTR-10 reactor.

2. Based on this model, develop computer programs which can be used to make predictions on the response of the neutron noise field to the vibrating absorber for the experimental configuration to be studied.

3. Use an experimental apparatus consisting of a vibrating neutron absorber placed in the reactor, which approximates the conditions of (1) and (2), to study the response of a neutron detector as a function of position in the reactor.

4. Compare and verify the predictions of the analytical model with the results of the experiment.

The analytical model developed is a two-dimensional Green's function solution using the two-group diffusion equations for the response of the neutron flux to a vibrating neutron absorber. The diffusion equations are written as linear differential equations which can then be solved essentially exactly using Green's function methods. The technique of Morse and Feshbach is applied to the equations resulting in a series form of solution equations which can be solved using computer programs [7].

Computer programs were written to solve the large number of multiple mode equations resulting from this development. These programs are called GFP-24, GFP-25, GFP-27, and GFP-28 and are listed in Appendix A. The computer was also used to solve the equations for

the unperturbed reactor in the fundamental mode to ensure the model represented, as nearly as possible, a critical system. This program is called GFP20 and is also listed in Appendix A. The function of each program and its relationship to the model are discussed in Section IV. The LEOPARD code [8] was used to generate the cross sections for the analytical calculations.

In the experimental phase of the work, the apparatus shown in Figure 5.4, which was designed by Borland [6], was used to simulate a moving neutron absorber. The vibrating component of the apparatus consists of a piece of cadmium attached to the end of an aluminum rod which pivots on a pin located near the end of the rod, resulting in a pendulum-like motion. The rod is driven by two electrical coils. The frequency of the absorber vibration can be varied, and its position is indicated by a Linear Variable Differential Transformer (LVDT), which is attached to the top of the rod. This apparatus was inserted into the CVS in the central reflector region of the UTR-10 core. Detectors for measuring the reactor's response were positioned around the apparatus. One detector was placed in the body of the vibrating absorber apparatus and, therefore, very close (3.6 cm) to the vibrating absorber. The other detector was also placed in the central reflector region of the reactor, but in a stringer located 16.8 cm. radially away from the vibrating absorber. Figure 5.3 shows the exact detector locations.

A third detector was placed in the Thermal Column of the reactor (See Figures 5.1 and 5.2). This detector location was not used in the computer analysis, but the experimental results from this detector are used and analyzed. This detector provides a measure of the global response.

Signals from the detectors were analyzed using a frequency spectrum analyzer and a microcomputer. The results are interpreted in terms of APSDs, CPSDs (magnitude and phase), and coherence functions. These experimental results are then compared with the predicted responses based on the analytical model.

II. DEVELOPMENT OF THE TWO-DIMENSIONAL GREEN'S FUNCTION SOLUTIONS OF THE DIFFUSION EQUATIONS

The Green's function method for solving linear differential equations outlined by Hildebrand [9] will be discussed in this section.

The form of the diffusion equations for a moving neutron absorber as used in the analytical model is introduced. The Green's function solution technique will be used to solve the resulting equations and a final expression for the real part of the frequency dependent neutron flux as a function of position in the reactor will be obtained.

The Green's function method for solving differential equations is as follows: Given the differential equation

$$Ly = -S(x)$$

or

$$Ly + S(x) = 0 \quad . \tag{2.1}$$

where L indicates the differential operator

$$L = \frac{d}{dx}\,(P\ d/dx) + q = P\ d^2/dx^2 + dP/dx\ d/dx + q \tag{2.2}$$

and noting that y satisfies the homogeneous boundary conditions of the form

$$\sigma y + \beta\ dy/dx = 0 \tag{2.3}$$

for constant values of σ and β on the interval $a \leq x \leq b$, a Green's function, G, is determined which for a given point x_o in

(a,b) is G_1 for $x < x_o$ and G_2 for $x > x_o$. The Green's functions G_1 and G_2 are found by the application of four properties:

1. G_1 and G_2 satisfy $LG = 0$. That is $LG_1 = 0$ for $x < x_o$ and $LG_2 = 0$ for $x > x_o$,

2. G_1 and G_2 satisfy the boundary conditions of Equation 2.3 at the endpoints a and b. G_1 satisfies the conditions at $x = a$ and G_2 satisfies the conditions at $x = b$.

3. The Green's functions are continuous at $x = x_o$; i.e., G_1 at $x = x_o$ equals G_2 at $x = x_o$, and

4. dG/dx has a discontinuity of magnitude of $-1/P(x_o)$ at x_o. This means $\frac{dG_2(x_o)}{dx} - \frac{dG_1(x_o)}{dx} = -1/P(x_o)$.

Once the Green's functions G_1 and G_2 are found, the solution to the problem of (2.1) may be determined from

$$Y(x) = \int_a^b G(x,x_o)S(x_o)dx_o \qquad (2.4)$$

As an alternate representation, the Green's function is also identified as the solution of the differential equation

$$LG = -\delta(x-x_o) \quad .$$

In order to apply the Green's function technique to the solution of the diffusion equations, the equations must be written in a form which can be applied directly to this method. The development carried out will be limited to two neutron energy groups. To this end, let Group 1 represent the fast neutron group and Group 2 represent

the thermal neutron group. If the assumption is made that all fissions occur in Group 2 and that these fissions produce neutrons in Group 1, the usual two-group diffusion equations result

$$D_1\nabla^2\phi_1 - (\Sigma_{a1} + \Sigma_{R1})\phi_1 + \lambda C + (1-\beta)\nu\Sigma_f \phi_2 = 1/V_1 \, \partial\phi_1/\partial t \quad (2.5)$$

and

$$D_2\nabla^2\phi_2 + \Sigma_{R1}\phi_1 - \Sigma_{a2}\phi_2 = 1/V_2 \, \partial\phi_2/\partial t \quad . \quad (2.6)$$

If the following additional assumptions are made:

1. Use one group of delayed neutrons, i.e.

$$\beta\nu\Sigma_f\phi_2 - \lambda C = \partial C/\partial t, \quad (2.7)$$

2. Assume small changes in the absorption cross-section, i.e.

$$\Sigma_{a2} = \Sigma_{a2o} + \delta\Sigma_{a2}, \quad (2.8)$$

3. Assume that small changes in the neutron flux due to condition 2 above take place

$$\phi_1 = \phi_{10} + \delta\phi_1 \quad (2.9)$$

and

$$\phi_2 = \phi_{20} + \delta\phi_2, \quad (2.10)$$

and 4. Further, assume that small changes in the precursor concentration due to condition 2 take place so that

$$C = C_o + \delta C \tag{2.11}$$

the two-group diffusion equations become,

$$D_1\nabla^2\delta\phi_1 - (\Sigma_a + \Sigma_{R1})\delta\phi_1 + \lambda\delta C + (1-\beta)\nu\Sigma_f\ \delta\phi_2 =$$

$$1/V_1\ \ \partial\,\delta\phi_1/\partial t \tag{2.12}$$

$$D_2\nabla^2\delta\phi_2 + \Sigma_{R1}\delta\phi_1 - \Sigma_{a20}\delta\phi_2 - \delta\Sigma_{a2}\phi_{20} = 1/V_2\ \partial\delta\phi_2/\partial t \tag{2.13}$$

and

$$\beta\nu\Sigma_f\delta\phi_2 - \lambda\delta C = \partial\delta C/\partial t\ . \tag{2.14}$$

Note that when the substitutions of (2.8), (2.9), (2.10), and (2.11) were made into (2.5), (2.6), and (2.7), the steady state terms were neglected as well as terms involving double differentials, i.e., $\delta\delta << \delta$.

Application of the Fourier transform yields

$$D_1\nabla^2\Delta\phi_1 - (\Sigma_{a1} + \Sigma_{R1})\Delta\phi_1 + \lambda\Delta C + (1-\beta)\nu\Sigma_f\Delta\phi_2 =$$

$$j\omega/V_1\ \Delta\phi_1 \tag{2.15}$$

$$D_2\nabla^2\Delta\phi_2 + \Sigma_{R1}\Delta\phi_1 - \Sigma_{a20}\Delta\phi_2 - \Delta\Sigma_{a2}\phi_{20} = \frac{j\omega}{V_2}\ \Delta\phi_2 \tag{2.16}$$

$$\beta\nu\Sigma_f\Delta\phi_2 - \lambda\Delta C = j\omega\Delta C \tag{2.17}$$

where $\Delta\phi_1$, $\Delta\phi_2$, ΔC and $\Delta\Sigma_a$ represent the Fourier transforms of $\delta\phi_1$, $\delta\phi_2$, δC, and $\delta\Sigma_a$, respectively.

There are two approaches used to obtain the response of a thermal neutron detector to the perturbation in the absorption cross section. One method is to solve equations (2.15), (2.16), and (2.17) for $\Delta\phi_2$ and form the detector response, R, as the integral over the detector volume, V_d, of the product of $\Delta\phi_2$ and the detector cross section, Σ_d,

$$R = \int_{V_d} \Delta\phi_2 \Sigma_d \, dv \quad .$$

An alternate and equivalent formulation is to solve for the detector adjoint function [1,2] ψ and form the detector response as

$$R = \int_{V_R} \psi \, S \, dv$$

where V_R is the reactor volume and S is the perturbation sources. The first approach is more direct for a single fixed perturbation point with variable detector placement, and the formulation in terms of the detector adjoint function is more useful for a fixed detector with variable source locations. For the applications in this research, the first formulation was used since the driving source was fixed in position.

Equation (2.17) may be rewritten as

$$\Delta C = \frac{\beta \nu \Sigma_f \Delta\phi_2}{\lambda + j\omega} \quad . \tag{2.18}$$

which upon substitution into (2.15) gives

$$D_1 \nabla^2 \Delta\phi_1 - (\Sigma_{a1} + \Sigma_{R1})\Delta\phi_1 + \frac{\lambda\beta\nu\Sigma_f}{\lambda + j\omega} \Delta\phi_2 + (1-\beta)\nu\Sigma_f \Delta\phi_2 =$$

$$\frac{j\omega}{V_1} \Delta\phi_1 \quad . \tag{2.19}$$

If the equations are assumed to be frequency independent in the plateau region of the reactor frequency response (approximately 1 to 10 Hz), $j\omega$ can, in effect, be set equal to zero and the Fourier transformed flux interpreted as the real part of the complex flux. With this assumption, Equations (2.16) and (2.19) become

$$D_1 \frac{\partial^2 \Delta\phi_1}{\partial x^2} + D_1 \frac{\partial^2 \Delta\phi_1}{\partial y^2} - (\Sigma_{a1} + \Sigma_{R1})\Delta\phi_1 + (1-\beta)\nu\Sigma_f \Delta\phi_2 = 0 \tag{2.20}$$

and

$$D_2 \frac{\partial^2 \Delta\phi_2}{\partial x^2} + D_2 \frac{\partial^2 \Delta\phi_2}{\partial y^2} - \Sigma_{a20} \Delta\phi_2 + \Sigma_{R1}\Delta\phi_1 = \Delta\Sigma_{a2}\phi_{20} \tag{2.21}$$

where $\Delta\phi_1$ and $\Delta\phi_2$ now represent the real part of the Fourier transformed flux.

As described previously, Equations (2.20) and (2.21) are to be solved using the Green's function technique. In two dimensions, the equations for the Green's functions are

$$\frac{\partial^2 G_1}{\partial x^2} + \frac{\partial^2 G_1}{\partial y^2} - \frac{(\Sigma_{a1} + \Sigma_{R1})G_1}{D_1} + \frac{(1-\beta)\nu\Sigma_f G_2}{D_1} = 0 \tag{2.22}$$

and

$$\frac{\partial^2 G_2}{\partial x^2} + \frac{\partial^2 G_2}{\partial y^2} - \frac{\Sigma_{a20}}{D_2} G_2 + \frac{\Sigma_{R1}}{D_2} G_1 = -\delta(x-x_o)\delta(y-y_o). \tag{2.23}$$

Since only the thermal group equation contains a nonhomogeneous term, the equation for the thermal component of the Green's function, G_2, contains the delta function. The equation for the fast component, G_1, is set equal to zero. Equations (2.22) and (2.23) are solved using the procedure outlined by Morse and Feshbach [7]. This is done by expanding the Green's function in terms of a complete set of sine functions involving all coordinates except one, in this case, y.

$$G_1(x,x_o,y) = \frac{2}{a} \sum_{n=1}^{\infty} \text{Sin } B_n x_o \text{ Sin } B_n x \, Y_{1n}(y) \tag{2.24}$$

and

$$G_2(x,x_o,y) = \frac{2}{a} \sum_{n=1}^{\infty} \text{Sin } B_n x_o \text{ Sin } B_n x \, Y_{2n}(y). \tag{2.25}$$

It is required that the Green's function solutions be zero at both boundaries in the x direction. If the x dimension extends from 0 to a, then the boundary condition is satisfied by letting

$$B_n = \frac{n\pi}{a}. \tag{2.26}$$

Substituting Equations (2.24) and (2.25) into Equations (2.22) and (2.23) yields

$$\frac{2}{a}\sum_{n=1}^{\infty}(-B_n^2)\ \text{Sin}\ B_n x_o\ \text{Sin}\ B_n x\ Y_{1n}(y) + \frac{2}{a}\sum_{n=1}^{\infty}\text{Sin}\ B_n x_o\ \text{Sin}\ B_n x$$

$$\frac{d^2 Y_{1n}(y)}{dy^2} - \frac{(\Sigma_{a1} + \Sigma_{R1})}{D_1}\ \frac{2}{a}\sum_{n=1}^{\infty}\text{Sin}\ B_n x_o\ \text{Sin}\ B_n x\ Y_{1n}(y) +$$

$$\frac{(1-\beta)\nu\Sigma_f}{D_1}\ \frac{2}{a}\sum_{n=1}^{\infty}\text{Sin}\ B_n x_o\ \text{Sin}\ B_n x\ Y_{2n}(y) = 0 \qquad (2.27)$$

and

$$\frac{2}{a}\sum_{n=1}^{\infty}(-B_n^2\ \text{Sin}\ B_n x_o\ \text{Sin}\ B_n x\ Y_{2n}(y)) + \frac{2}{a}\sum_{n=1}^{\infty}\text{Sin}\ B_n x_o\ \text{Sin}\ B_n x$$

$$\frac{d^2 Y_{2n}(y)}{dy^2} - \frac{\Sigma_{a20}}{D_2}\ \frac{2}{a}\sum_{n=1}^{\infty}\text{Sin}\ B_n x_o\ \text{Sin}\ B_n x\ Y_{2n}(y) +$$

$$\frac{\Sigma_{R1}}{D_2}\frac{2}{a}\sum_{n=1}^{\infty}\text{Sin}\ B_n x_o\ \text{Sin}\ B_n x\ Y_{1n}(y) = -\delta(x-x_o)\delta(y-y_o). \qquad (2.28)$$

To take advantage of the orthogonality of the sine functions

$$\int_o^a \text{Sin}\ B_n x_o\ \text{Sin}\ (B_k x)dx = \frac{a}{2} \text{ if } k = n$$

or 0 if $k \neq n$

Equation (2.27) is multiplied by Sin $(B_k x)$ and integrated from 0 to a with respect to x. This gives

$$-B_k^2\ \text{Sin}\ B_k x_o\ Y_{1k} + \text{Sin}\ B_k x_o\ \frac{d^2 Y_{1k}}{dy^2} - \frac{(\Sigma_{a1} + \Sigma_{R1})}{D_1}$$

$$\text{Sin}\ B_k x_o\ Y_{1k} + \frac{(1-\beta)\nu\Sigma_f}{D_1}\ \text{Sin}\ B_k x_o\ Y_{2k} = 0 \qquad (2.29)$$

or

$$\frac{d^2Y_{1k}}{dy^2} - B_k^2 \; Y_{1k} - \frac{(\Sigma_{a1} + \Sigma_{R1})}{D_1} Y_{1k} + \frac{(1-\beta)\nu\Sigma_f}{D_1} Y_{2k} = 0 \quad . \quad (2.30)$$

This procedure is repeated for Equation (2.28) to obtain:

$$\frac{d^2Y_{2k}}{dy^2} - B_k^2 \; Y_{2k} - \frac{\Sigma_{a20}}{D_2} Y_{2k} + \frac{\Sigma_{R1}}{D_2} \; Y_{1k} = -\delta(y-y_o). \quad (2.31)$$

Equations (2.30) and (2.31) are to be solved for the one-dimensional Green's functions, Y_{1k} and Y_{2k}, $k = 1,2,3,\ldots$.

In equation (2.21), let the nonhomogeneous source term $\Delta\Sigma_{a2}\phi_{20}$ be represented by δS; i.e. let $\Delta\Sigma_{a2}\phi_{20} = \delta S$. For a moving neutron absorber in the form of a thin rod, δS can be represented by [3]

$$\delta S(x,y,\omega) = \gamma \int_{-\infty}^{\infty} dt \; e^{-j\omega t} \; \phi(x_o,y_o) \; [\delta(x-x_o-\Delta x(t))\delta(y-y_0-\Delta y(t))$$

$$- \delta(x-x_o)\delta(y-y_o)] \quad (2.32)$$

where $\phi(x_o,y_o)$ = steady state flux,

x_o,y_o = the equilibrium position of the absorber,

γ = the relative absorber strength,

and $\Delta x(t),\Delta y(t)$= motion of the absorber.

Based on the Green's function method, the solution for the thermal flux response is given as the integral over the reactor volume, V_R, of the Green's function and the driving source.

$$\Delta\phi_2(x,y,\omega) = \int_{V_R} G(x,x_o,y,y_o,\omega)\ \delta S\ (x_o,y_o,\omega)\ dx_o dy_o. \qquad (2.33)$$

Substituting Equation (2.32) into Equation (2.33) gives

$$\Delta\phi_2(x,y,\omega) = \gamma \int_{V_R} G(x,x_o,y,y_o,\omega)\ dx_o\ dy_o \int_{-\infty}^{\infty} dt\ e^{-j\omega t}\phi(x_o,y_o)$$

$$[\delta(x-x_o-\Delta x(t))\cdot\delta(y-y_o-\Delta y(t)) - \delta(x-x_o)\delta(y-y_o)] \qquad (2.34)$$

Integrating over V_R and using the property of the delta function results in the expression

$$\Delta\phi_2(x,y,\omega) = \gamma \int_{-\infty}^{\infty} dt\ e^{-j\omega t}\ [\phi(x_o+\Delta x,y_o+\Delta y)G(x,x_o+\Delta x,y,y_o+\Delta y,\omega)$$

$$- \phi_2(x_o,y_o)G(x,x_o,y,y_o,\omega)]. \qquad (2.35)$$

The expression $\phi(x_o+\Delta x,y_o+\Delta y)G(x,x_o+\Delta x,y,y_o+\Delta y,\omega)$ in Equation (2.35) is expanded about x_o and y_o using a two-dimensional Taylor's series. The Taylor's series for a function of two variables is

$$f(a+h,b+k) = f(a,b) + \left(h\frac{\partial}{\partial x} + k\frac{\partial}{\partial y}\right) f(x,y)\Big|_{\substack{x=a\\y=b}} + \ldots$$

$$+ \frac{1}{N!}\left(h\frac{\partial}{\partial x} + K\frac{\partial}{\partial y}\right)^N f(x,y)\Big|_{\substack{x=a\\y=b}} + \ldots \quad . \qquad (2.36)$$

In this case, the series is terminated after two terms. For convenience, let $\phi(x_o,y_o)$ be written as ϕ and $G(x,x_o,y,y_o,\omega)$ be written

as G. Applying the Taylor's series and neglecting the $\Delta x\Delta x$, $\Delta y\Delta y$, $\Delta x\Delta y$ terms yields:

$$\Delta\phi_2(x,y,\omega) = \gamma \int_{-\infty}^{\infty} dt e^{-i\omega t} + \{\Delta x[\frac{\partial\phi}{\partial x_o} G + \phi\frac{\partial G}{\partial x_o}]$$

$$+ \Delta y[\frac{\partial\phi}{\partial y_o} G + \phi\frac{\partial G}{\partial y_o}]\} \qquad (2.37)$$

Carrying out the Fourier transform indicated in Equation (2.37) results in

$$\Delta\phi_2(\omega) = \gamma[(\frac{\partial\phi}{\partial x_o} G + \phi\frac{\partial G}{\partial x_o})\Delta x(\omega) + (\frac{\partial\phi}{\partial y_o} G + \phi\frac{\partial G}{\partial y_o})\Delta y(\omega)]. \qquad (2.38)$$

Equation (2.38) provides a means of predicting the fluctuations in the thermal neutron flux resulting from changes in group parameters due to a vibrating neutron absorber. If the motion is in one dimension only (i.e., y), the term $\delta x(\omega) = 0$ and the expression becomes

$$\Delta\phi_2(\omega) = \gamma\Delta y(\omega) (\frac{\partial\phi}{\partial y_o} G + \phi\frac{\partial G}{\partial y_o}). \qquad (2.39)$$

If G is assumed to be independent of frequency (as is the case for this development), Equation (2.39) may be inverted back to the time domain to obtain

$$\Delta\phi_2(t) = \gamma \Delta y(t) (\frac{\partial\phi}{\partial y_o} G + \phi\frac{\partial G}{\partial y_o}). \qquad (2.40)$$

Equations (2.30) and (2.31) and equations for the neutron flux will be used to find the four terms of Equation (2.39), namely, $\frac{\partial\phi}{\partial y_o}$, G, ϕ

and $\frac{\partial G}{\partial y_o}$, which are necessary to find $\Delta\phi_2$. Note that since a thermal detector and absorber are assumed, the thermal component of ϕ and G are used in Equation (2.39). Also, for a point detector $\Delta\phi_2$ is proportional to the detector response, and integration over the detector volume is not required.

III. ANALYTICAL MODEL OF THE GREEN'S FUNCTION SOLUTIONS TO THE DIFFUSION EQUATIONS

In this section, the procedures for obtaining the Green's functions solutions for a model of the Iowa State University UTR-10 reactor will be described. These solutions will form the basis of the analytical model which was then analyzed using the computer programs described in Appendix A.

It can be seen from the two-dimensional plan view of the UTR-10 reactor shown in Figure 5.1, that a potential difficulty exists in applying the series expansion procedure described previously directly in that the core material properties are not continuous in either direction in the reactor. Since the most significant flux variation takes place along an axis perpendicular to the fuel regions (called the y direction), it was decided to use the sine function expansion parallel to the fuel regions (the x direction). This, in effect, models the reactor, as shown in Figure 3.1, with the fuel regions extending to the edges of the graphite core since the sine functions do not account for variations in core properties. Since the variation of the flux parallel to the fuel region is approximately sinusoidal, expansion of the x component of the Green's function in sine functions should be a reasonable approximation at least for points not too near the boundary of the reactor.

As shown in Figure 5.1, the UTR-10 reactor core consists of different regions containing either fuel or graphite. In a multi-

region system, some modifications of the basic procedures, as described in Chapter II, for obtaining the one-dimensional Green's function solution must be made. Continuity of each mode and the equivalent of continuity of current is required at each interface. The special Green's function conditions of continuity of the modes and jump in the derivative of the thermal component of the modes are applied at the location of the perturbation. For this model, the vibrator is located in the center of the internal graphite reflector.

In the fuel regions, Equations (2.30) and (2.31), repeated here, apply directly without modification,

$$\frac{d^2Y_{1k}}{dy^2} - B_k^2 Y_{1k} - \frac{(\Sigma_{a1} + \Sigma_{R1})}{D_1} Y_{1k} + \frac{(1-\beta)\nu\Sigma_f}{D_1} Y_{2k} = 0 \qquad (2.30)$$

and

$$\frac{d^2Y_{2k}}{dy^2} - B_k^2 Y_{2k} - \frac{\Sigma_{a20}}{D_2} Y_{2k} + \frac{\Sigma_{R1}}{D_2} Y_{1k} = 0 \qquad (2.31)$$

In the graphite regions, Equation (2.30) must be changed since $\Sigma_f=0$ there

$$\frac{d^2Y_{1k}}{dy^2} - B_k^2 Y_{1k} - \frac{(\Sigma_{a1} + \Sigma_{R1})}{D_1} Y_{1k} = 0. \qquad (3.1)$$

In order to solve for the Green's functions in the graphite regions, Equation (3.1) is rewritten as

$$\frac{D^2 Y_{1k}}{dy^2} - \alpha_k^2 Y_{1k} = 0 \tag{3.2}$$

where

$$\alpha_k^2 = B_k^2 + \frac{(\Sigma_{a1} + \Sigma_{R1})}{D_1} . \tag{3.3}$$

Equation (2.31) is also rewritten as

$$\frac{d^2 Y_{2k}}{dy^2} - \beta_k^2 Y_{2k} + \frac{\Sigma_{R1}}{D_2} Y_{1k} = 0 \tag{3.4}$$

where

$$\beta_k^2 = B_k^2 + \frac{\Sigma_{a20}}{D_2}. \tag{3.5}$$

The solution for Equation (3.2) is immediately seen to be

$$Y_{1k} = A1e^{-\alpha_k y} + A2e^{\alpha_k y} . \tag{3.6}$$

The solution to Equation (3.4) will have two parts, a homogeneous solution Y_{2kH} and a particular solution Y_{2kP}. The homogeneous solution comes from

$$\frac{d^2Y_{2kH}}{dy^2} - \beta_k^2 Y_{2kH} = 0 \tag{3.7}$$

and its solution is given as

$$Y_{2kH} = A3e^{-\beta_k y} + A4e^{\beta_k y}. \tag{3.8}$$

The solution for Y_{2KP} is written as

$$Y_{2kP} = C1A1e^{-\alpha_k y} + C2A2e^{\alpha_k y} \tag{3.9}$$

where C1 and C2 are coupling constants which are to be determined. Substituting Equation (3.9) into Equation (3.4) and equating like exponentials leads to

$$C1 = C2 = \frac{-\Sigma_{R1}/D_2}{(\alpha_k^2-\beta_k^2)}. \tag{3.10}$$

Inserting Equation (3.10) into Equation (3.9) and then writing the complete solution for Y_{2K} gives

$$Y_{2k} = Y_{2kH} + Y_{2kP} = A3e^{-\beta_k y} + A4e^{\beta_k y} - \frac{\Sigma_{R1}/D_2}{(\alpha_k^2-\beta_k^2)}$$

$$+ [A1e^{-\alpha_k y} + A2e^{\alpha_k y}]. \qquad (3.11)$$

To solve for the Green's functions in the fuel regions, Equations (3.4) and (3.5) are used and Equation (2.30) is rewritten as

$$\frac{d^2Y_{1k}}{dy^2} - \alpha_k^2 Y_{1k} + \frac{(1-\beta)\nu\Sigma_f}{D_1} Y_{2k} = 0 \qquad (3.12)$$

where α_K^2 has the same meaning as in Equation (3.3). A fourth order equation is next written for Y_{1K} alone. This is done by differentiating (3.12) twice to obtain (letting D = d/dy).

$$D^4 Y_{1k} - \alpha_k^2 D^2 Y_{1k} + \frac{(1-\beta)\nu\Sigma_f}{D_1} D^2 Y_{2k} = 0. \qquad (3.13)$$

Solving Equation (3.4) for D^2Y_{2K} yields

$$D^2 Y_{2k} = \beta_k^2 Y_{2k} - \frac{\Sigma_{R1}}{D_2} Y_{1k} \qquad (3.14)$$

which may be combined with Equation (3.12) to obtain an expression for Y_{2K}

$$Y_{2k} = \frac{\alpha_k^2 Y_{1k} - D^2 Y_{1k}}{\frac{(1-\beta)\nu\Sigma_f}{D_1}} . \qquad (3.15)$$

Substitute Equation (3.15) into Equation (3.14), and then substitute the resulting expression into Equation (3.13) to obtain

$$D^4 Y_{1k} - D^2 Y_{1k} (\alpha_k^2 + \beta_k^2) + Y_{1k} (\beta_k^2\alpha_k^2 - \frac{(1-\beta)\nu\Sigma_f}{D_1} . \frac{\Sigma_{R1}}{D_2}) = 0. \qquad (3.16)$$

This can be factored into two terms

$$(D^2-\mu^2) (D^2-\nu^2) Y_{1k} = 0, \qquad (3.17)$$

where μ^2 and ν^2 are obtained by solving the roots of

$$D^4 - D^2 (\alpha_k^2 + \beta_k^2) + \beta_k^2\alpha_k^2 - \frac{(1-\beta)\nu\Sigma_f\Sigma_{R1}}{D_1D_2} = 0. \qquad (3.18)$$

The roots of Equation (3.18) are found by solving the quadratic equation, thus

$$D^2 = \mu^2, \nu^2 = \frac{(\alpha_k^2 + \beta_k^2)}{2} \pm [(\alpha_k^2 + \beta_k^2)^2 - 4(\beta_k^2\alpha_k^2 - \frac{(1-\beta)\nu\Sigma_f\Sigma_{R1}}{D_1D_2})]^{\frac{1}{2}} /2 \qquad . \qquad (3.19)$$

The solution of Equation (3.12) may be written as

$$Y_{1k} = A5e^{-\mu y} + A6e^{\mu y} + A7e^{-\nu y} + A8e^{\nu y} \tag{3.20}$$

In solving Equation (3.4) for Y_{2K}, let

$$Y_{2k} = C1e^{-\mu y} + C2e^{\mu y} + C3e^{-\nu y} + C4e^{\nu y} \tag{3.21}$$

where C1, C2, C3, and C4 are coupling coefficients incorporating the constants A5, A6, A7, and A8. Differentiating Equation (3.21) twice yields

$$\frac{d^2Y_{2k}}{dy^2} = C1\mu^2e^{-\mu y} + C2\mu^2e^{\mu y} + C3\nu^2e^{-\nu y} + C4\nu^2e^{\nu y}. \tag{3.22}$$

Equations (3.20), (3.21), and (3.22) are substituted into Equation (3.4)

$$C1\mu^2e^{-\mu y} + C2\mu^2e^{\mu y} + C3\nu^2e^{-\nu y} + C4\nu^2e^{\nu y} - \beta_k^2\, C1e^{-\mu y} - \beta_k^2\, C2e^{\mu y}$$
$$- \beta_k^2\, C3e^{-\nu y} - \beta_k^2\, C4e^{\nu y} + \frac{\Sigma_{R1}}{D_2} A5e^{-\mu y} + \frac{\Sigma_{R1}}{D_2} A6e^{\mu y} + \frac{\Sigma_{R1}}{D_2} A7e^{-\nu y} +$$
$$\frac{\Sigma_{R1}}{D_2} A8e^{\nu y} = 0 \tag{3.23}$$

Equating like exponentials gives

$$C1 = \frac{-\Sigma_{R1}/D_2}{(\mu^2-\beta_k^2)} A5 \tag{3.24}$$

$$C2 = \frac{-\Sigma_{R1}/D_2}{(\mu^2-\beta_k^2)} A6 \tag{3.25}$$

$$C3 = \frac{-\Sigma_{R1}/D_2}{(\nu^2-\beta_k^2)} A7 \tag{3.26}$$

$$C4 = \frac{-\Sigma_{R1}/D_2}{(\nu^2-\beta_k^2)} A8 \tag{3.27}$$

and Equation (3.21) becomes, therefore,

$$Y_{2k} = \frac{-\Sigma_R/D_2}{(\mu^2-\beta_k^2)} (A5e^{-\mu y} + A6e^{\mu y}) - \frac{\Sigma_{R1}/D_2}{(\nu^2-\beta_k^2)} (A7e^{-\nu y} + A8e^{\nu y}). \tag{3.28}$$

The Green's functions for the two-dimensional, two-group problem are given by Equations (3.6), (3.11), (3.20), and (3.28). To determine the coefficients A1 through A8, appropriate boundary conditions are applied.

As the analysis progressed, it was discovered that for the first few modes the root ν^2 of Equations 3.20 and 3.28 is negative. Because of this, the terms of (3.20) and (3.28) associated with ν^2 become, as long as ν^2 is negative,

$$Y_{1k} = A5e^{-\mu y} + A6e^{\mu y} + A7\cos\nu y + A8\sin\nu y \qquad (3.20a)$$

and

$$Y_{2k} = \frac{-\Sigma_R/D_2}{(\mu^2-\beta_k^2)} (A5e^{-\mu y} + A6e^{\mu y}) - \frac{\Sigma_{R1}/D_2}{(\nu^2-\beta_k^2)} (A7\cos\nu y + A8\sin\nu y). \qquad (3.28a)$$

A model of the UTR-10 reactor is now developed. The ISU UTR-10 reactor is a graphite reflected, light water cooled and moderated, coupled core machine. There are two fuel regions surrounded and separated by a graphite matrix. The model used in this study defines a plane through the reactor core which is at the level of the center-line of the vibrating neutron absorber. Both the graphite and fuel regions of the model core are homogeneous. Figure 3.1 illustrates the model. The core dimensions used in this model are taken from Salih [10].

As pointed out previously, in obtaining the Green's function modes for the model, the appropriate equations were used for each region of the reactor with appropriate boundary conditions. Properties 3 and 4 for the Green's function, as discussed in Section III, were used at the point of perturbation (y_o).

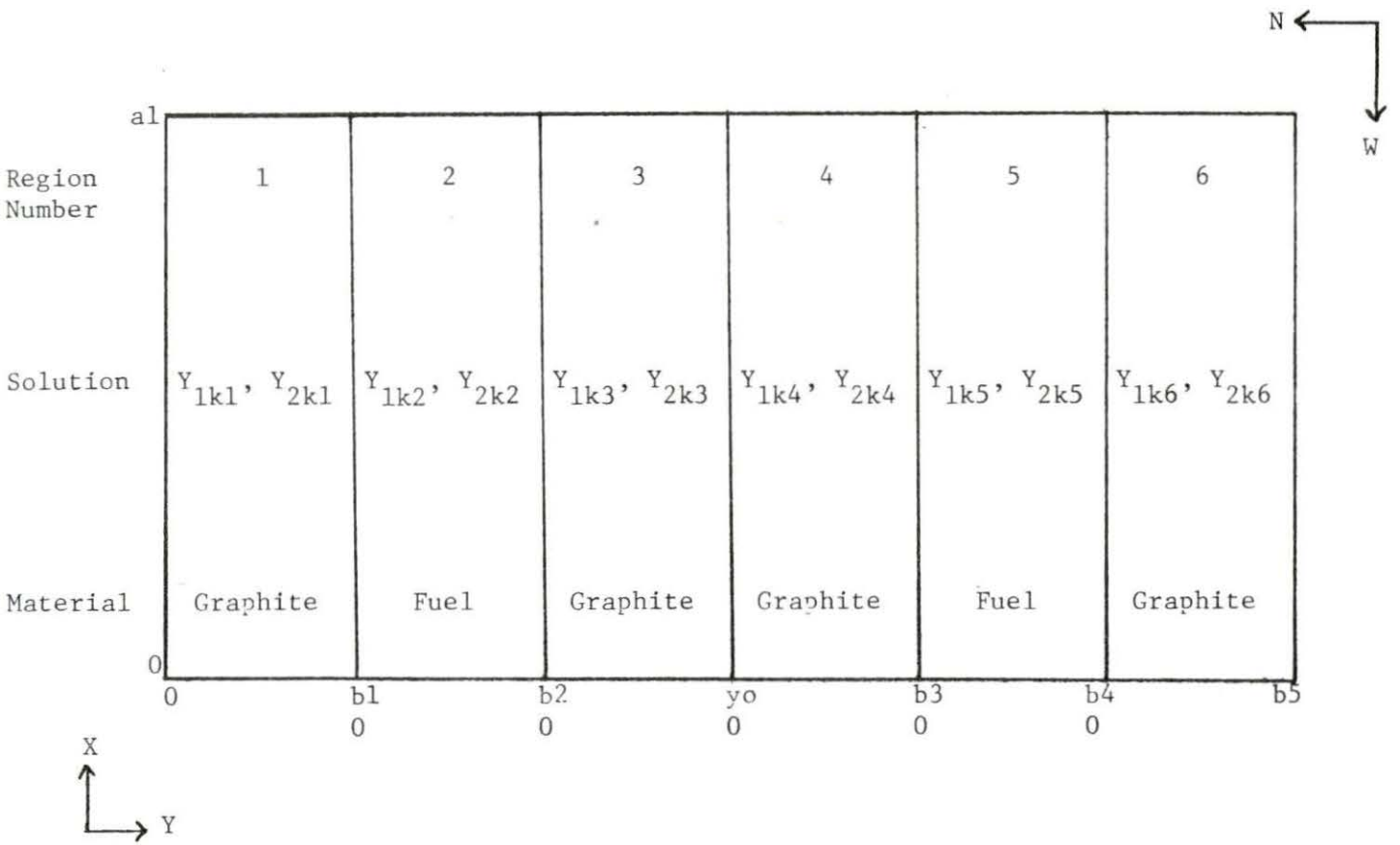

Figure 3.1 Analytical model of the UTR-10 reactor

Referring to Figure 3.1 for the locations of the appropriate Green's function solutions, $Y_{ikj}(y)$, the application of the boundary condition requirements will now be illustrated. In the term $Y_{ikj}(y)$, i refers to the group number and j refers to the region number. The conditions being applied require a Green's function solution of zero at both endpoints of the reactor. At each region interface, the solutions are required to have continuity of flux and current. Continuity of flux implies the solution on one side of the interface must equal the solution on the other side of the interface when both solutions are evaluated at the interface. The current is the derivative of the solution times the diffusion constant, D, for the region. Continuity of current means the solutions on either side of an interface will have equal currents at the interface. As an example, the boundary/interface conditions for the first graphite and first fuel region require

$$Y_{1k1}(0) = 0 \tag{3.29}$$

$$Y_{2k1}(0) = 0 \tag{3.30}$$

$$Y_{1k1}(b_1) = Y_{1k2}(0) \tag{3.31}$$

$$Y_{2k2}(b_1) = Y_{2k2}(0) \tag{3.32}$$

$$D_{1M} \frac{dY_{1k1}(b_1)}{dy} = D_{2F} \frac{dY_{1k2}(0)}{dy} \tag{3.33}$$

$$D_{2M} \frac{dY_{2k1}(b_1)}{dy} = D_{2F} \frac{dY_{2k2}(0)}{dy} \tag{3.34}$$

$$Y_{1k2}(b_2) = Y_{1k3}(0). \tag{3.35}$$

Note that a moving coordinate system was used in the model for the y dimension. This was done to avoid computer overflow and underflow as a result of large spatial coordinate values. The imposed Green's functions conditions give

$$Y_{1k3}(yo) = Y_{1k4}(0) \tag{3.36}$$

$$Y_{2k3}(yo) = Y_{2k4}(0) \tag{3.37}$$

$$D_{1M} \frac{dY_{1k3}(yo)}{dy} = D_{1M} \frac{dY_{1k4}(0)}{dy} \tag{3.38}$$

$$\frac{dY_{2k3}(yo)}{dy} - \frac{dY_{2k4}(0)}{dy} = 1. \tag{3.39}$$

A total of 24 boundary conditions result.

The next step in the modeling is to form the set of equations which describe the reactor. The boundary conditions are applied to

the solution equations (3.6), (3.11), (3.20), and (3.28). The result is 24 coupled equations with 24 unknown coefficients. For the fuel regions, several additional equations must be written to account for the different solution equations, (3.20a) and (3.28a), which are used when the root ν^2 is negative. When ν^2 is negative, these equations are substituted for the equations used when ν^2 is positive. As an example, boundary condition (3.31) yields the following equation when imposed on Equations (3.6) and (3.20):

$$A1e^{-\alpha_k b1} + A2e^{\alpha_k b1} = A5e^{-\mu(0)} + A6e^{\mu(0)} + A7e^{-\nu(0)} + A8e^{\nu(0)}$$

or

$$A1e^{-\alpha_k b1} + A2e^{\alpha_k b1} - A5 - A6 - A7 - A8 = 0. \qquad (3.40)$$

The same is done for all boundary conditions to form the solution to the two-group problem. The equations are solved simultaneously to find the desired coefficients. This is done using the computer, as outlined in the next section.

IV. COMPUTER MODELING OF THE GREEN'S FUNCTION SOLUTIONS

In this section, the computer programs which were written to solve the Green's function solution equations are discussed, and each program is described individually. Listing of the programs is also given in Appendix A. All programs used double precision arithmetic. Graphs indicating the results of individual programs are presented, and predictions of the changing neutron flux due to the moving neutron absorber are made.

The 24 coupled equations discussed in Section III are to be solved simultaneously using computer programs. Solving the equations means determining the coefficients of each solution equation (3.6), (3.11), (3.20), and (3.28) in appropriate regions of the reactor. To solve them, the equations are first written in the matrix form

$$\underline{A}\,\underline{X} = \underline{B}. \tag{4.1}$$

The vector $\underline{X}$ contains the 24 unknown coefficients of the solution equations. Matrix $\underline{A}$ consists of the array of system constants multiplying the unknown coefficients. Vector $\underline{B}$ contains the elements of the right hand side of the solution equations.

The first step in the analysis was to insure that the modeled reactor represented a critical system as closely as possible. For a critical reactor, the vector $\underline{B}$ in Equation (4.1) will be zero. This leads to

$$\underline{A}\,\underline{X} = 0$$

or

$$\text{determinant } \underline{A} = \left|\underline{A}\right| = 0. \tag{4.2}$$

The criticality calculation was done for an unperturbed core. This means that the Green's function conditions at y_o are not applied and, in fact, the interface at y_o is eliminated. Graphite regions 3 and 4 (see Figure 3.1) are combined. This reduces the size of the set of simultaneous equations to be solved to 20.

In the criticality calculation, all diffusion coefficients, cross sections, and all other parameters are the same ones that are to be used in the perturbed reactor. It was decided to iterate on the vertical buckling, B_Z^2, to zero the determinant of $\underline{A}$ to obtain a critical system. B_Z^2 is introduced into the equations in the α^2 and β^2 terms of Equations (3.3) and (3.5). These equations now become

$$\alpha_K^2 = B_K^2 + \frac{(\Sigma_{a1} + \Sigma_{R1})}{D_1} + B_Z^2 \tag{4.3}$$

$$\beta_K^2 = B_K^2 + \frac{\Sigma_{a20}}{D_2} + B_Z^2.$$

Addition of the B_Z^2 term is justified if $\nabla^2\phi$ of Equations (2.5) and (2.6) is separated into the three components

$$\nabla^2\phi = \frac{\partial^2\phi}{\partial x^2} + \frac{\partial^2\phi}{\partial y^2} - B_Z^2\phi. \qquad (4.4)$$

When this addition is made, it can be easily shown that the derivations of Sections II and III are not changed. The value of B_Z^2 is approximately $(\pi/Z)^2$, where Z is the vertical dimension of the reactor.

The computer program GFP-20 was written to do the criticality calculations. GFP-20 calls the library subroutine LINV3F to solve for the determinant of $\underline{A}$. In GFP-20 the reactor parameters, cross sections, etc. are first assigned. As discussed in Appendix B, reactor parameters were obtained using the LEOPARD code [8]. Next, the 20 x 20 matrix $\underline{A}$ is initialized to zero and the elements of $\underline{A}$ representing the solution equations are inserted. The program then calls the library subroutine LINV3F and the determinant of $\underline{A}$ is calculated. The program was set up to step through incremental values of Z until the Z which resulted in a zero determinant was found. At this point, it was important to make sure that the value of Z found corresponds to the fundamental mode solution. This was checked by calculating the neutron fluxes. The desired value of Z (or B_Z^2) will result in all positive fluxes. Any Z other than the fundamental value gives some positive and some negative fluxes. The critical value of Z was found to be 74.583 cm based on the reactor parameters given in Appendix B. The solution was also checked by using the finite difference, two-dimensional computer code EXTERMINATOR-2 [11] to

perform an eigenvalue calculation for the reactor model used in the analytical calculation. The resulting eigenvalue of 0.9974 confirmed that the correct critical buckling was found.

Four computer programs were written to solve for the four terms needed for the reactor response, Equation (2.40). These programs solve for the terms of Equation (2.40) and then produce punched output so that the total flux response across the reactor can be calculated. Since the detectors and vibrator used in the experiment are sensitive to the thermal flux, the computer programs were written to solve for the Green's functions, the flux, and their derivatives for the thermal group only. The general form of each program is the same. First, all reactor parameters are assigned. Next, the elements of the matrix $\underline{A}$, and vector $\underline{B}$, if applicable, are calculated and inserted into the proper locations. The programs then call the library subroutine LINV3F to solve the equations. The coefficients which are found (as the elements of vector $\underline{x}$) are then used in the proper solution equation and a numerical answer is produced. Choosing the proper solution equation to use depends on the position (y) being solved for.

The program GFP-24 calculates the term G in Equation (2.40), which is the Green's function term. The program, as listed in Appendix A, will calculate the Green's functions at 61 points across the reactor core for any value of x. Because the equations for the Green's functions were originally expanded into a series form (Equations (2.24) and (2.25)), the Green's functions calculated by

the program is the sum of many modes. As the mode number k increased, the matrix $\underline{A}$ appeared to become progressively ill-conditioned until a point was reached where the routine LINV3F failed to find the solution vector. It was observed that for the maximum value of k, the solution in the fuel and external graphite regions had converged. For the region containing the perturbation, where the Green's function is sharply peaked, convergence was found not to be satisfactory when the limiting value of k was reached for the whole core calculation. The program is designed to run the maximum number of modes possible (13 were used) when the solutions for the whole core are calculated. The program then refines the numbers by repeating the mode calculation for the central graphite region only using zero boundary conditions on the additional modes, which, in effect, forces the solution to the converged values at the edge of the fuel. This procedure allowed 8 more modes to be added to the 13 modes already calculated. This method produced a convergence of 0.005 at the point of perturbation. That is, the difference between the 20th mode and the 21st mode is 0.005. Since the value of the Green's function at this point is 0.32825, this convergence represents an error of 1.5%. A plot of the Green's functions across the midplane of the reactor through the perturbation point is shown in Figure 4.1. In this graph, and the others which follow, the perturbation is located in the center of the central graphite region of the reactor. Since the Green's function describes the response as a function of position due to a point

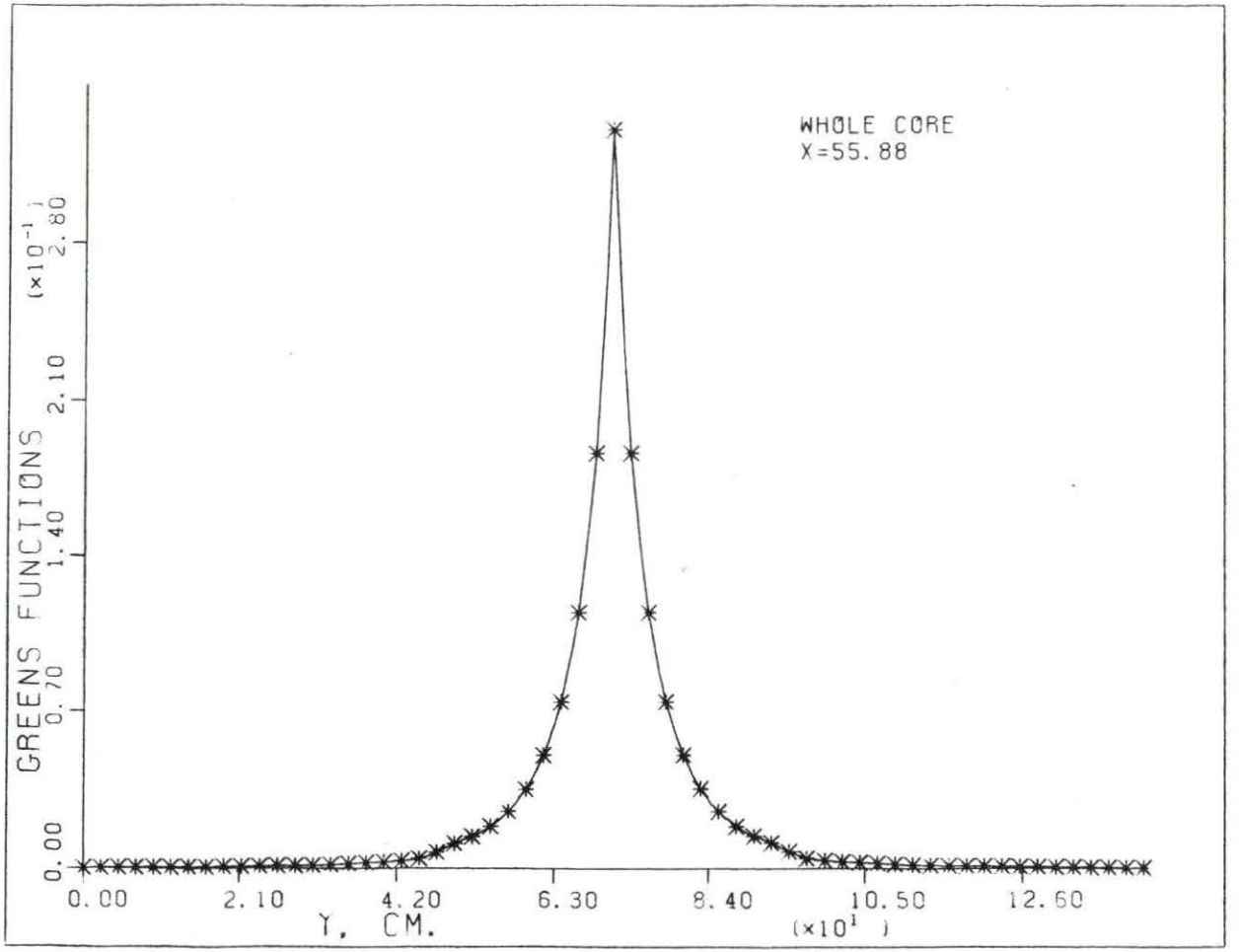

Figure 4.1 Green's functions at x=55.88 cm as calculated by GFP-24

perturbation, the sharply peaked nature of G implies that the response near the perturbation should be sensitive to changes in vibrator position (the dG/dy_o term).

The next computer program, GFP-25, calculates the term dG/dy_o, the change in the Green's function associated with a change in perturbation position. Since the variable y_o does not appear explicitly in G, a finite-difference technique was employed. The Green's function is calculated twice at each desired point, once with the perturbation located at the center of the core and once with the perturbation moved an amount $\Delta y_o = 0.02$ cm in the +y or south direction. The difference between the two Green's functions at each space point is divided by the step size and an approximate derivative is produced. It should be noted that the derivative is a function of x and y for a given y_o. As is expected, dG/dy_o was found to be greatest where the Green's function is increasing the fastest, at the center of the core. Because of the approximate nature of the calculation, the sensitivity of the result to the step size and two point approximation was checked using different step sizes and also a three point calculation. As might be expected, because of the nature of the Green's function, the solution was found to be sensitive to these parameters for locations near the perturbation point. Based on the sensitivity study, it was concluded that a two point estimate of the derivative with a Δy_o of 0.02 cm yielded acceptable estimates of dG/dy_o for the experimental locations used in the study.

The flux term of Equation (2.40) is calculated by the computer program GFP-27. The flux solutions are the fundamental mode solutions to the steady state diffusion equations. The thermal flux solutions can be written as

$$\phi_2 = \sin \frac{\pi x}{a} \left(Y_{21j}\right) \tag{4.5}$$

where Y_{21j} is the solution to the one-dimensional diffusion equation. GFP-27 finds the fluxes using the same matrix as is used in GFP-20. The coefficients of the solution equations are found by adding the identity matrix to matrix $\underline{A}$ and then calling library subroutine EIGRF to evaluate the eigenvectors and eigenvalues of the resultant matrix. The coefficients are the elements of the eigenvector corresponding to the unity eigenvalue. Figure 4.2 shows a plot of the relative thermal flux. This shows a higher peaking in the south core due to the larger fuel loading there (see Appendix B).

The last program used to evaluate the reactor response was GFP-28. This program calculates $d\phi/dy$ at the point of the perturbation. Since $d\phi/dy$ is a function of the perturbation location and not detector location, it was necessary to find only one value. The program is a modification of GFP-27 which uses a finite-difference technique similar to GFP-25. The value of $d\phi/dy$ found by GFP-28 is 0.01353 for the center of the core.

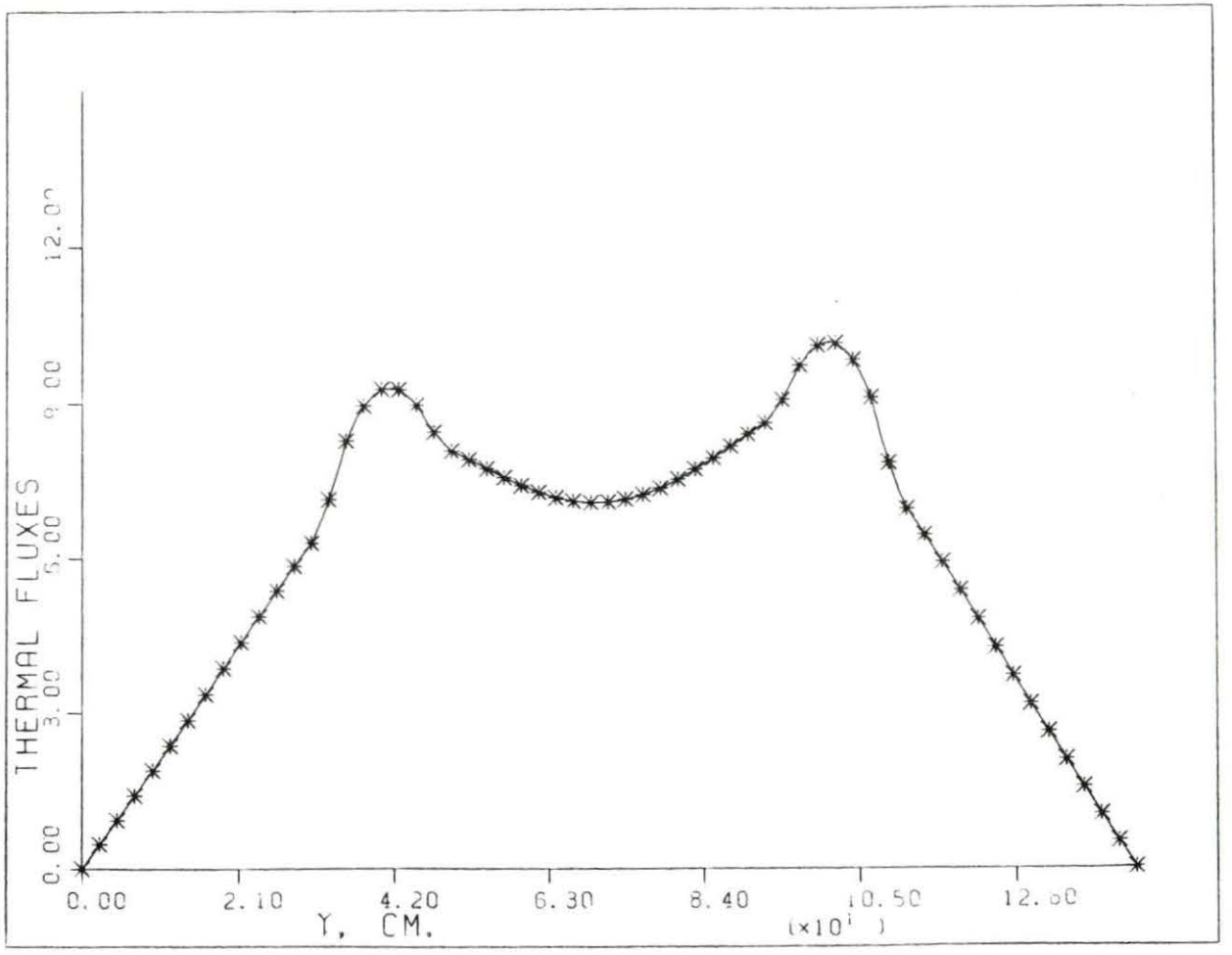

Figure 4.2 Thermal fluxes at x=55.88 cm as calculated by GFP-27

The next step in the analysis was to combine the four terms of Equation (2.40) calculated by the programs GFP-24, GFP-25, GFP-27, and GFP-28 into one result which represents the reactor thermal flux response. This was done by obtaining program output for G, dG/dy_o, ϕ, and $d\phi/dy_o$ on punched cards, which were then assembled as the data deck for a plotting program. The program is called PLOT and is listed in Appendix A. PLOT was used to generate four graphs. The graphs illustrate the detector response across the core in the y direction for two fixed positions in x corresponding to locations used in the experimental measurements. Each x position is shown for the whole core, and also for the central graphite region. Figures 4.3 and 4.4 show the response through the center of the core where the perturbation is positioned with the x plane located at x = 55.88 cm. The point at 71.12 cm on these graphs (the perturbation point), therefore, represents the maximum flux response made at this point. In Figures 4.5 and 4.6, the x plane is moved to x = 41.67 cm.

Figures 4.3 and 4.4 illustrate that the detector response drops off rapidly along the centerline of the reactor with increasing separation between the vibrator and detector. This is indicative of a large local component of the response near the vibrator. The change in sign across the vibrator location simply indicates that there is a 180° phase difference between the responses on each side of the vibrator.

Several other features were noted from the data used to plot Figures 4.3 and 4.4. The small peak in the response shown in

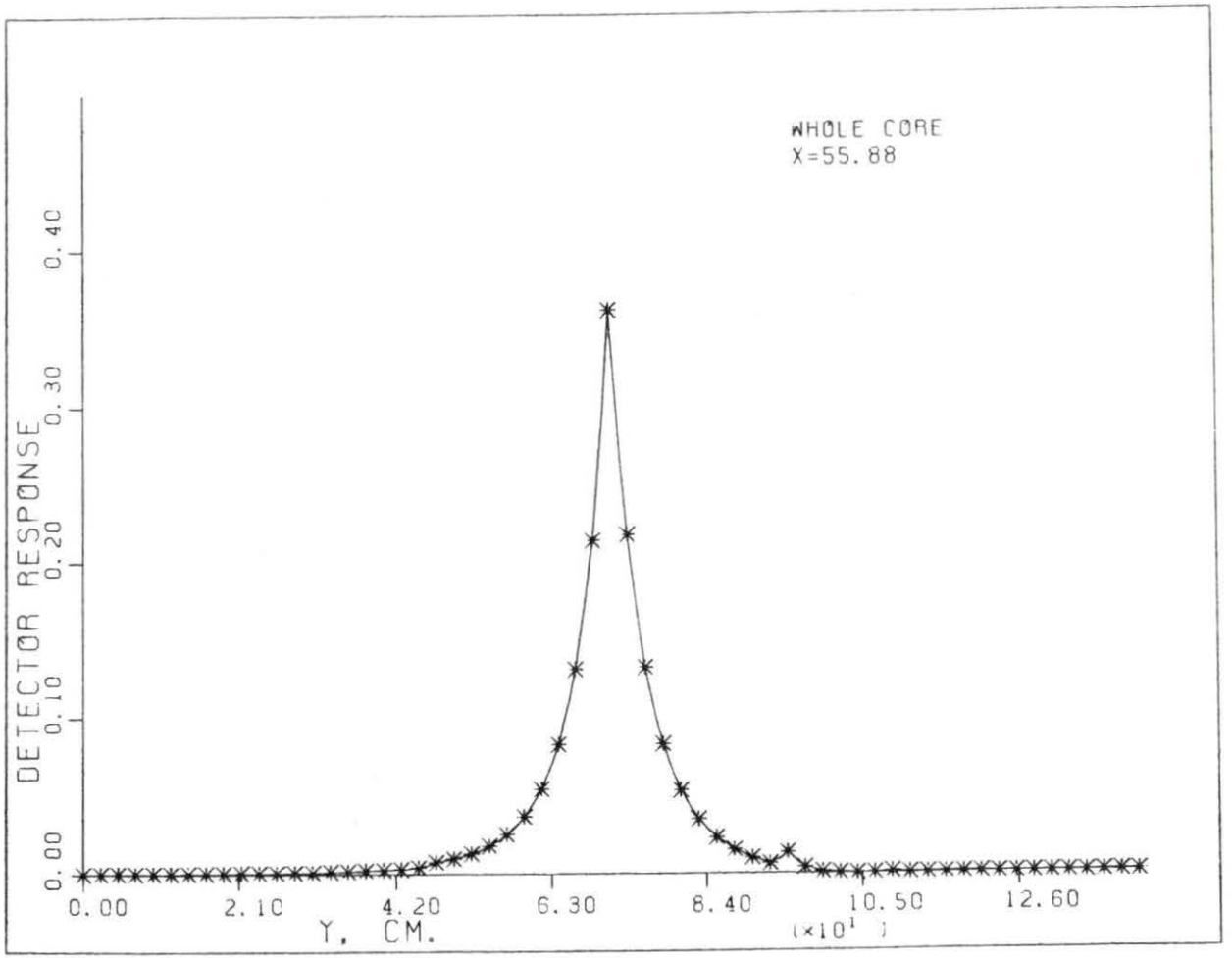

Figure 4.3 Reactor flux response for the whole core, x=55.88 cm

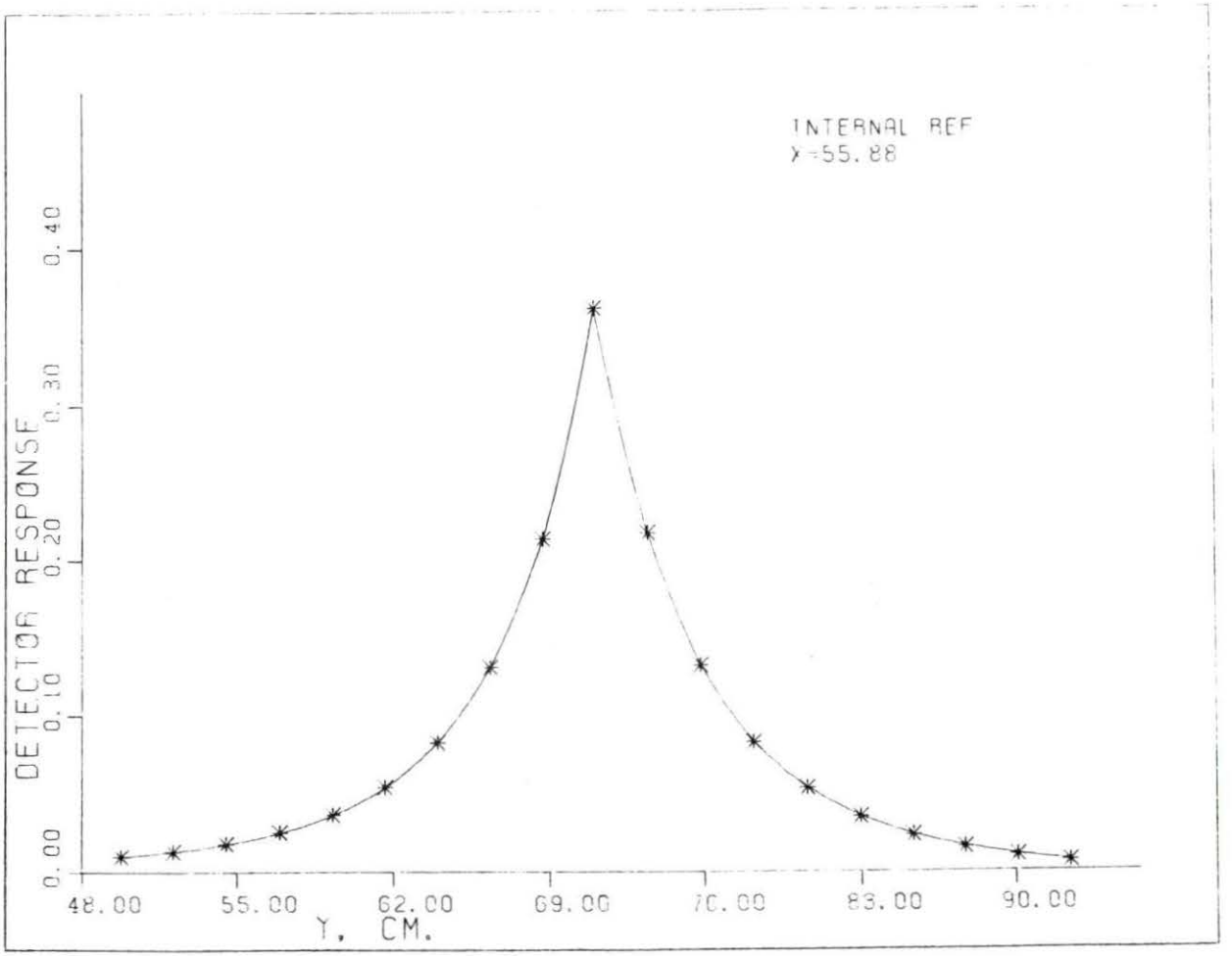

Figure 4.4 Reactor flux response for the central graphite region, x=55.88 cm

Figure 4.3 is located just inside the south fuel region. There is also a similar peak, although smaller, just inside the fuel on the other side of the south core. These peaks were not found in the north core. It is not known if these peaks are real or simply the result of residual oscillations from the modal solution for G. It was also noted that in a small region (from approximately 111 to 128 cm) just outside the south fuel region toward the edge of the core in the graphite, the sign of the response changes. This would indicate that the response in this region is in-phase with the response on the opposite side of the vibrator. Again, it is not known if this effect is real or simply due to oscillations in the modal solution.

Figures 4.5 and 4.6 show the response across the reactor in a plane approximately 14.2 cm from the vibrator. The response, in this case, also shows a strong local component. The small peaks in the south fuel region and the change in sign in the graphite region appear also in these calculations. In both cases, the two terms in Equation (2.40) add on the right side of the absorber and subtract of the left side. The term dG/dy_o dominates the solution for the detector so the sign of the response is the same as the sign of the derivative.

In the experimental portion of this work, neutron detectors were placed at three locations; two in the central reflector (at x = 55.88 cm, y = 68.26 cm and x = 41.67 cm, y = 59.61 cm), and one fully inserted in the central stringer of the thermal column with the near end of the detector approximately 58.42 cm from the center of the reactor. One of the purposes of this study is to compare the measured

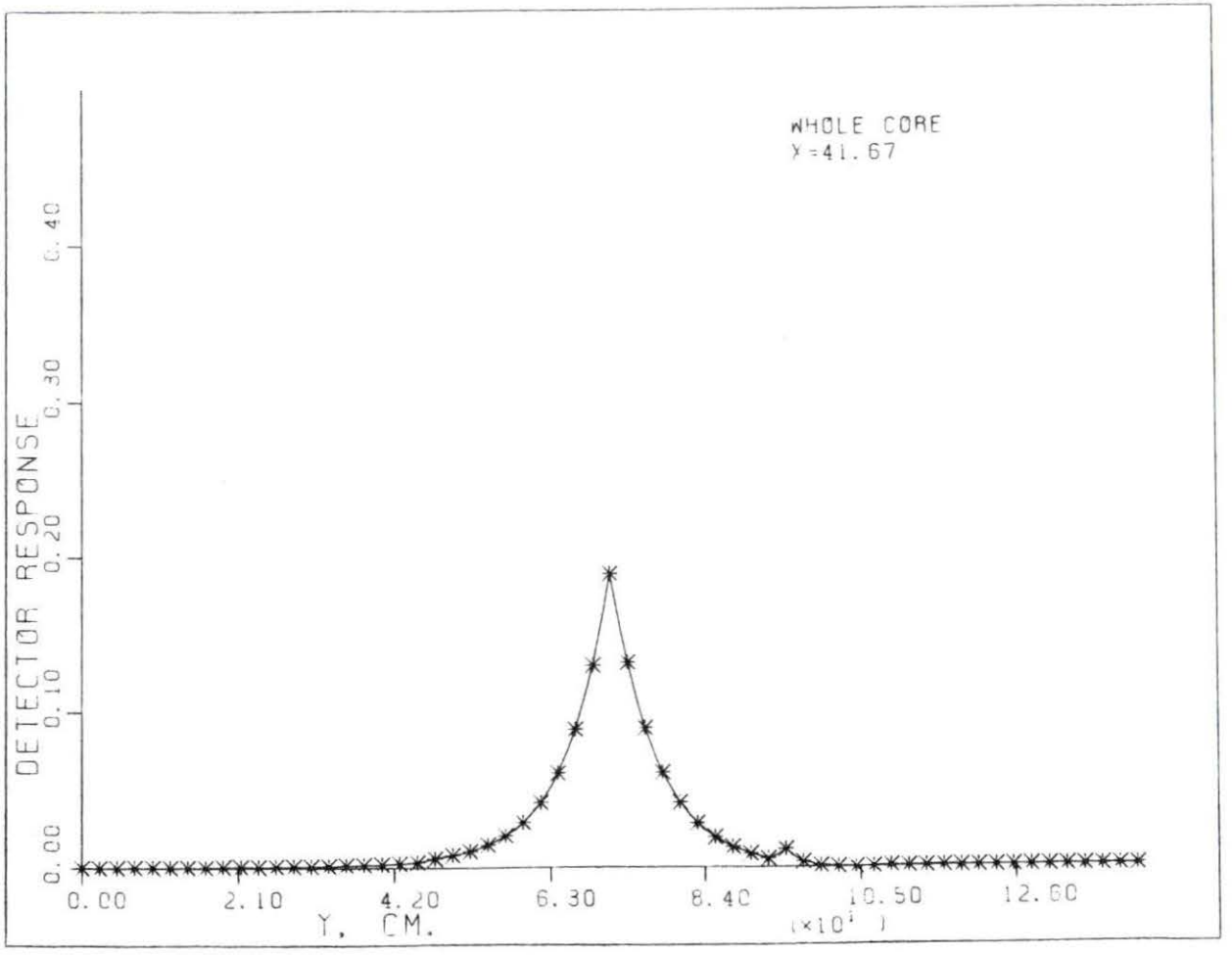

Figure 4.5 Reactor flux response for the whole core, x=41.672 cm

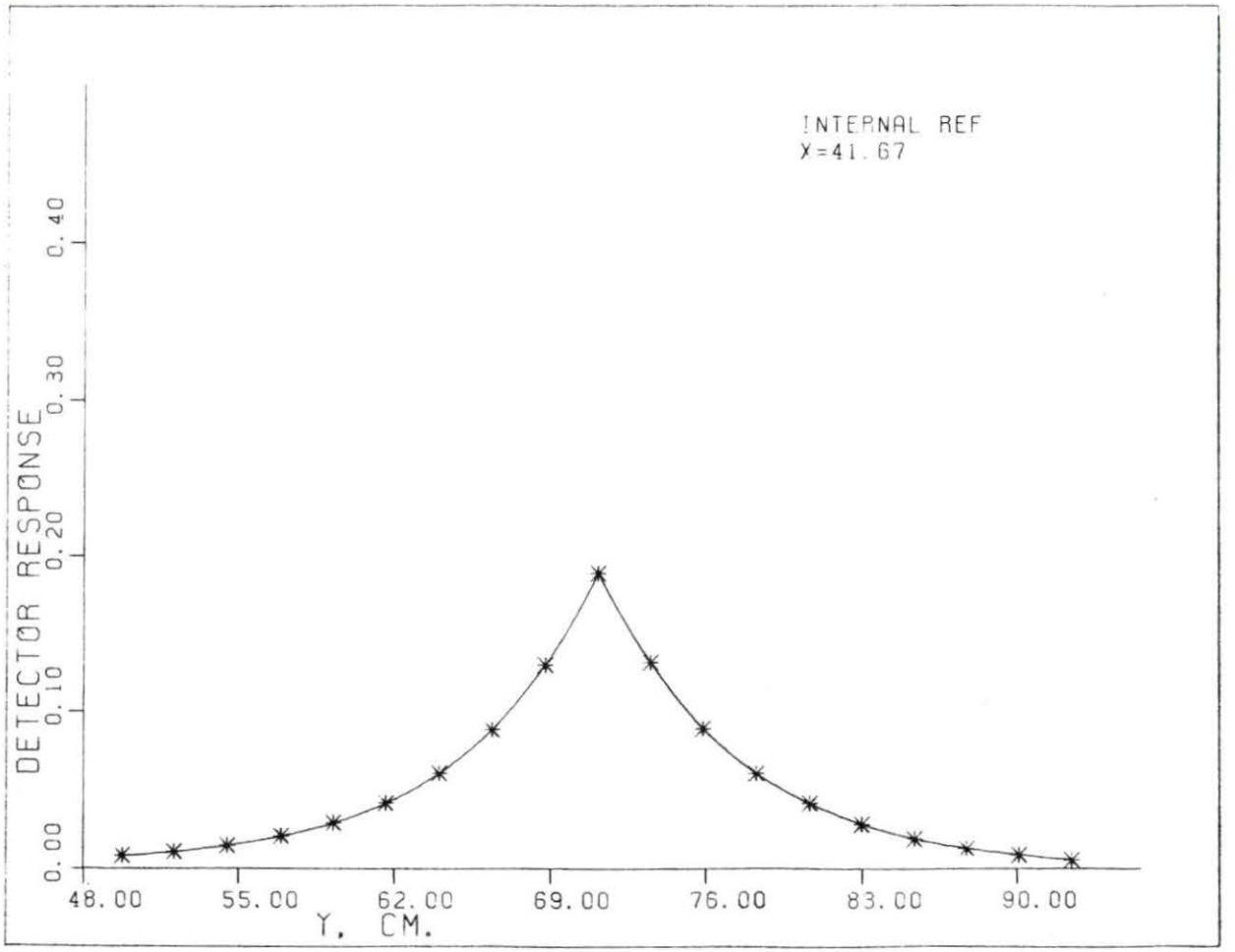

Figure 4.6 Reactor flux response for the central graphite region, x=41.672 cm

and predicted responses of the detectors located in the central reflector. To eliminate the need to estimate an appropriate value for γ to use in Equation (2.40), results were interpreted in terms of the ratio of the response rather than an absolute value. A summary of the prediction is shown in Table 1.

The calculated ratios of detector responses shown in Table 1 confirm the highly localized characteristics of the response. These results also illustrate the sensitivity of the calculated response of the detector near the vibrator to the assumed detector position. This behavior should be kept in mind when comparing the experimental and theoretical responses.

Table 1. Computer based predictions of flux response to a moving absorber

Detector Position	G	$\partial G/\partial y_o$	ϕ	$\partial\phi/\partial y$	$\frac{\Delta\phi_2(\omega)}{\gamma\Delta Y(\omega)}$	Ratio$[\frac{\Delta\phi_2\ y=68}{\Delta\phi_2\ y=59}]$
x = 55.88 cm						
y = 68.26 cm[a]	0.1675	-0,03602	7.086	0,01353	-0,2576	
x = 41.67 cm						8.587
y = 59.61 cm[a]	0,02971	-0.004290	7.086	0.01353	-0,03000	
x = 55.88 cm						
y = 69.06 cm[b]	0,2401	-0.04524	7.086	0.01353	-0.3173	10.58

[a]Based on distance from detector centerline to vibrator centerline.

[b]Based on distance from detector edge to vibrator centerline.

V. EXPERIMENTAL EQUIPMENT AND RESULTS OF MEASUREMENTS

In this section, the results of the experiment which was performed to verify the predictions of Section IV will be presented. In addition to the actual flux response ratio, other data such as detector phase plots and coherence functions will be discussed. Short descriptions of the UTR-10 reactor, experimental equipment, and experimental methods are also included.

The UTR-10 reactor is an Argonaut type coupled-core system. It is light water moderated and cooled. Each core region is surrounded by graphite which serves as a reflector. The maximum licensed power of the reactor is 10 kilowatts.

The central graphite region of the reactor contains five removable stringers which may be replaced with experimental devices. The experimental work done for this research involved using two of the stringer locations. The vibrating neutron absorber and one detector (detector 1 of Figure 5.3) were placed in the Central Vertical Stringer (CVS). Another detector was placed in a stringer located northwest of the CVS (detector 2 of Figure 5.3) in the internal reflector. Figures 5.1 and 5.2 show plan and elevations views of the reactor core. A third detector was fully inserted in the central stringer location in the thermal column. The detectors used in the internal reflector were N. Wood model G-5-9, 5/8 inch (1.59 cm) x 9 inch (22.9 cm) BF_3 detectors operated as ion chambers, and the detector used in the

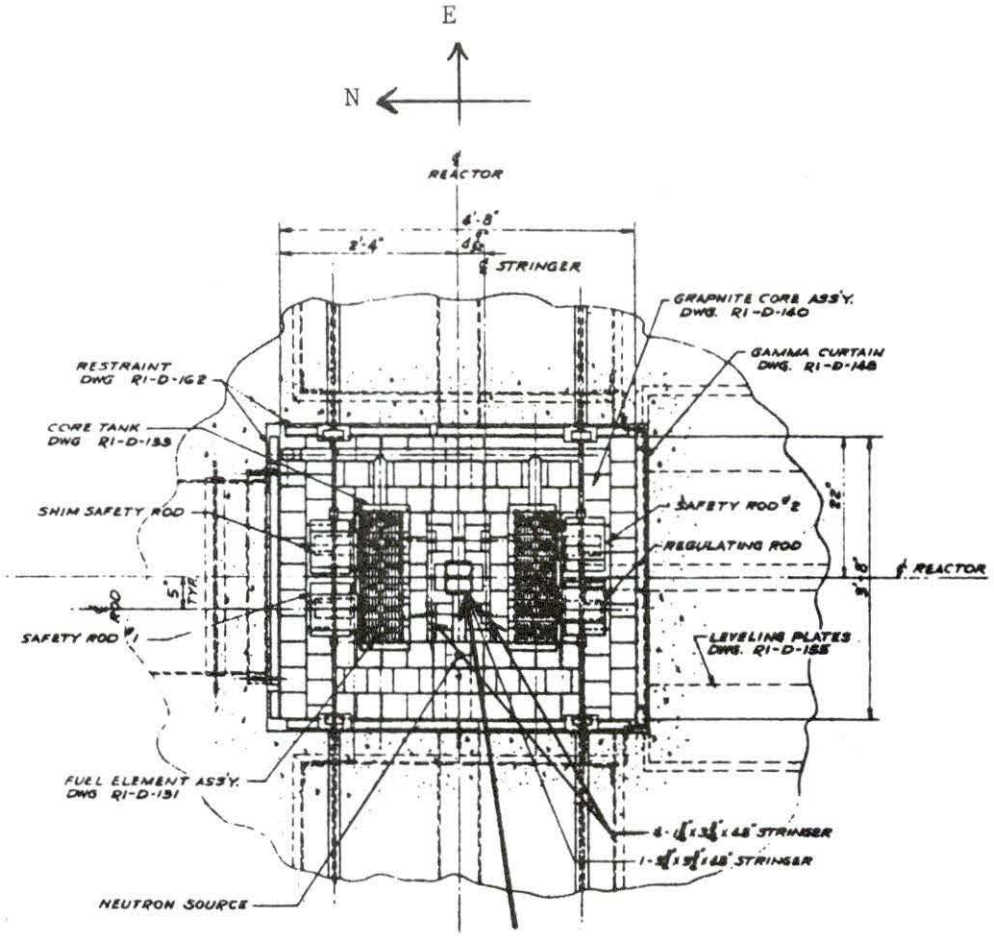

Central Vertical Stringer (CVS)

Figure 5.1 Plan view of the UTR-10 reactor showing locations of the CVS and the other central graphite region stringers

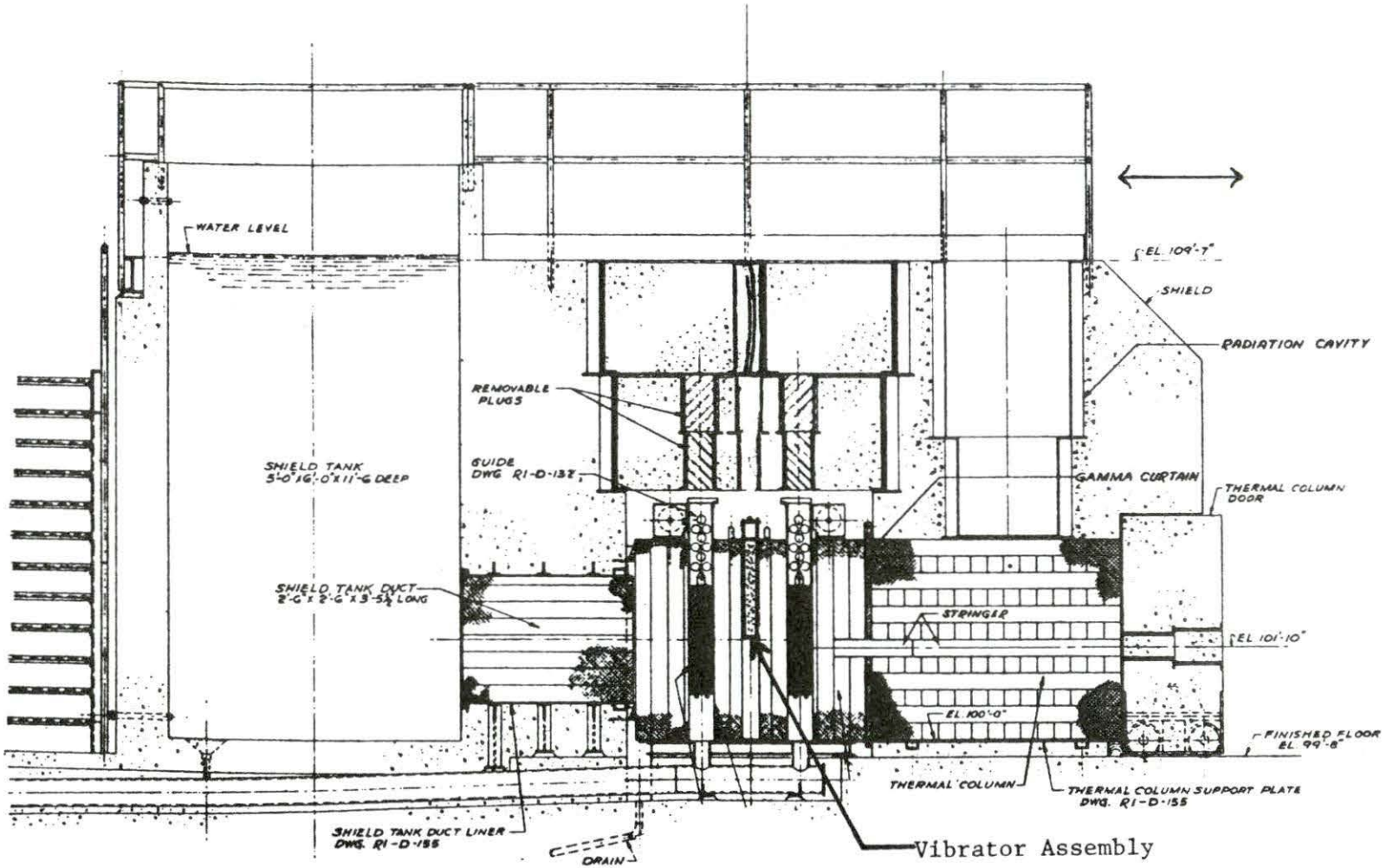

Figure 5.2 Elevation view looking east of the UTR-10 reactor showing location of the CVS

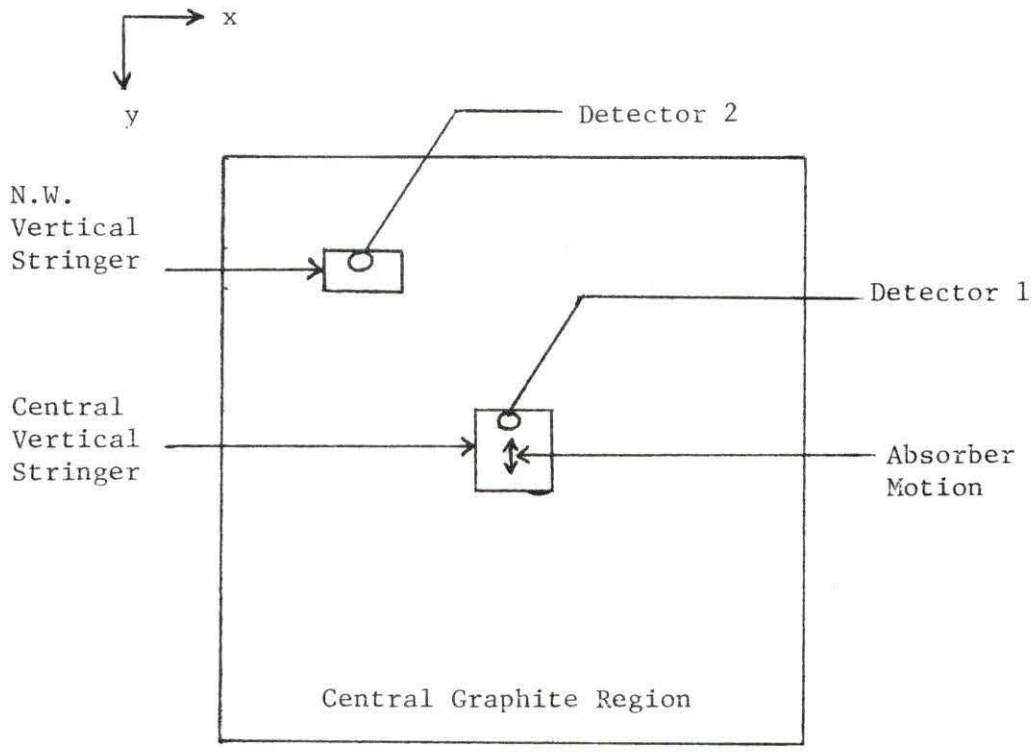

Detector Calculated Positions
(origin at N.W. corner of core)

N
W

	x (cm)[a]	y (cm)[a]
Detector 1	41.67	59.61
Detector 2	55.88	68.26

[a] To centerline of detector

Figure 5.3 Central graphite region showing exact detector locations

thermal column was a Westinghouse model 6377 compensated ion chamber (CIC). The current output from the BF_3 detectors was measured by pre-amplifiers locally constructed, (Ames Laboratory) which produced a voltage output. The output from the CIC was measured by Keithley model 417 picoameter. All signals were bandlimited using a high pass filter (Krohn-Hite model 3321) set at a cutoff of 0.1 Hz and a low pass filter (local construction) set at 15 Hz.

The vibrating neutron absorber used in this research is the same apparatus used by Borland [6]. It consists of a graphite block which fits into the CVS. It has slots for detectors, as well as a hollow center for the vibrating neutron absorber parts. The vibrating absorber is a small piece of cadmium metal attached to an aluminum rod. The rod is suspended in the graphite block by a pivot in the top of the assembly. The rod is driven back and forth in the graphite block by two electrical coils, also located in the top of the device. These coils alternately attract iron plates secured to the top of the rod creating a vibrating motion in the Cd strip. This motion has a maximum amplitude of 1.28 cm. The centerline of the motion is approximately 2 inches above the center plane of the reactor. A linear variable differential transformer (LVDT) was used to measure the motion of the absorber. The apparatus is shown in Figure 5.4.

The signals from the detectors and the LVDT were sent to a HP3582A Spectrum Analyzer. The analyzer uses the Fast Fourier transform to obtain the frequency content of the signals. The square

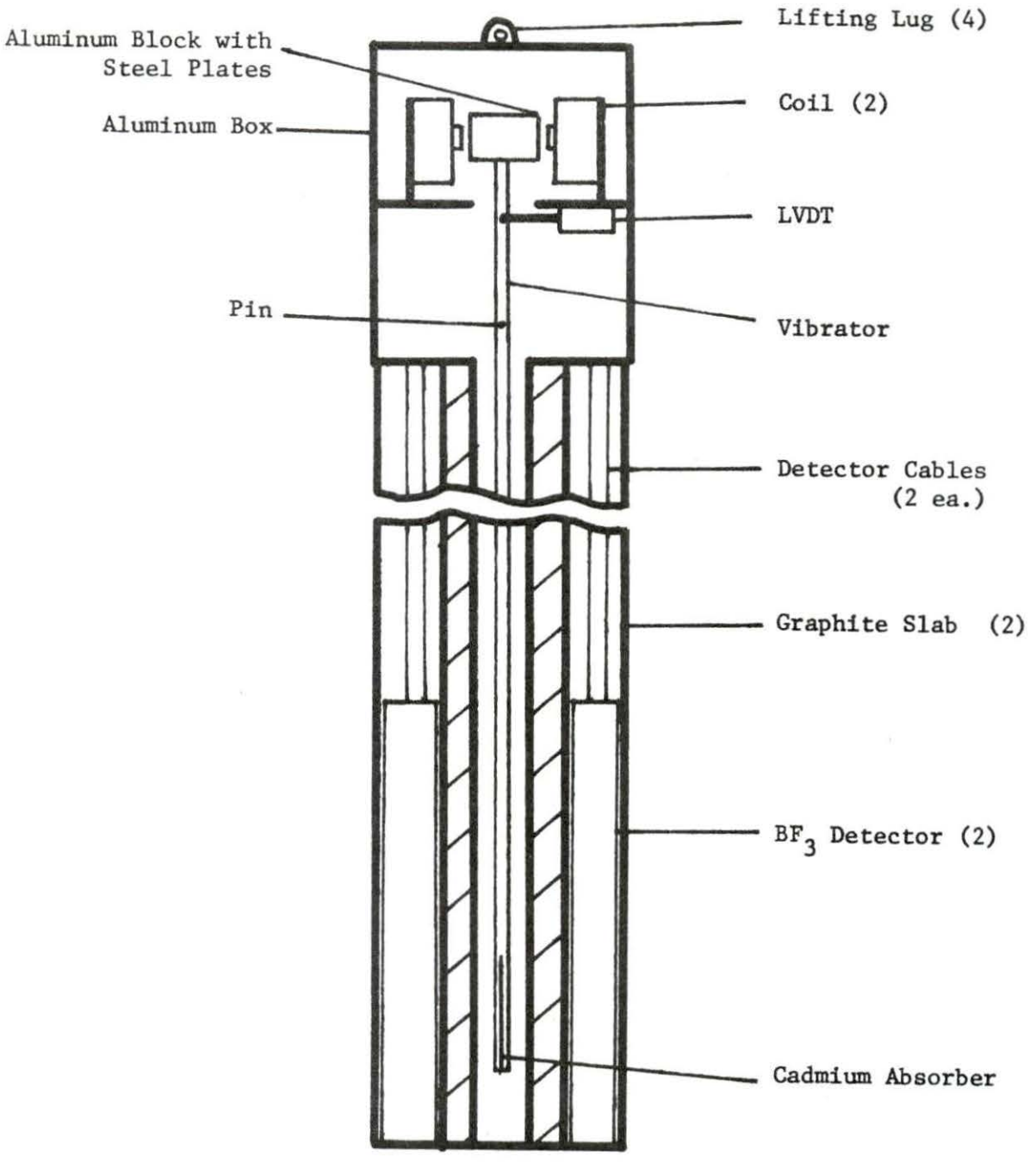

Figure 5.4 Vibrating absorber assembly [6]

root of the Auto Power Spectral Density (APSD), transfer functions, transfer function (TF) magnitude and phases, and coherence functions are all available on the analyzer. The cross power spectral density (CPSD) is not measured directly, but can be calculated from the appropriate APSD and transfer function (TF) using the equation CPSD = TF/APSD. A HP 85 minicomputer was used to store data from the analyzer, calculate the Cross Power Spectral Density and generate plots of the results. All runs used rms averaging with 16 averages.

Reactor flux response to a moving neutron absorber, such as was used in this experiment, can be thought of as having two separate components. These components are the local response and the global response [1,2]. The local response is due to the flux depression in the area of the reactor very near the neutron absorber. The global response is the overall reactor flux response to the absorber moving in a flux gradient. As the absorber moves into a region of greater flux, negative reactivity is added to the reactor and the whole reactor flux level falls. Similarly, when the absorber moves into a region of less flux, positive reactivity is added and the flux level increases. The effects of the local and global flux responses add or subtract depending on detector placement relative to the vibrator. A detector near enough to the neutron absorber to experience a local response will indicate a total response greater or less than either the local or global response alone depending on whether the components are in phase or not.

The detector in the CVS (detector 1 of Figure 5.3) is close enough to the absorber to see a large local effect. It is assumed that the other BF_3 detector (detector 2 of Figure 5.3) and the CIC will see only the global response. Since at the time the experiment was run, the south core had a larger fuel loading than the north core, calculations served to indicate that there was a positive flux gradient through the central graphite region from north to south (Figure 4.2). The higher flux was in the south core. For this distribution, when the absorber moved north it added reactivity and the overall flux level (i.e., the global response) increased. However, the detector in the CVS was on the north side of the apparatus and was exposed to a decreasing flux due to the local response. Thus, the local and global responses are out of phase for this detector. If the local response at the location of this detector is greater than the global response, the resulting composite signal will be out of phase with the rest of the detectors. Data will be presented which show that this is the case.

The LVDT signal was also found to be out of phase with the global response. This was determined by moving the absorber by hand and observing the LVDT signal on a digital multimeter. Both the CIC and the BF_3 detectors undergo a phase shift of 180^{o} due to the detection electronics. For this reason, the global response signals will be in phase with the LVDT. The local response signal will be out of phase with both the LVDT and global response signals. A summary of the

expected detector responses and LVDT signal is shown in Figure 5.5 where the global component is based on a positive flux gradient from north to south. Phase changes other than 180^{o} resulting from sign changes are assumed to be negligible. This includes the phase of the reactor frequency response (approximately 11^{o}) and a small phase shift through the instrumentation.

The experiment was run with the reactor at a power level of 200 watts. The vibrating absorber was excited with a 1.5 Hz square wave signal and with a pseudo random binary sequence (PRBS) signal. The graphs of interest, produced by the minicomputer, are the APSDs of the individual signals and the phase, coherence, and CPSD plots of combinations of the signals.

The APSD is a measure of how the "power" of a signal is distributed in frequency. The APSDs of the signals will first be examined. Figures 5.6 through 5.10 are plots of the background signals indicated by each detector. In these plots, and all that follow, detector 1 refers to the BF_3 detector in the CVS, detector 2 refers to the BF_3 detector in the other stringer, and thermal column detector refers to the CIC located in the thermal column. Figures 5.6, 5.7, and 5.8 show the detector spectra at a reactor power of 200 watts with no absorber motion. Figures 5.9 and 5.10 show the BF_3 detector's signals with the reactor shutdown but the vibrator in motion. These measurements were taken to check for noise from

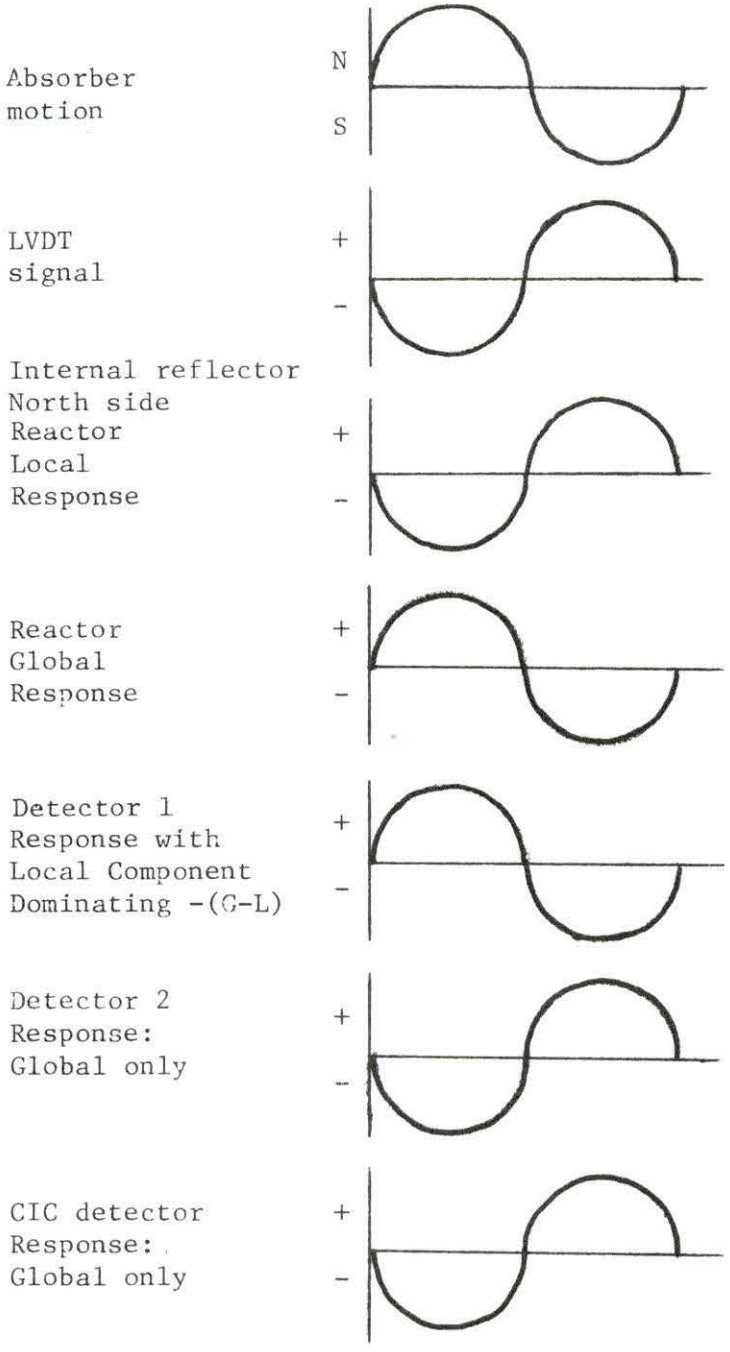

Figure 5.5 Reactor response and indicated detector response to absorber motion

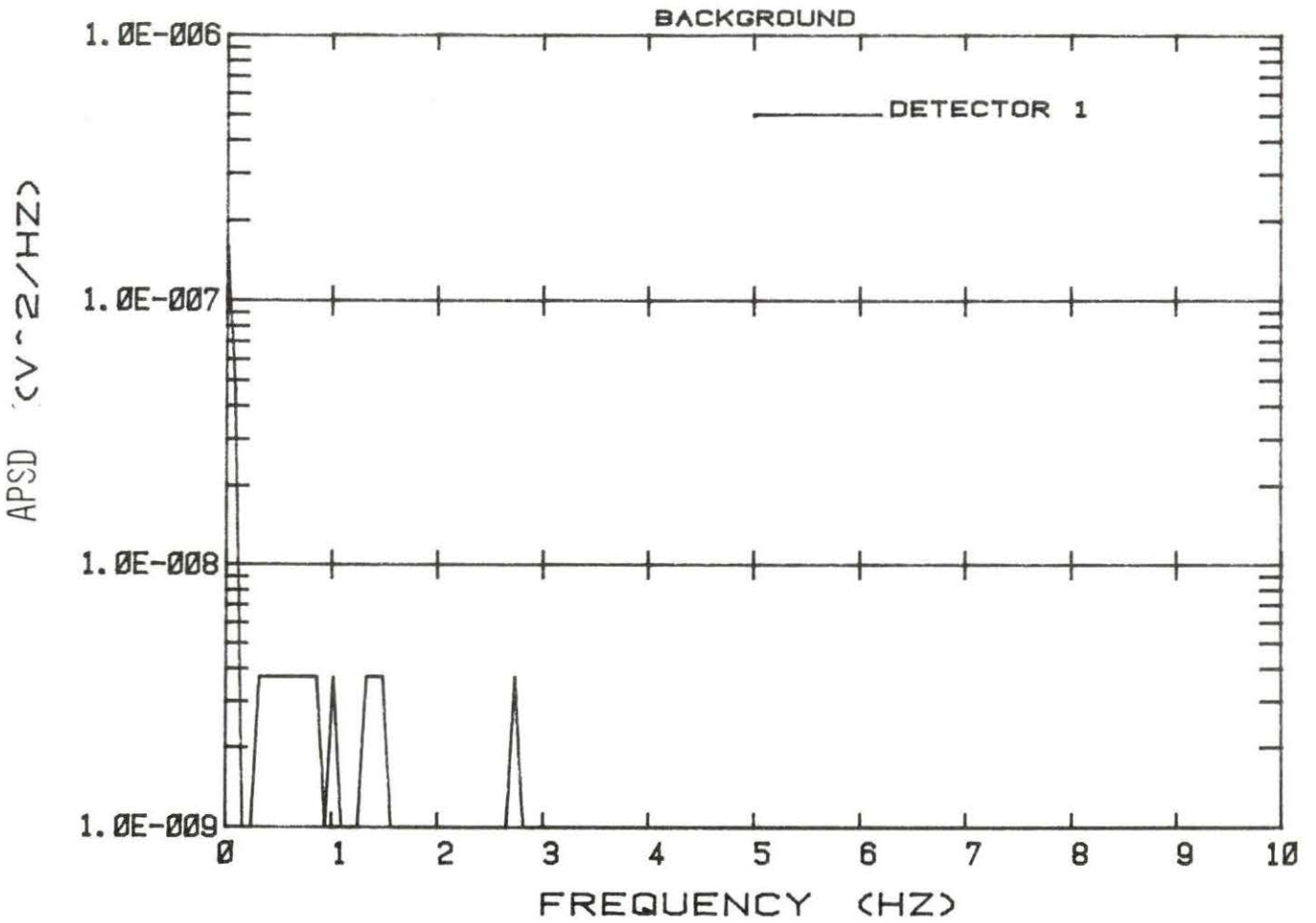

Figure 5.6 APSD of detector 1 background with reactor at 200 watts

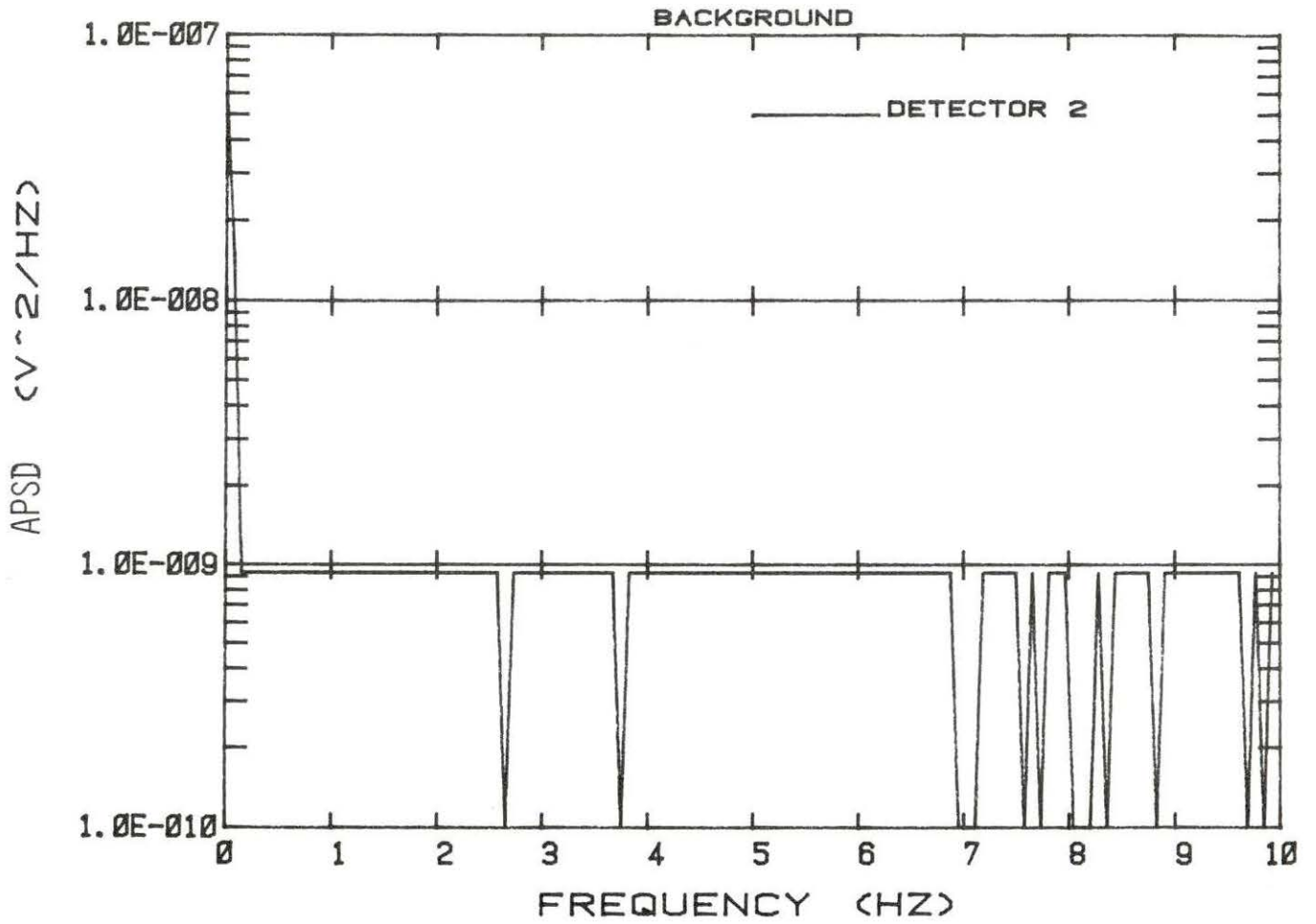

Figure 5.7 APSD of detector 2 with reactor at 200 watts

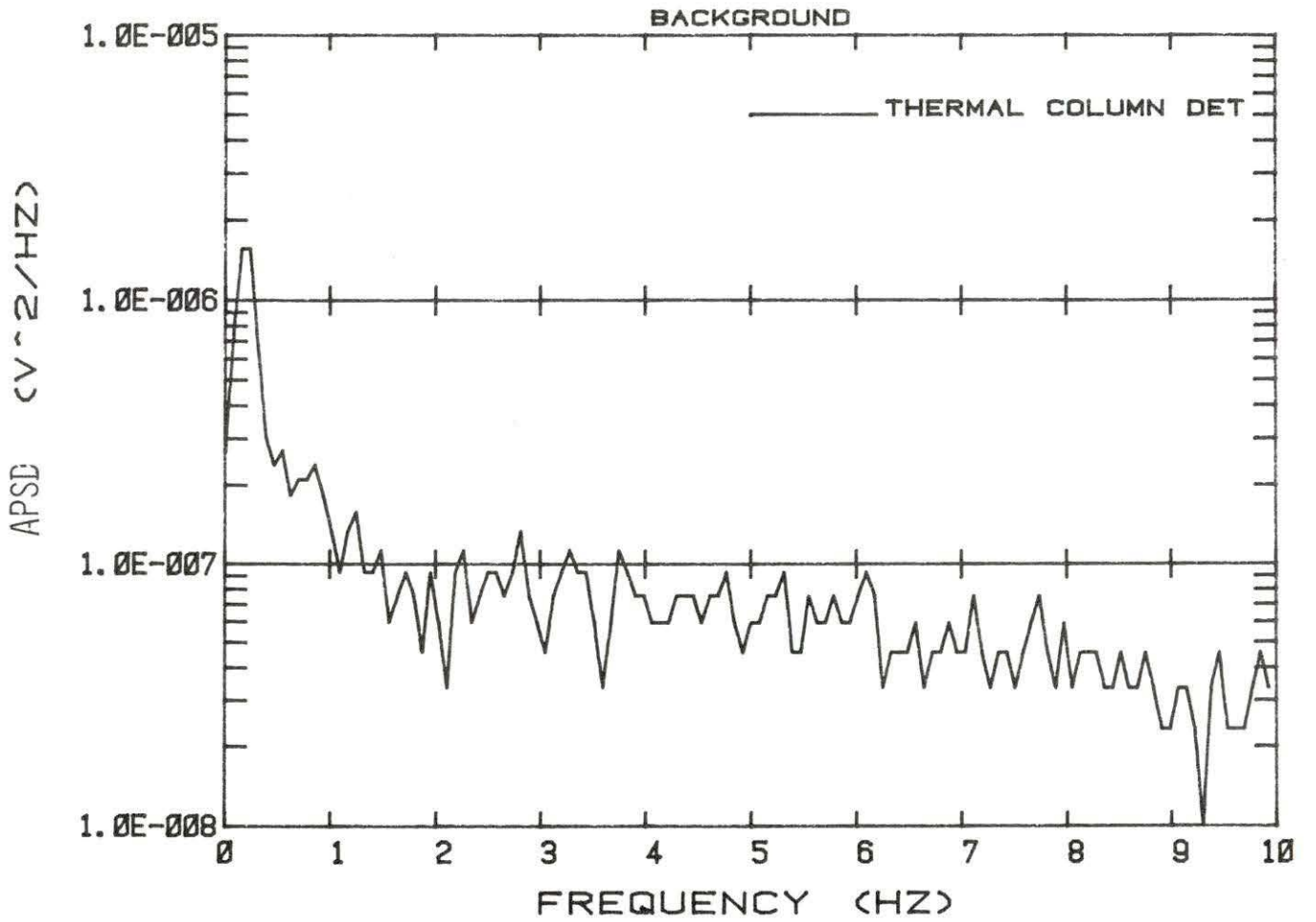

Figure 5.8 APSD of CIC detector with reactor at 200 watts

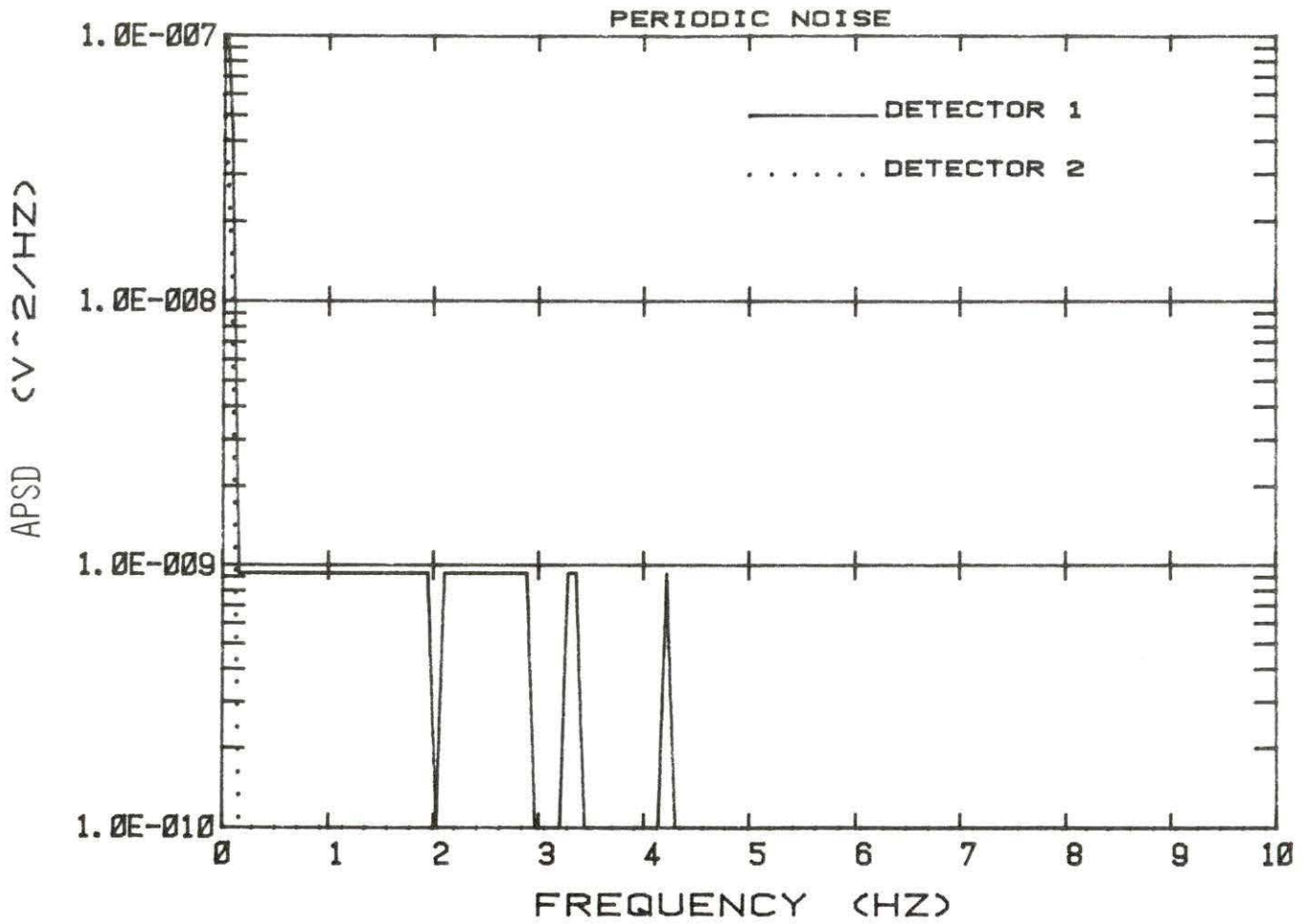

Figure 5.9 APSD of detector 1 and 2 background with reactor shutdown and periodic vibrating absorber motion

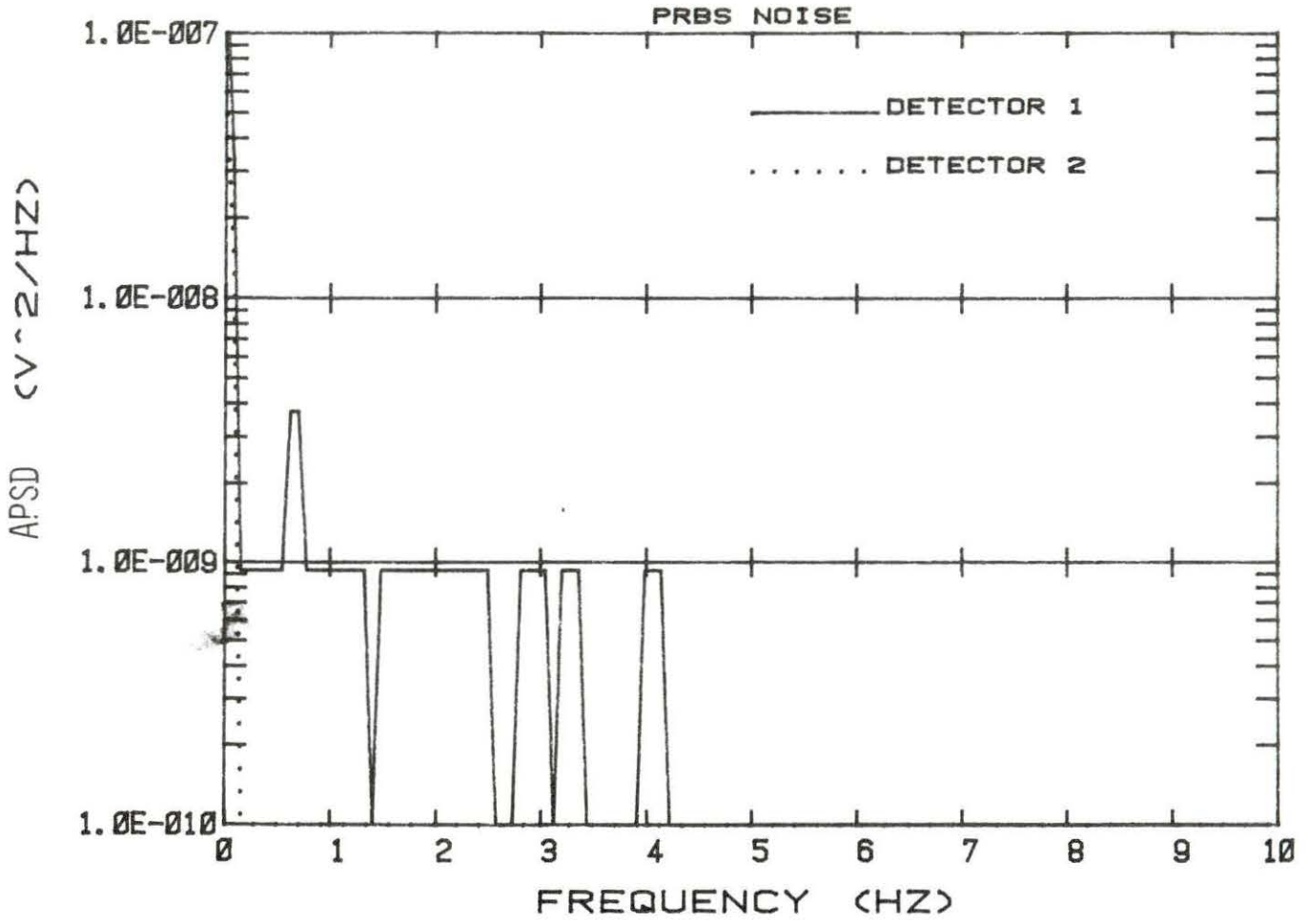

Figure 5.10 APSD of detectors 1 and 2 background with reactor shutdown and PRBS vibrating absorber motion

the coils or other parts of the detection system electronics. An additional check for noise pickup was made by operating the vibrator at 1.5 Hz with the vibrator blocked so that the cadmium strip could not move and with the reactor at 200 W. No indication of a 1.5 Hz response was found in the spectrum of any of the detectors. These plots establish a baseline which indicates a bottom level for determining the usefulness of data. For the BF_3 detectors, this level is approximately 10^{-9} v^2/Hz and for the CIC it is approximately 10^{-7} v^2/Hz.

Figures 5.11 through 5.17 show the APSDs of the three detector signals and the LVDT signal for the 1.5 Hz square wave and PRBS inputs. Several points are interesting to note on these graphs. Figure 5.12 shows the PRBS signal for detectors 1 and 2. The signal for detector 2 is seen to be only at the level of the background, thus, PRBS information from detector 2 is probably meaningless. The same is seen to be true for the CIC. This is because the "power" of the PRBS signal is spread out over a frequency band. The APSDs of each detector signal for the periodic absorber motion are seen to be well-above background levels. The LVDT signal for the PRBS input (Figure 5.17) shows that a frequency band out to about 5 Hz is present in the signal.

Next, the relationships between signals will be discussed. These relationships include phase information, coherences, and CPSDs. Of

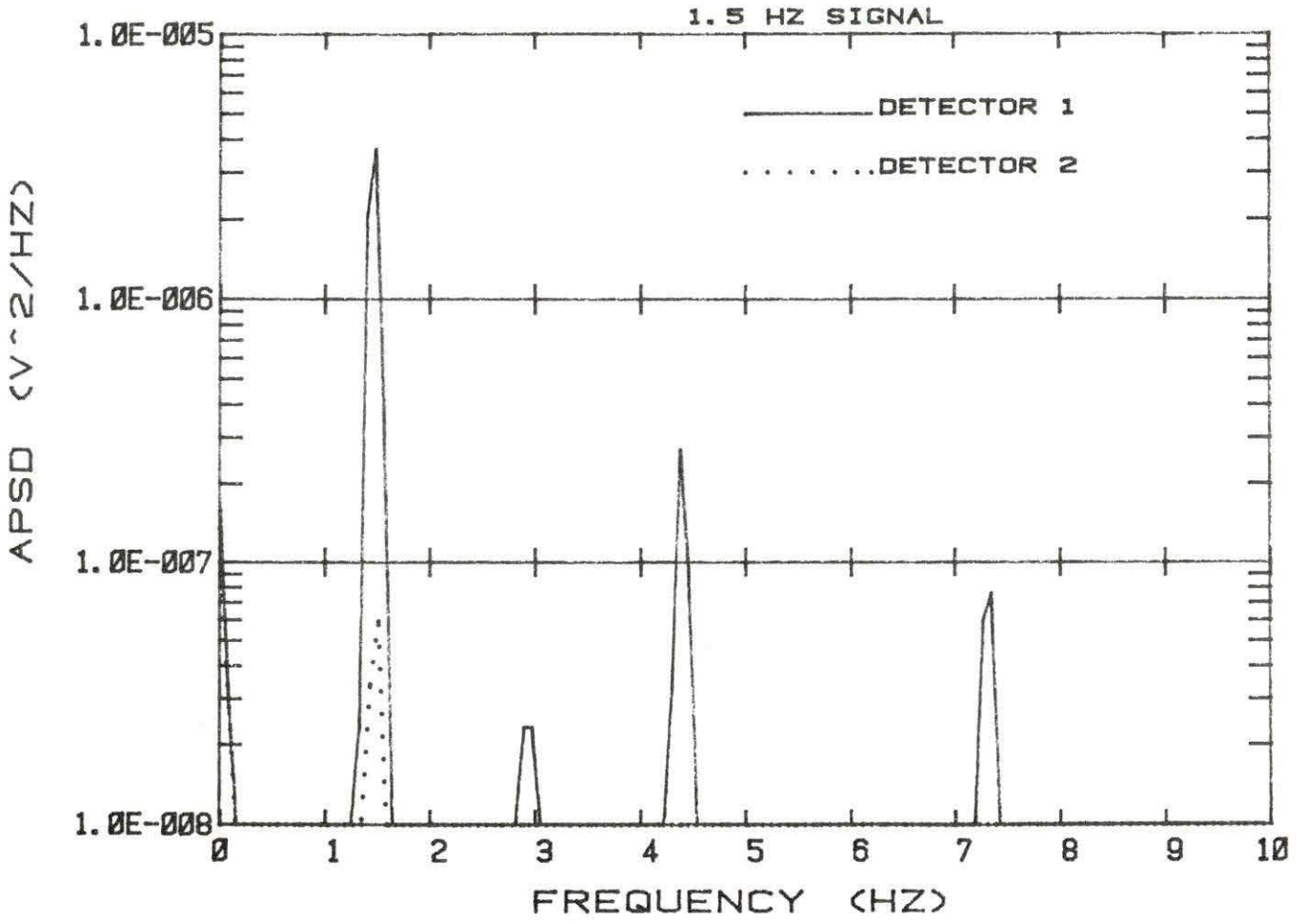

Figure 5.11 APSD of detectors 1 and 2 for a periodic vibrating absorber motion

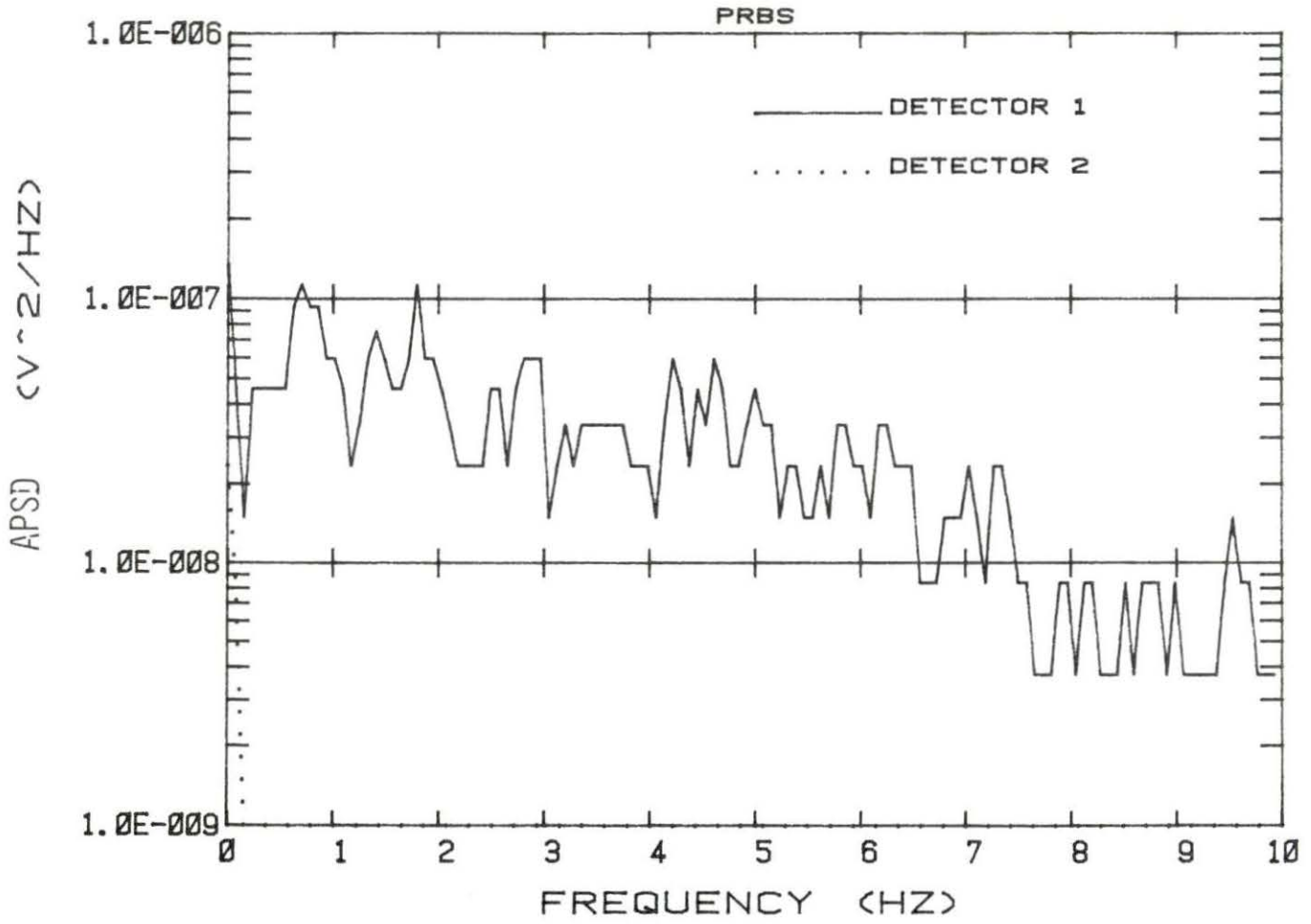

Figure 5.12 APSD of detectors 1 and 2 for a PRBS vibrating absorber motion

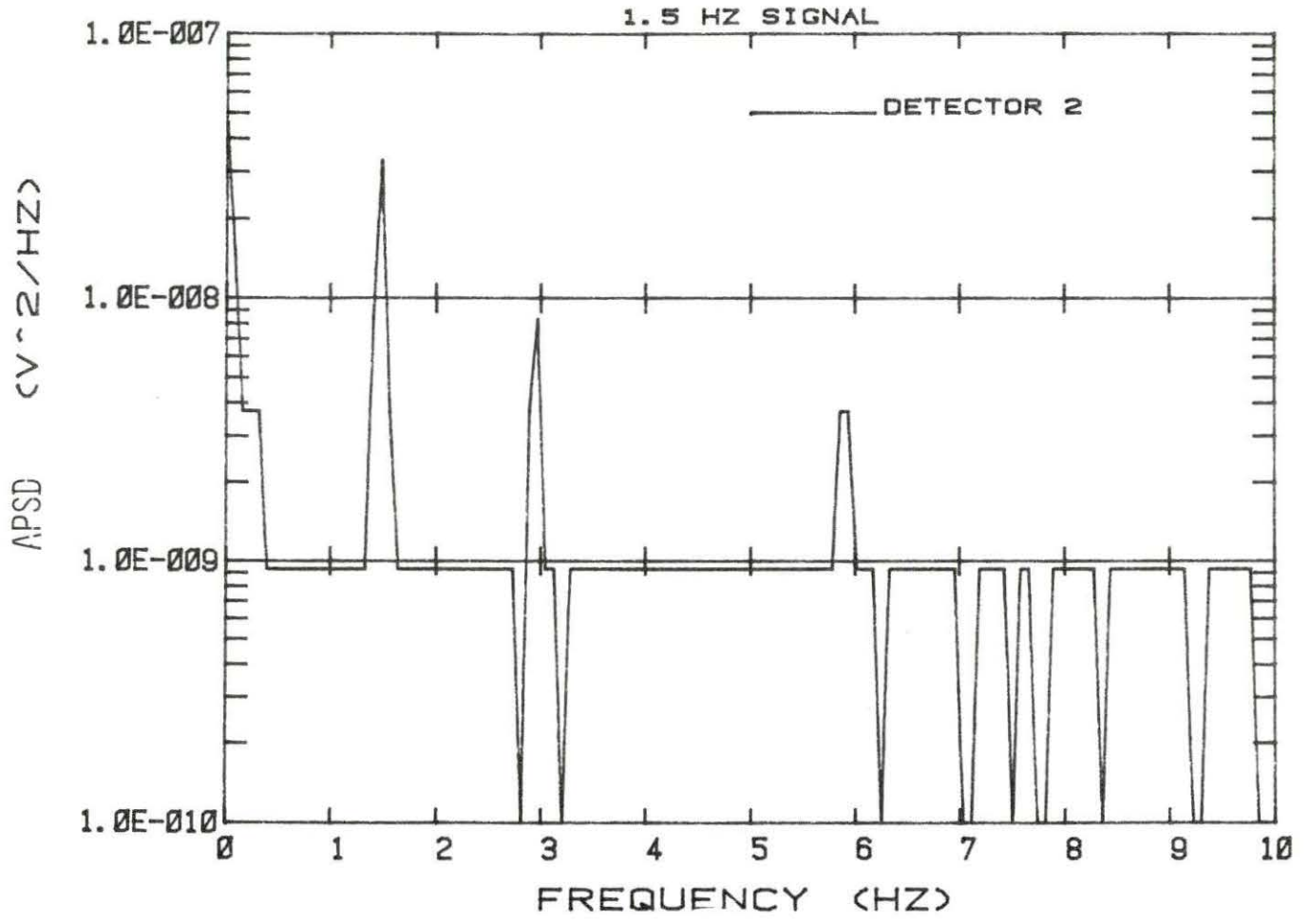

Figure 5.13 APSD of detector 2 for a periodic vibrating absorber motion

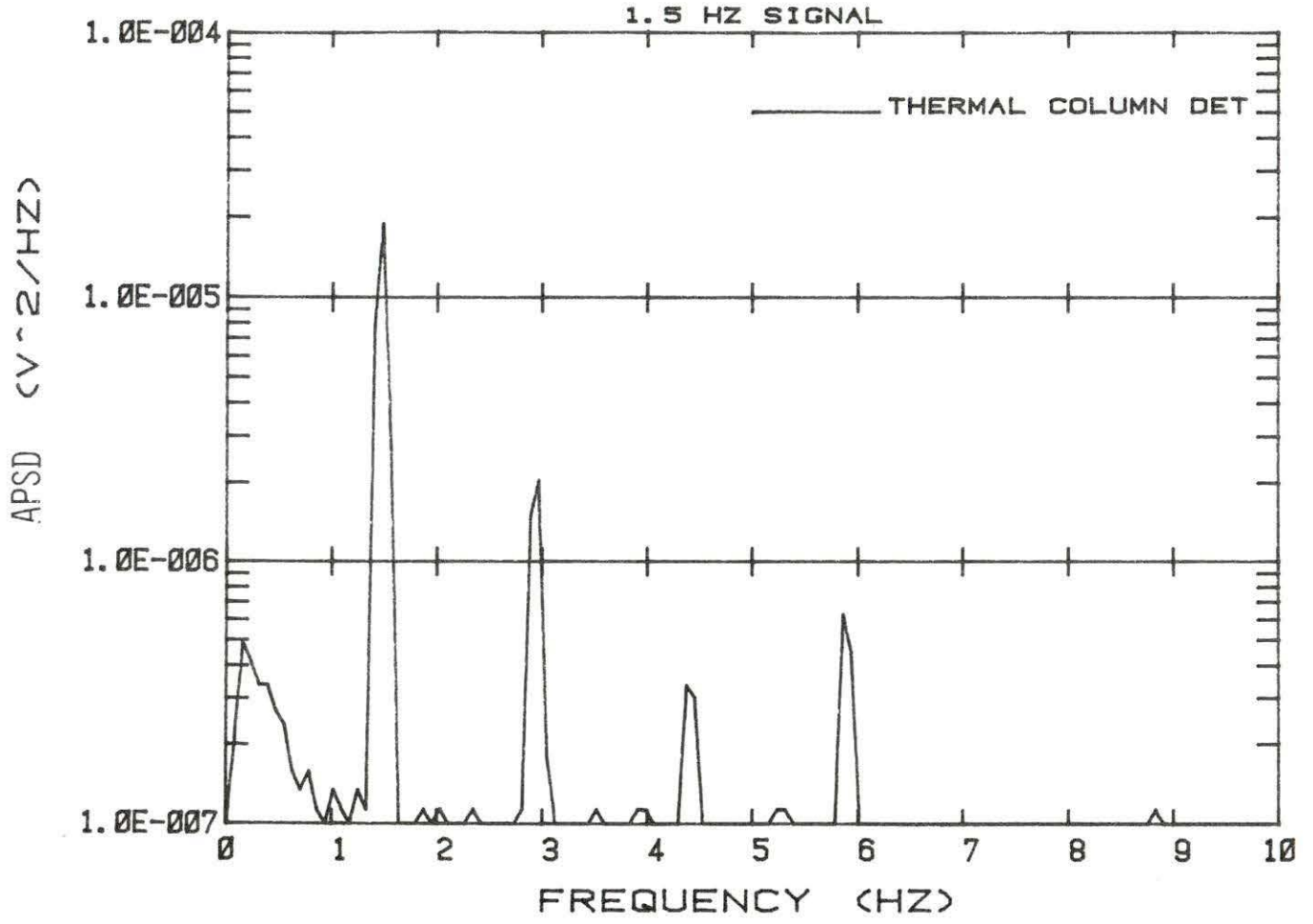

Figure 5.14 APSD of CIC detector for a periodic vibrating absorber motion

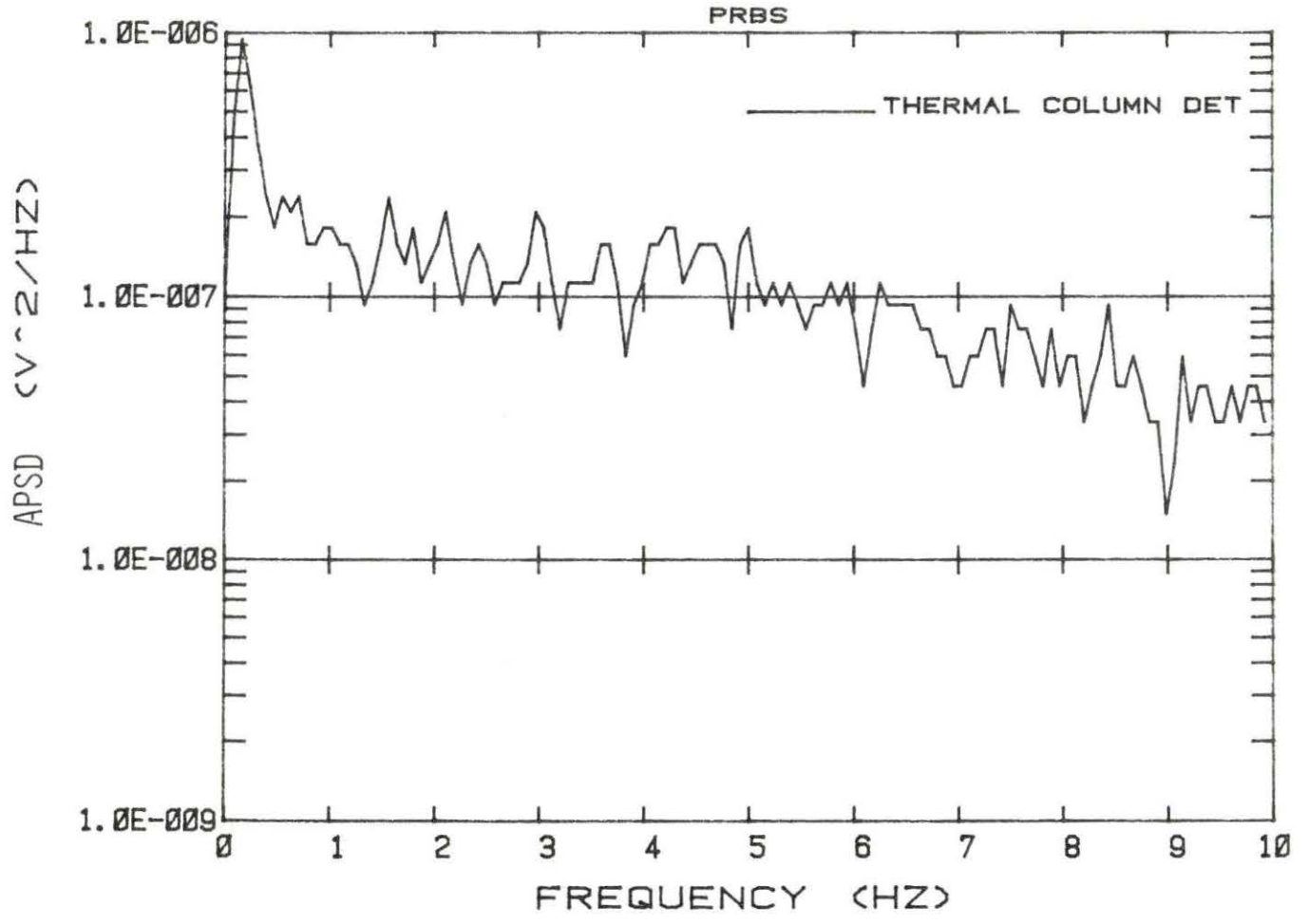

Figure 5.15 APSD of CIC detector for a PRBS vibrating absorber motion

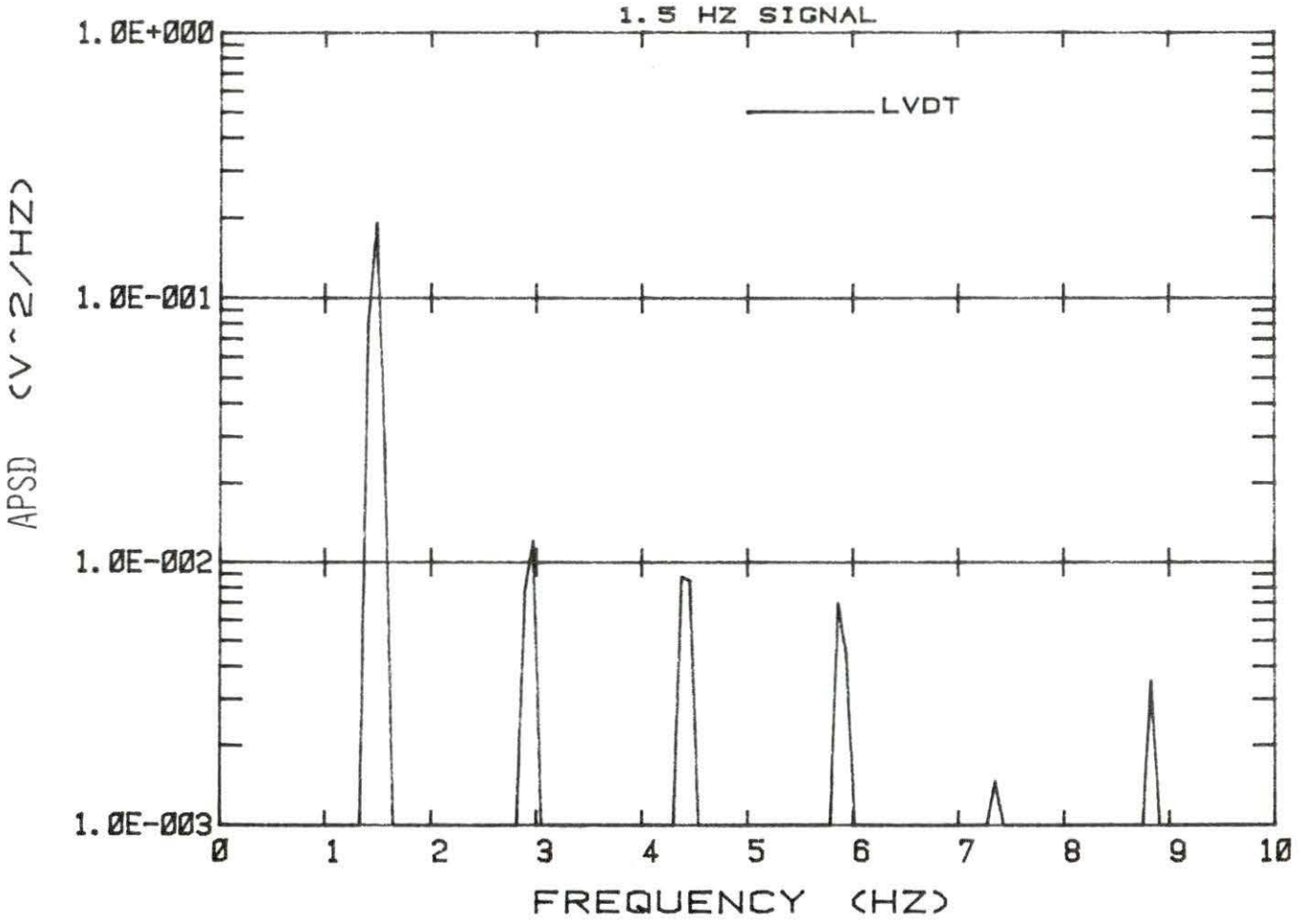

Figure 5.16 APSD of LVDT signal for a periodic vibrating absorber motion

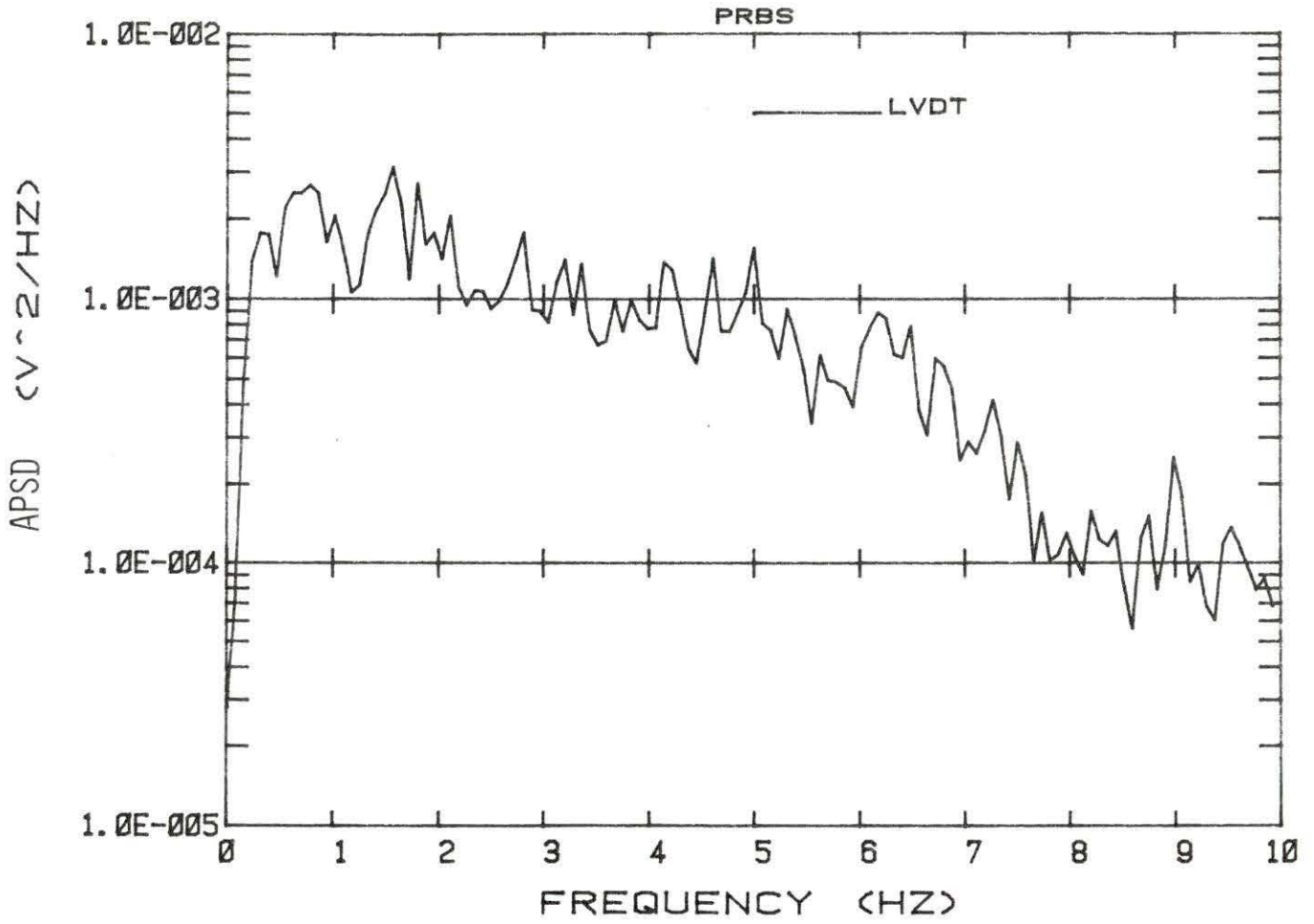

Figure 5.17 APSD of LVDT signal for a PRBS vibrating absorber motion

special interest are the coherence plots. The coherence function is defined as

$$\frac{CPSD_{12}^{\ 2}}{(APSD_1)(APSD_2)} \quad , \tag{5.1}$$

The coherence function provides a measure of how well two signals are correlated. A coherence of greater then 0.5 indicates strong correlation with a coherence of 1.0 being complete correlation. All phase information was found to be as expected, with detector 1 180^{o} out of phase with detector 2, the CIC, and LVDT. CPSD plots are used to show the relationship between signals as a function of frequency as seen by two detectors or a detector and the LVDT.

The Figures 5.18 through 5.23 show the phase, coherence, and CPSD information between detector 1 and detector 2. Figures 5.18 and 5.19 show the coherence functions for 1.5 Hz and PRBS inputs, respectively. The periodic signals are strongly coherent at the fundamental frequency and its harmonics but the PRBS case shows a very small coherence. This indicates that PRBS information for this combination of signals is essentially meaningless. The phase plots, Figures 5.20 and 5.21 show the expected 180^{o} phase shift for the periodic signal. No information can be inferred from the phase plots of the PRBS signal because of the very small coherence. The CPSD plots (Figures 5.22 and 5.23) show a strong signal for the periodic input; the PRBS CPSD is, however, not very meaningful.

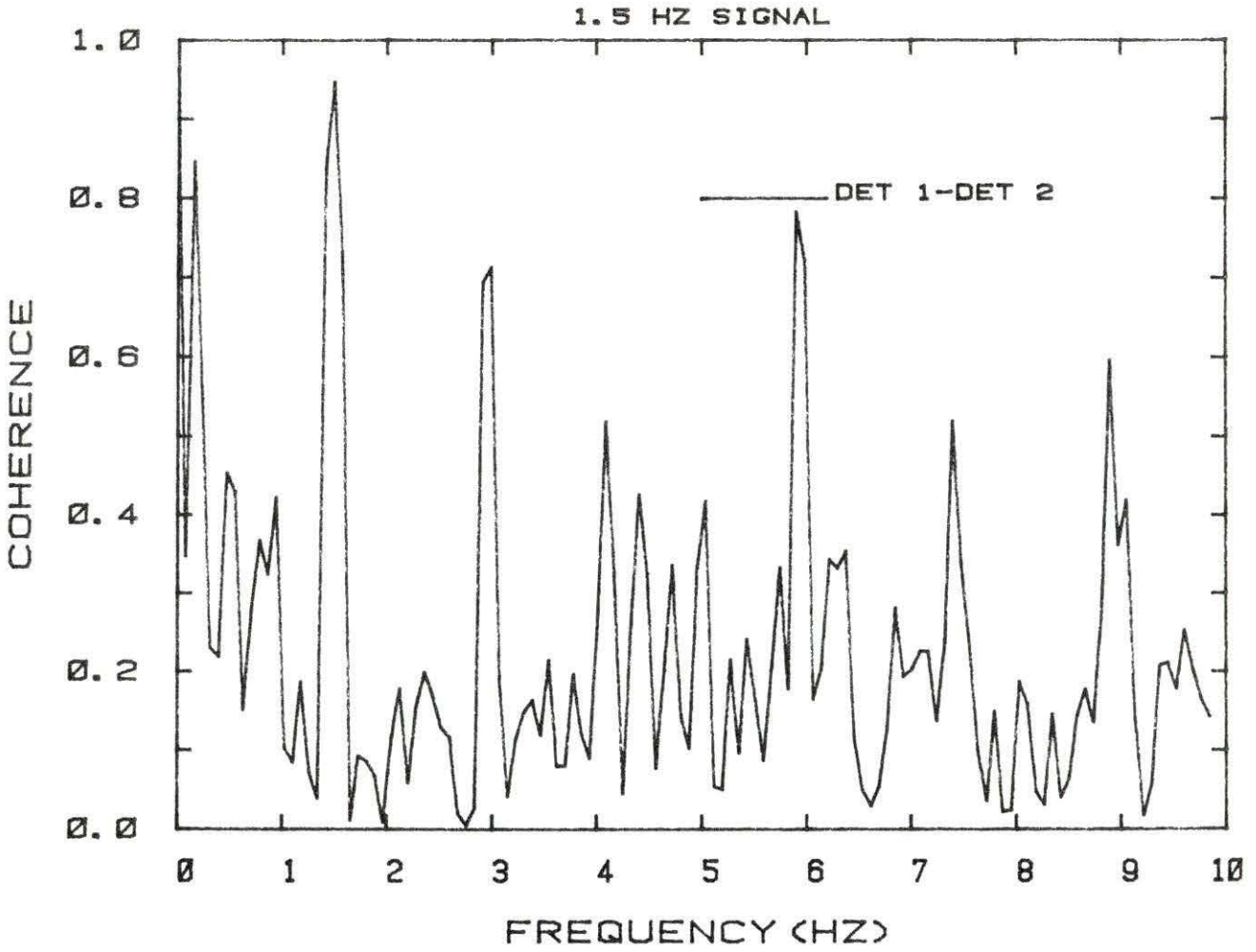

Figure 5.18 Detector 1 - detector 2 coherence for a periodic vibrating absorber motion

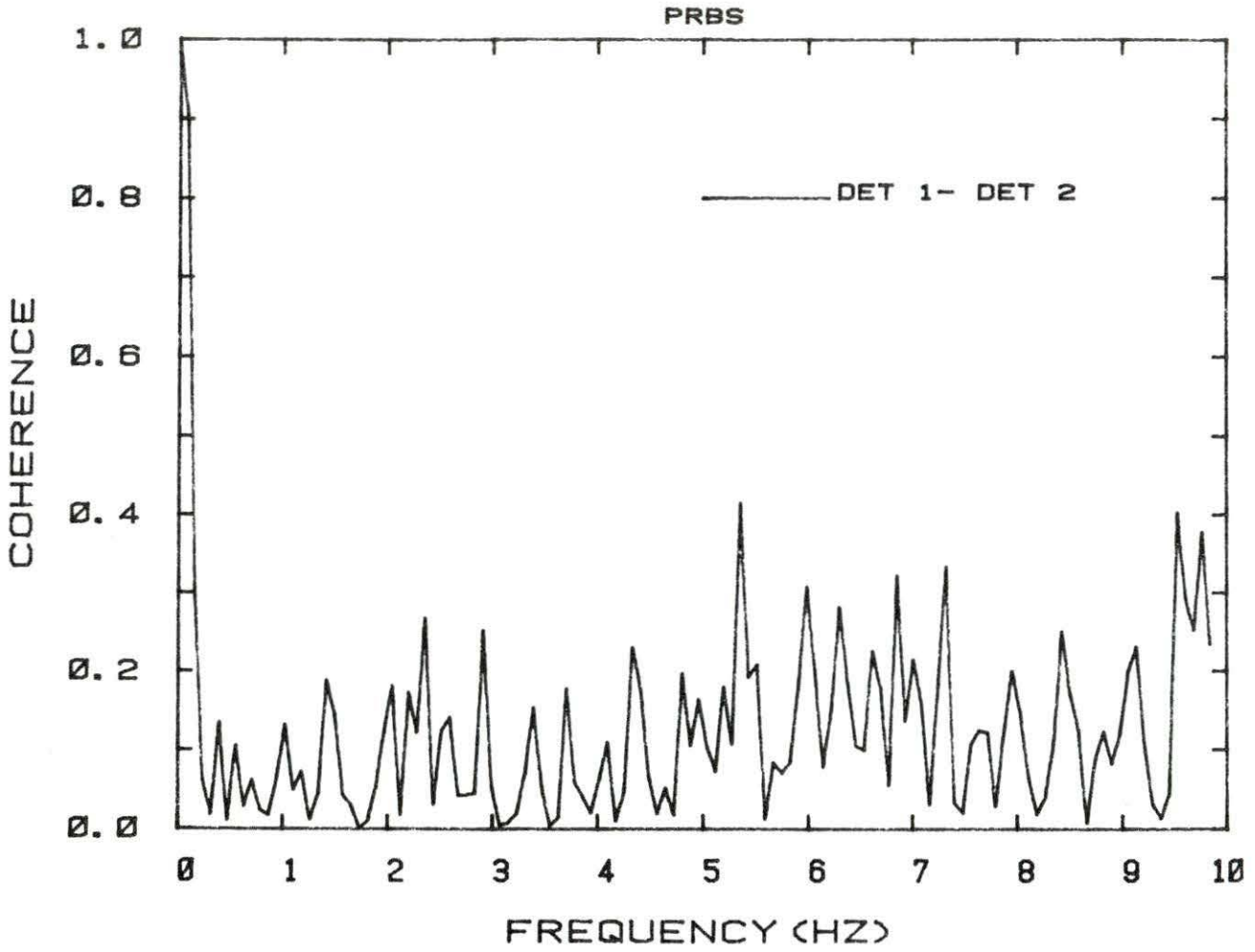

Figure 5.19 Detector 1 - detector 2 coherence for a PRBS vibrating absorber motion

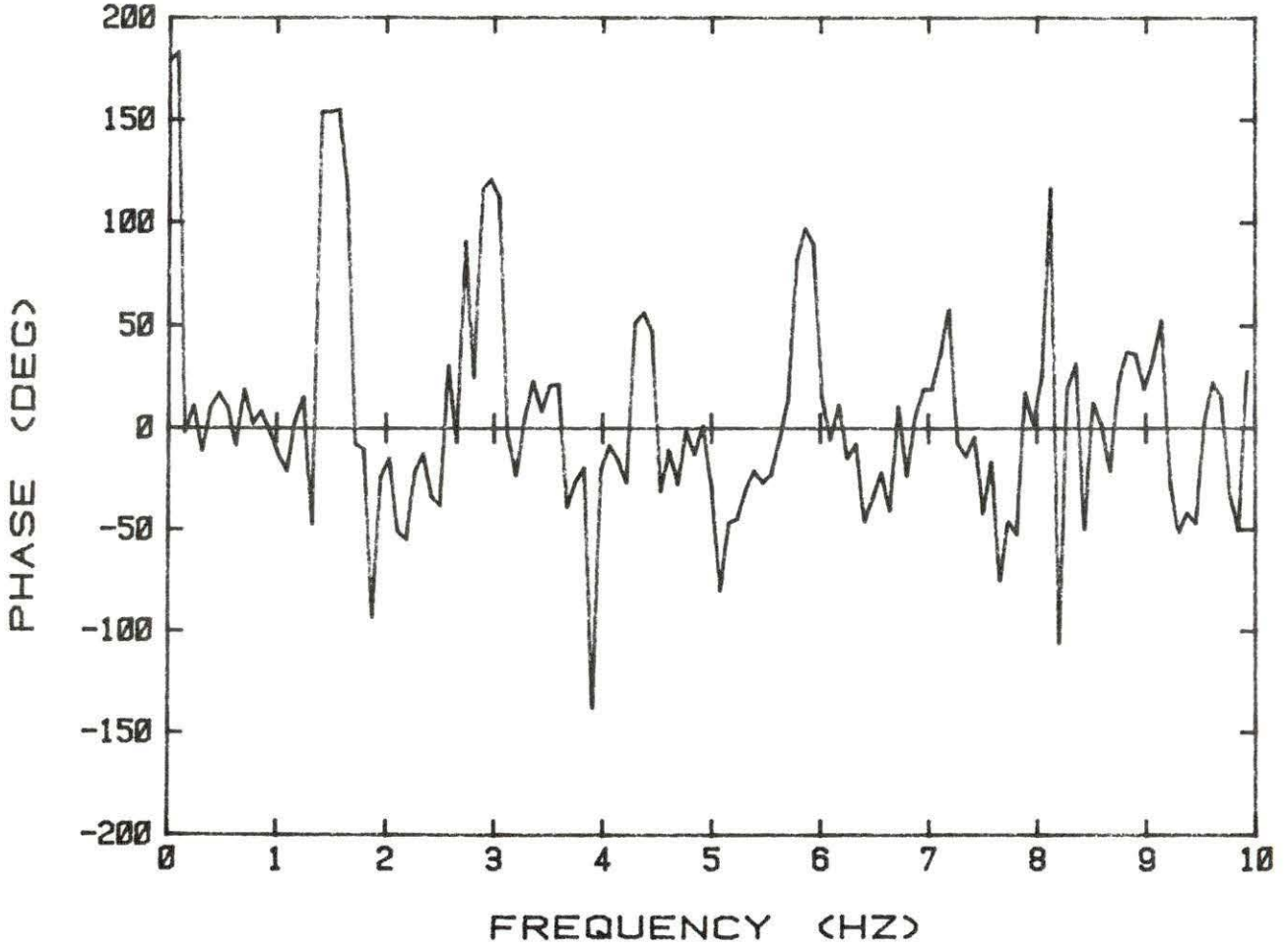

Figure 5.20 Detector 1 - detector 2 phase for periodic vibrating absorber motion

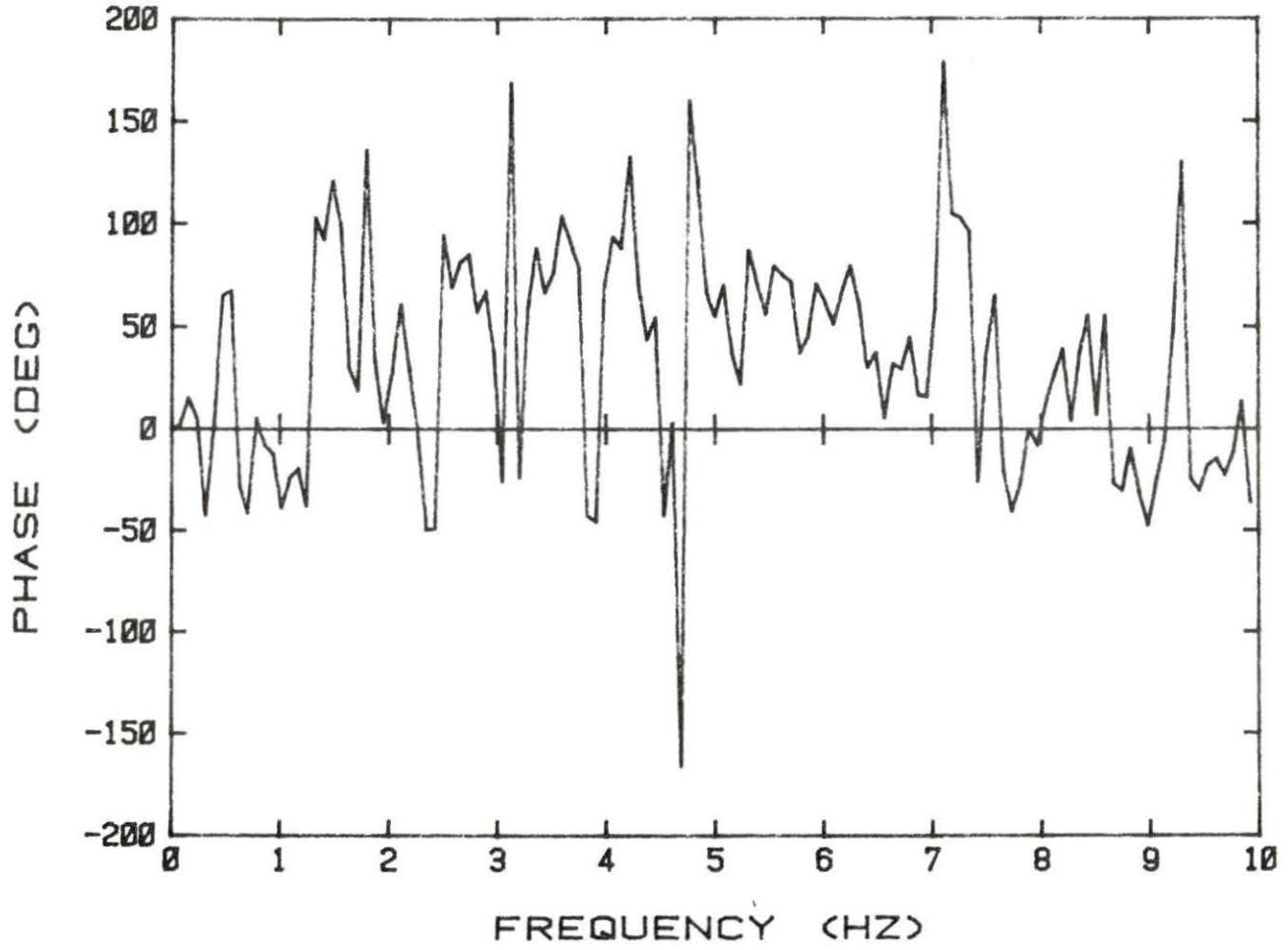

Figure 5.21 Detector 1 - detector 2 phase for PRBS vibrating absorber motion

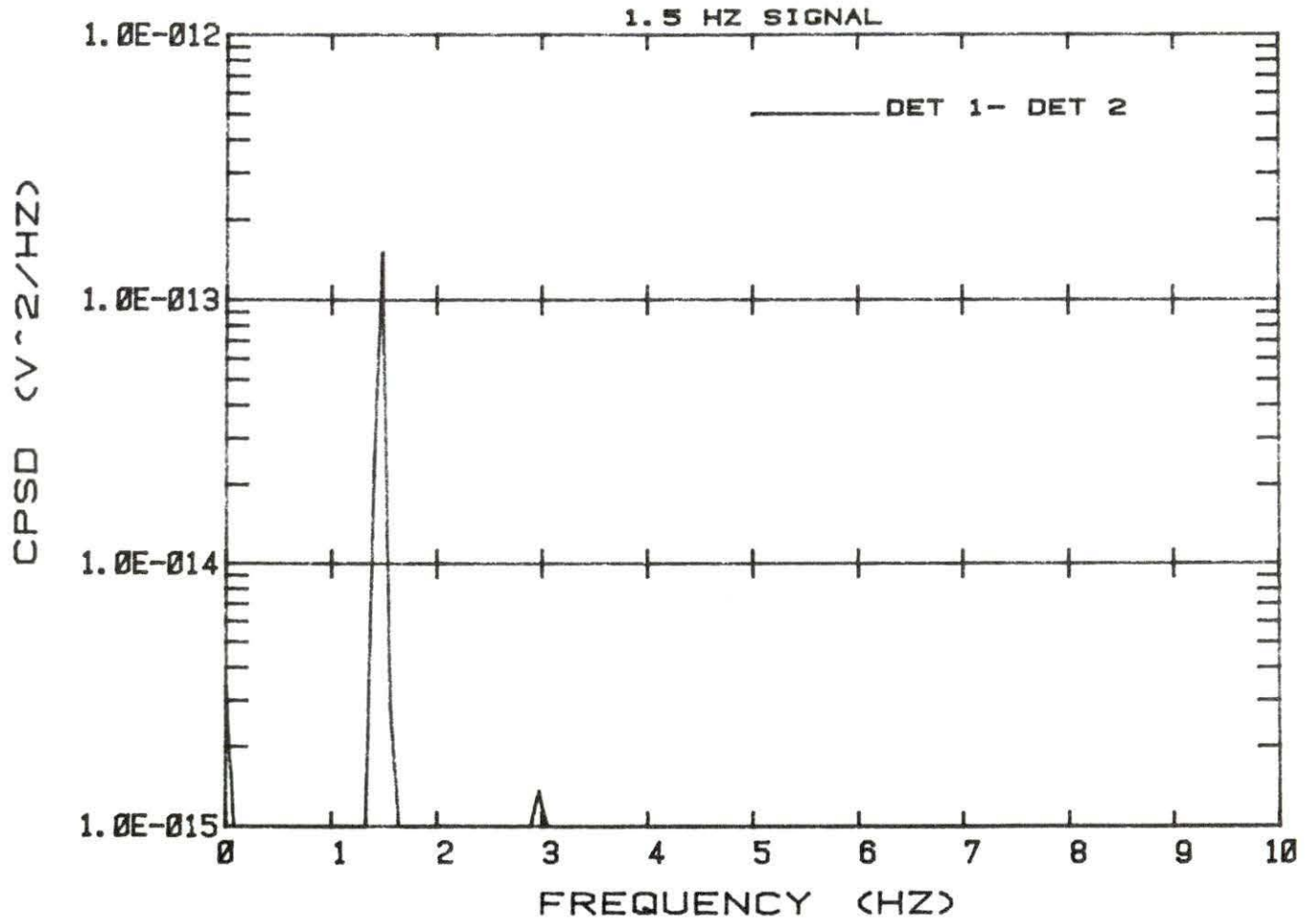

Figure 5.22 Detector 1 - detector 2 CPSD for PRBS vibrating absorber motion

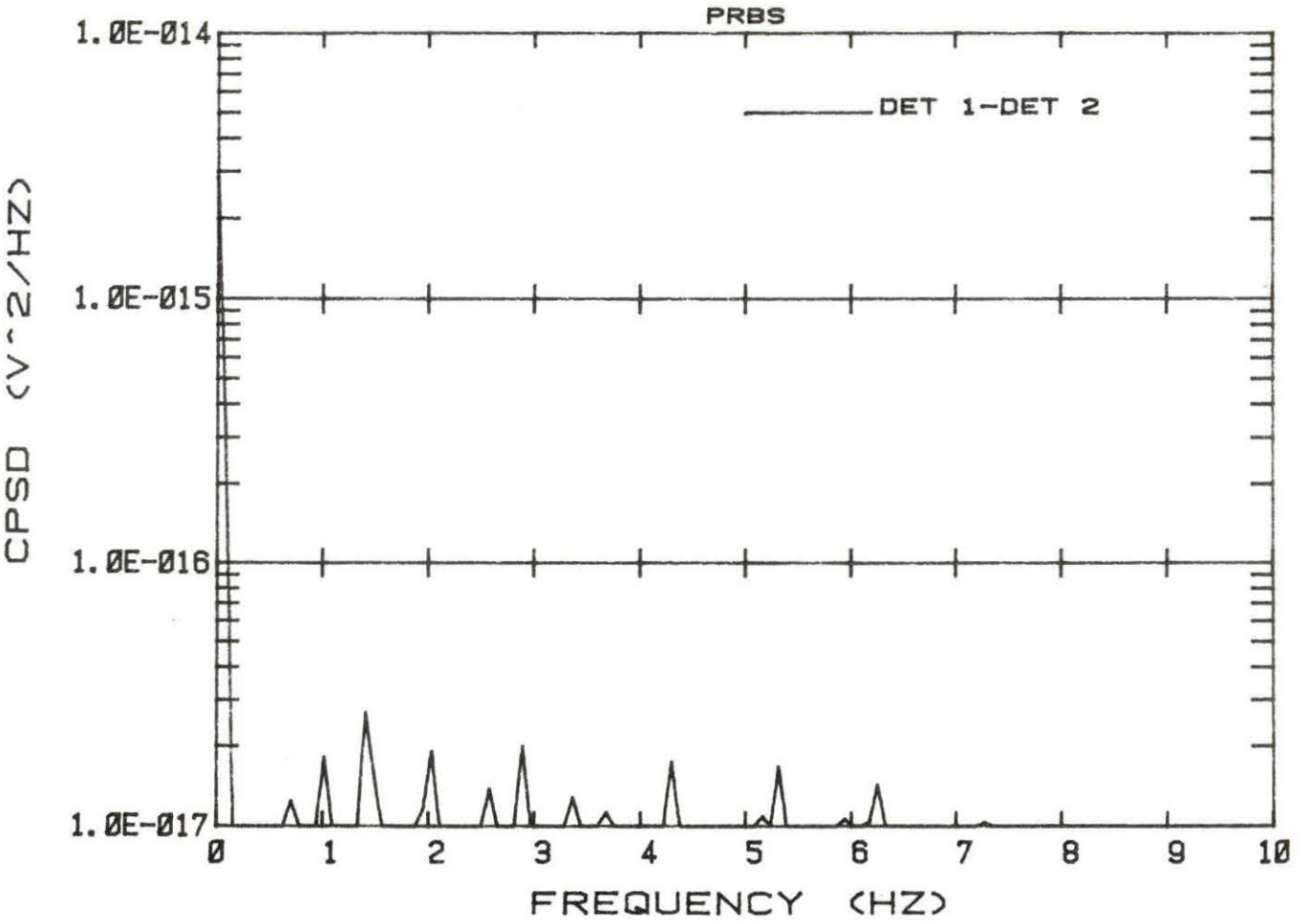

Figure 5.23 Detector 1 - detector 2 CPSD for PRBS vibrating absorber motion

Figures 5.24 through 5.29 show the detector 1 - CIC detector signal combinations. The coherence for the periodic input (Figure 5.24) shows a very strong correlation and the coherence of the PRBS (Figure 5.25) is low but larger than for the detector 1, detector 2 combination. The common induced components in the signals apparently are strong enough to contain some information. As expected, the phase plots (Figures 5.26 and 5.27) show the 180^{o} phase shift for both the 1.5 Hz and PRBS signals. At this time, it is necessary to note that when the spectrum analyzer sees a phase shift of more than 180^{o}, it flips the signal to the opposite sign. These phenomena can be seen in Figure 5.27 around 1 Hz and, in general, other phase plots. A comparison of the CPSDs (Figures 5.28 and 5.29) shows that the PRBS case generates considerably less common responses in the two signals than the periodic input.

The next set of graphs, Figures 5.30 through 5.35, show the detector 1 - LVDT signal combinations. These signals show the strongest relationship of the experiment. Strong coherence is seen (Figures 5.30 and 5.31) for both the periodic signals and the PRBS. The phase graphs (Figures 5.32 and 5.33) show the 180^{o} phase shift between the signals as expected.

Figures 5.36 through 5.41 are for the detector 2 - CIC detector combinations. The coherences, Figures 5.36 and 5.37, show trends similar to those previously observed with the periodic input having a stronger coherence than the PRBS input. Both the periodic and

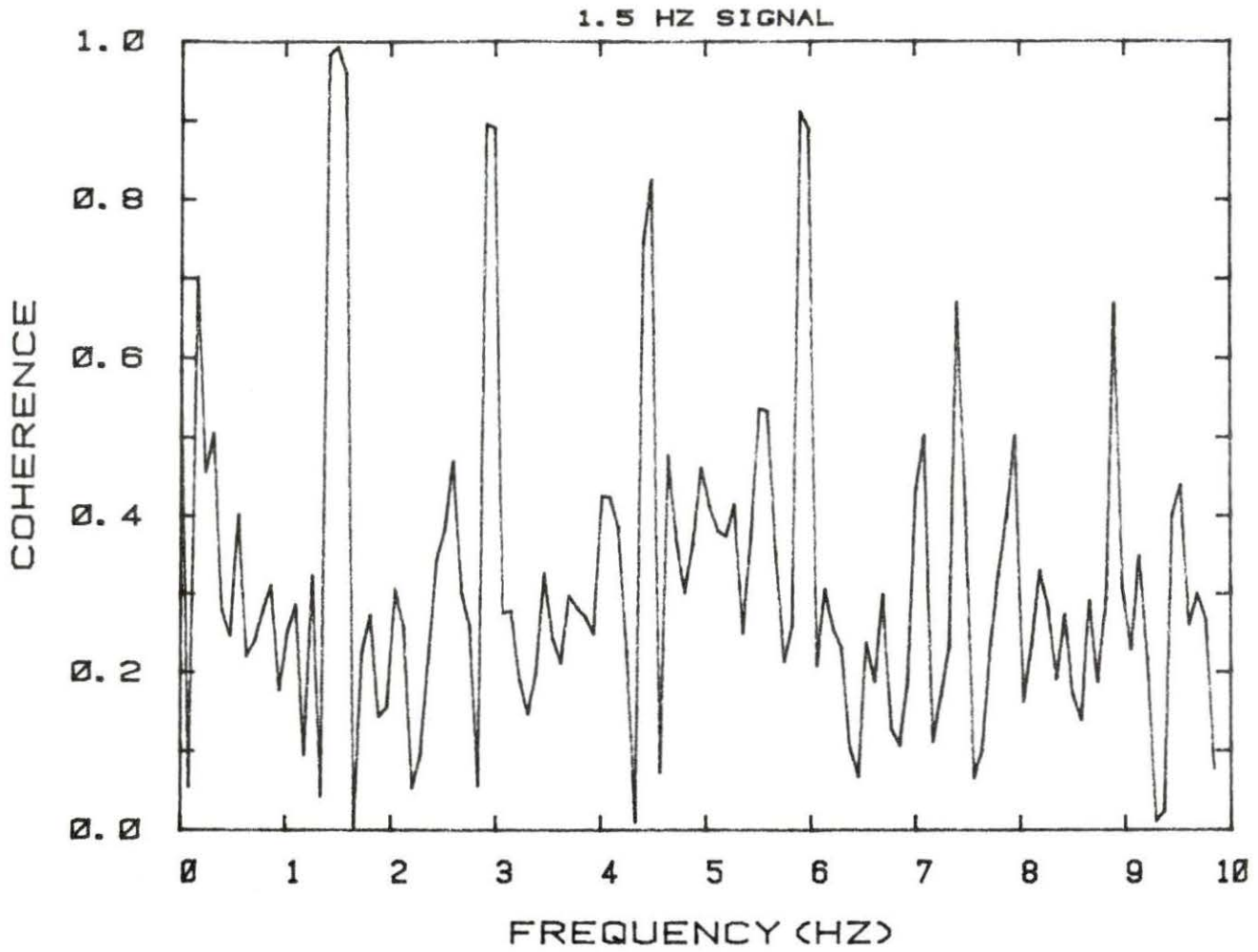

Figure 5.24 Detector 1 - CIC detector coherence for periodic vibrating absorber motion

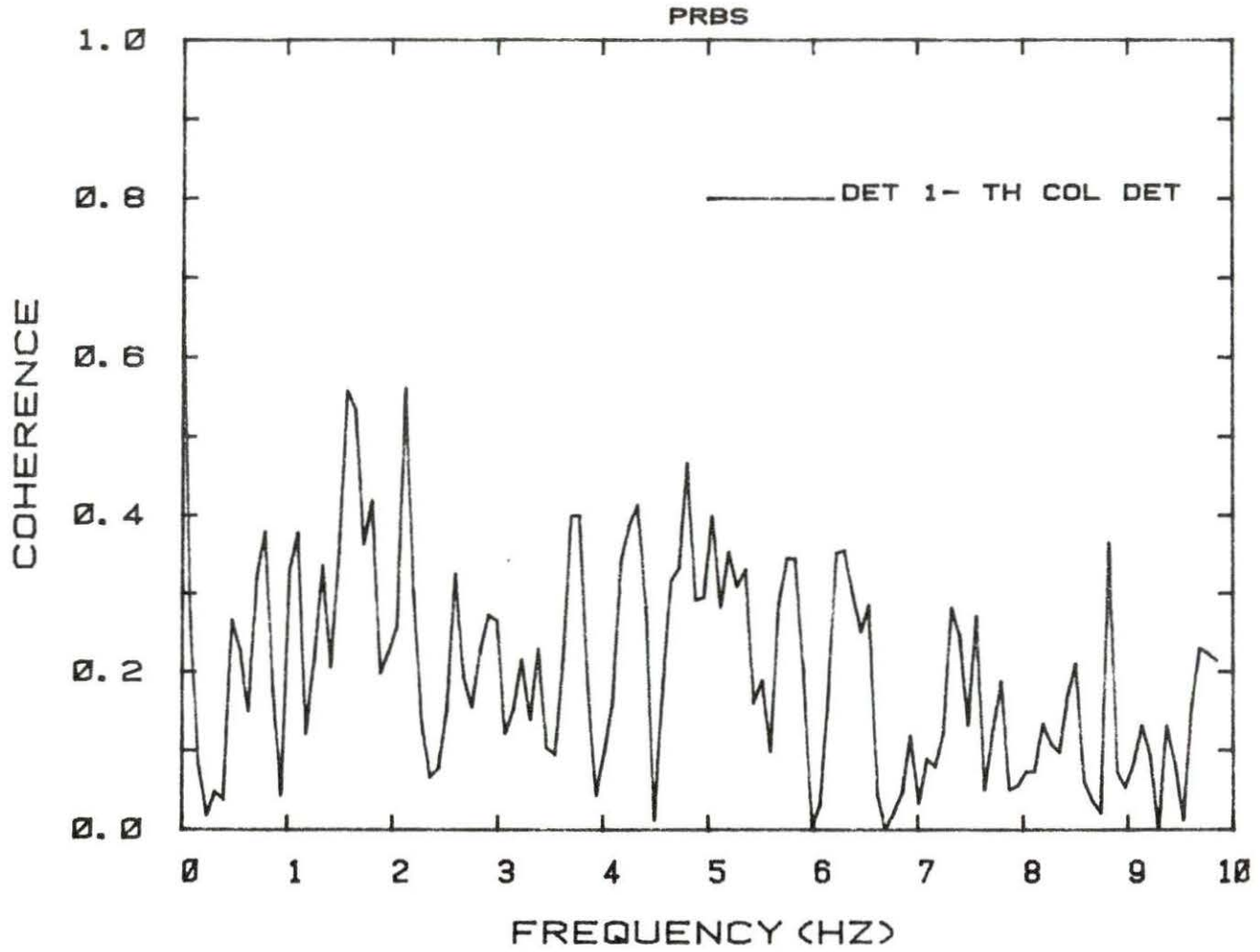

Figure 5.25 Detector 1 - CIC detector coherence for PRBS vibrating absorber motion

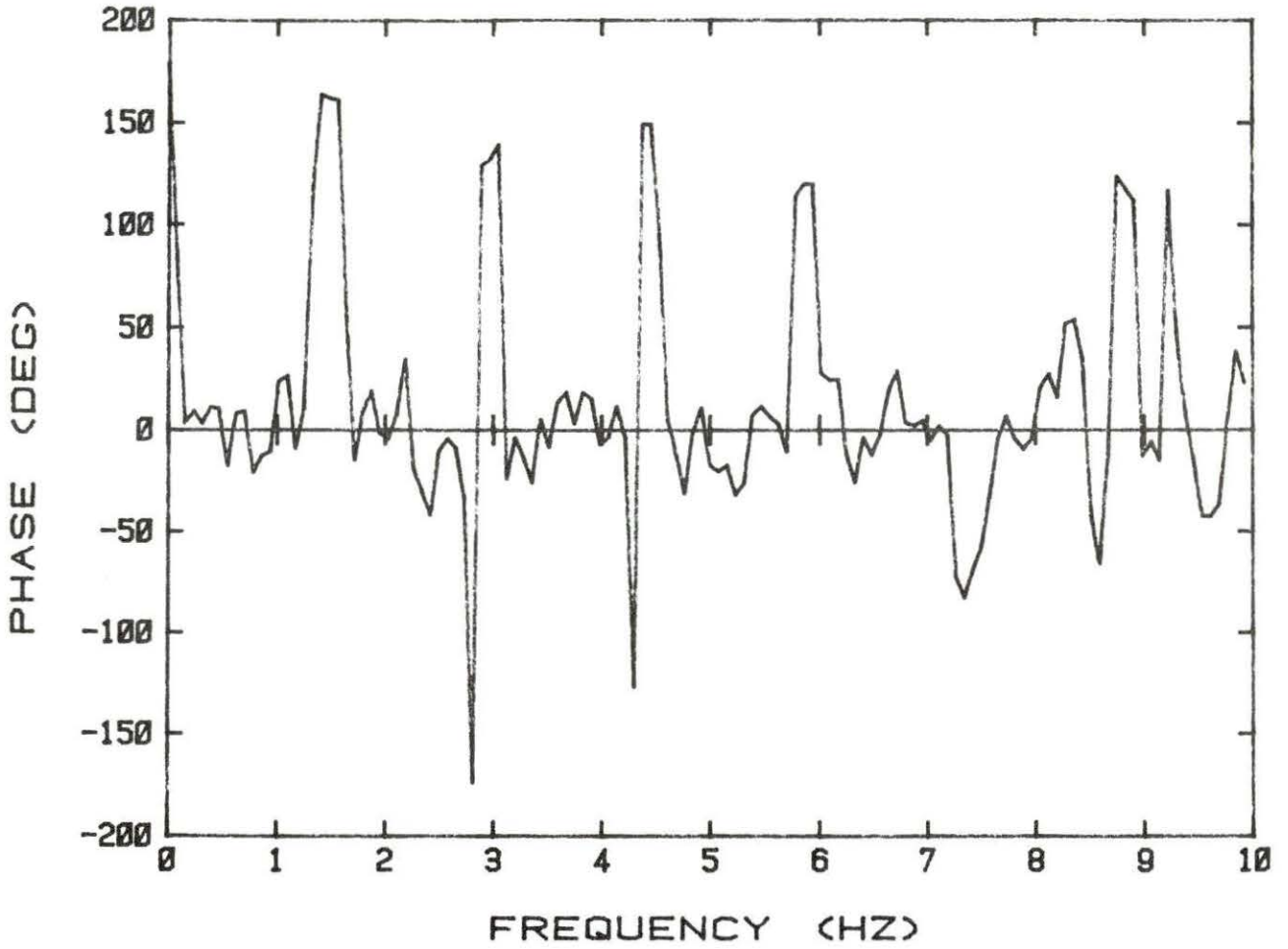

Figure 5.26 Detector 1 - CIC detector phase for periodic vibrating absorber motion

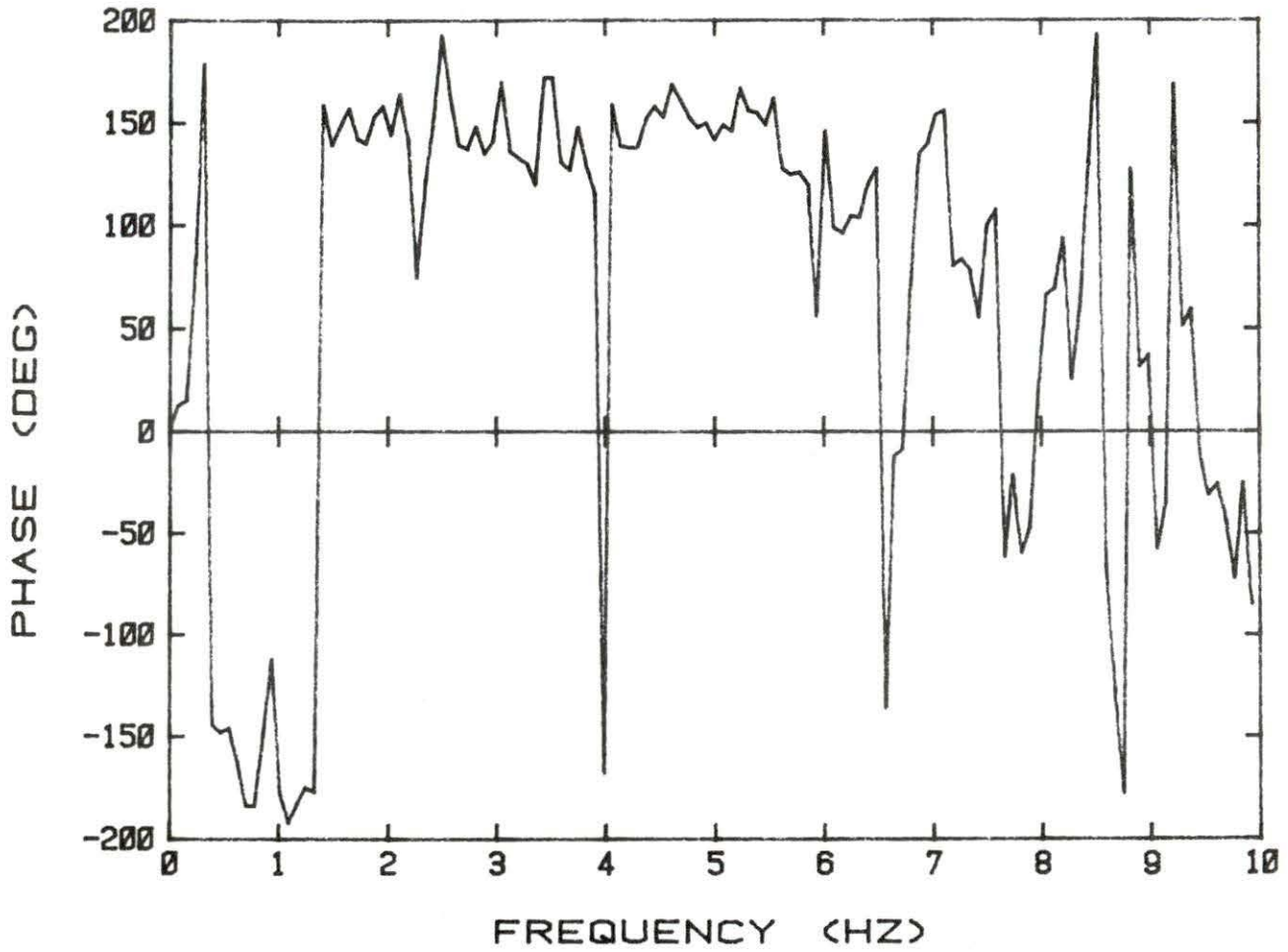

Figure 5.27 Detector 1 - CIC detector phase for PRBS vibrating absorber motion

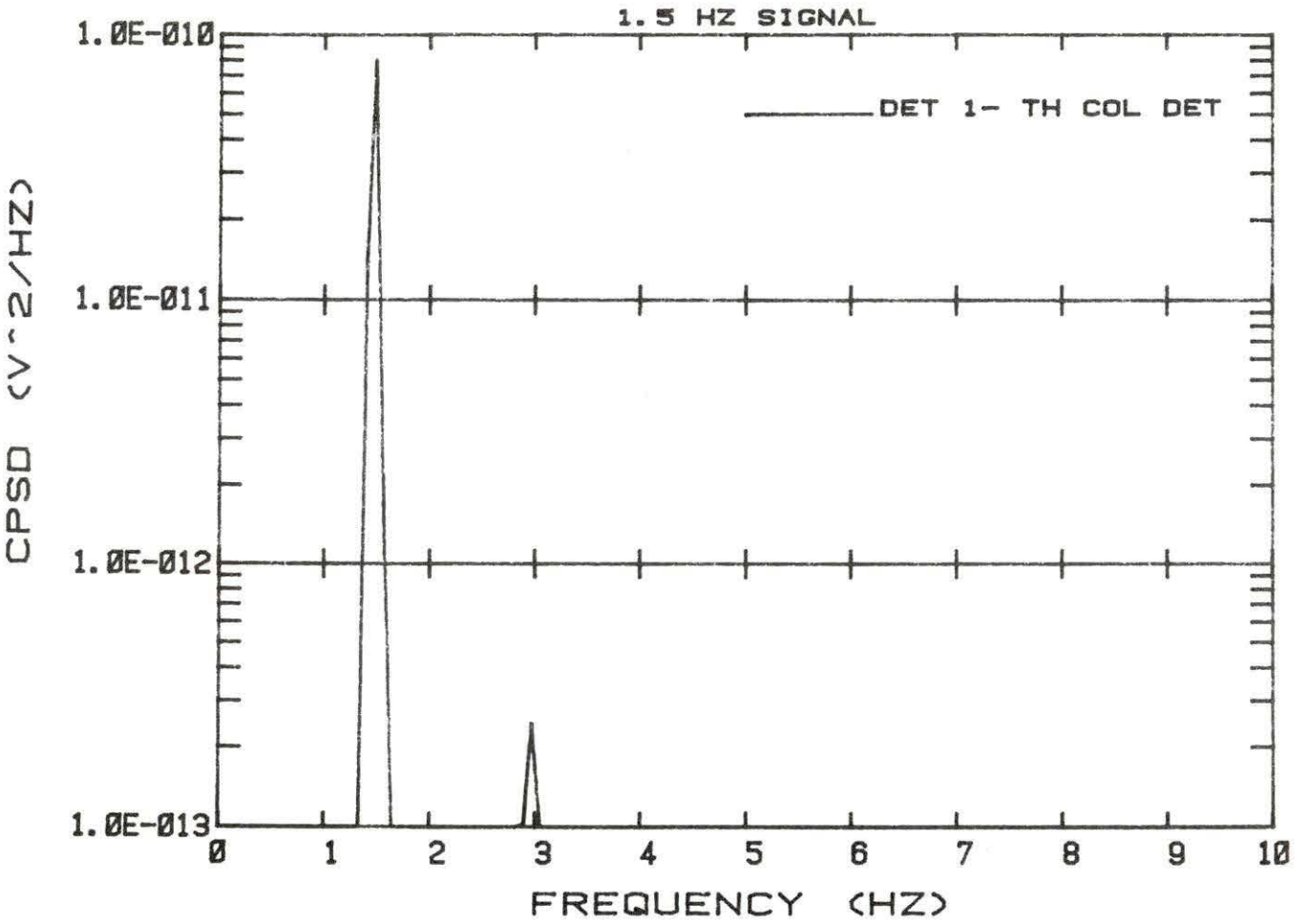

Figure 5.28 Detector 1 - CIC detector CPSD for periodic vibrating absorber motion

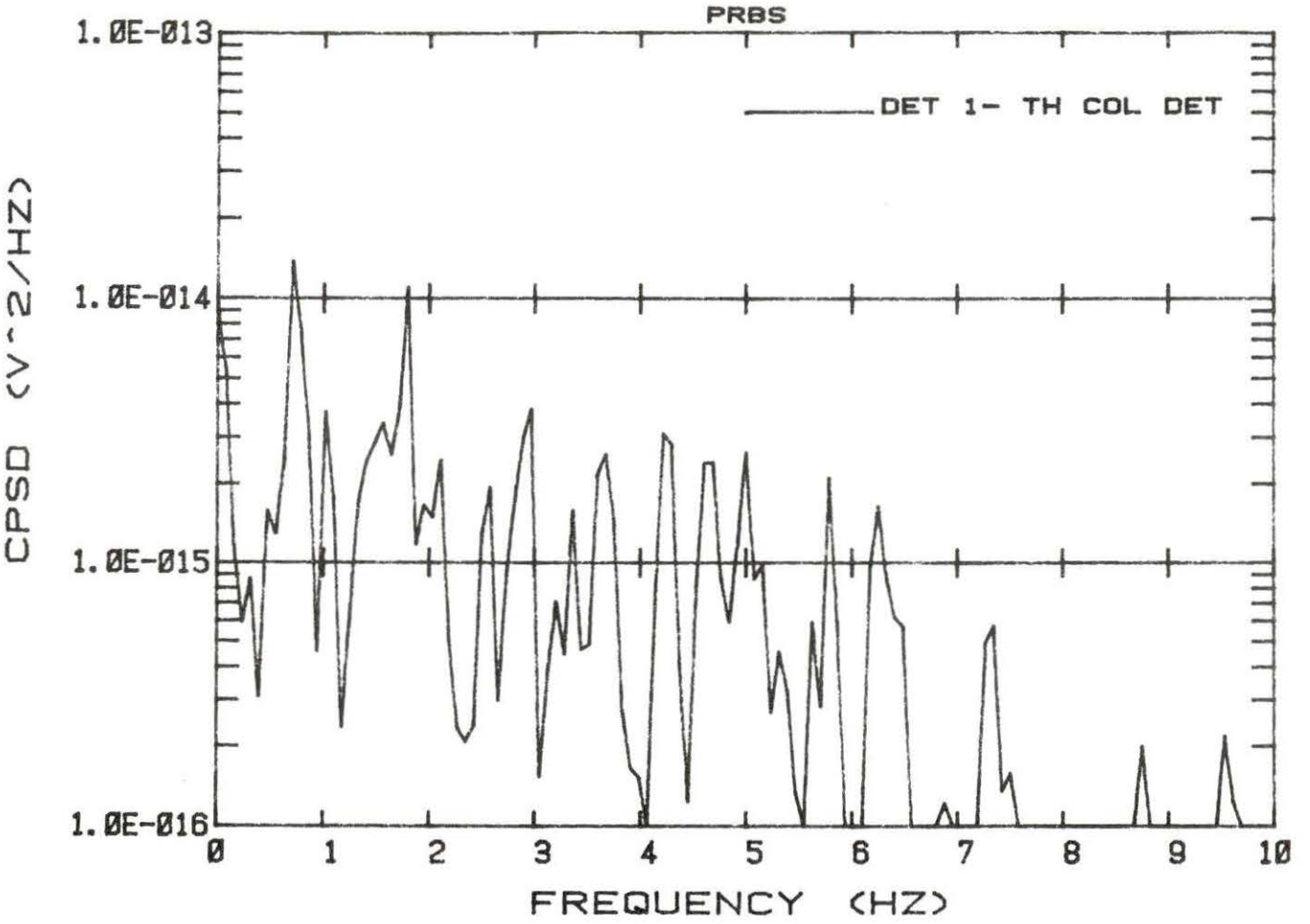

Figure 5.29 Detector 1 - CIC detector CPSD for PRBS vibrating absorber motion

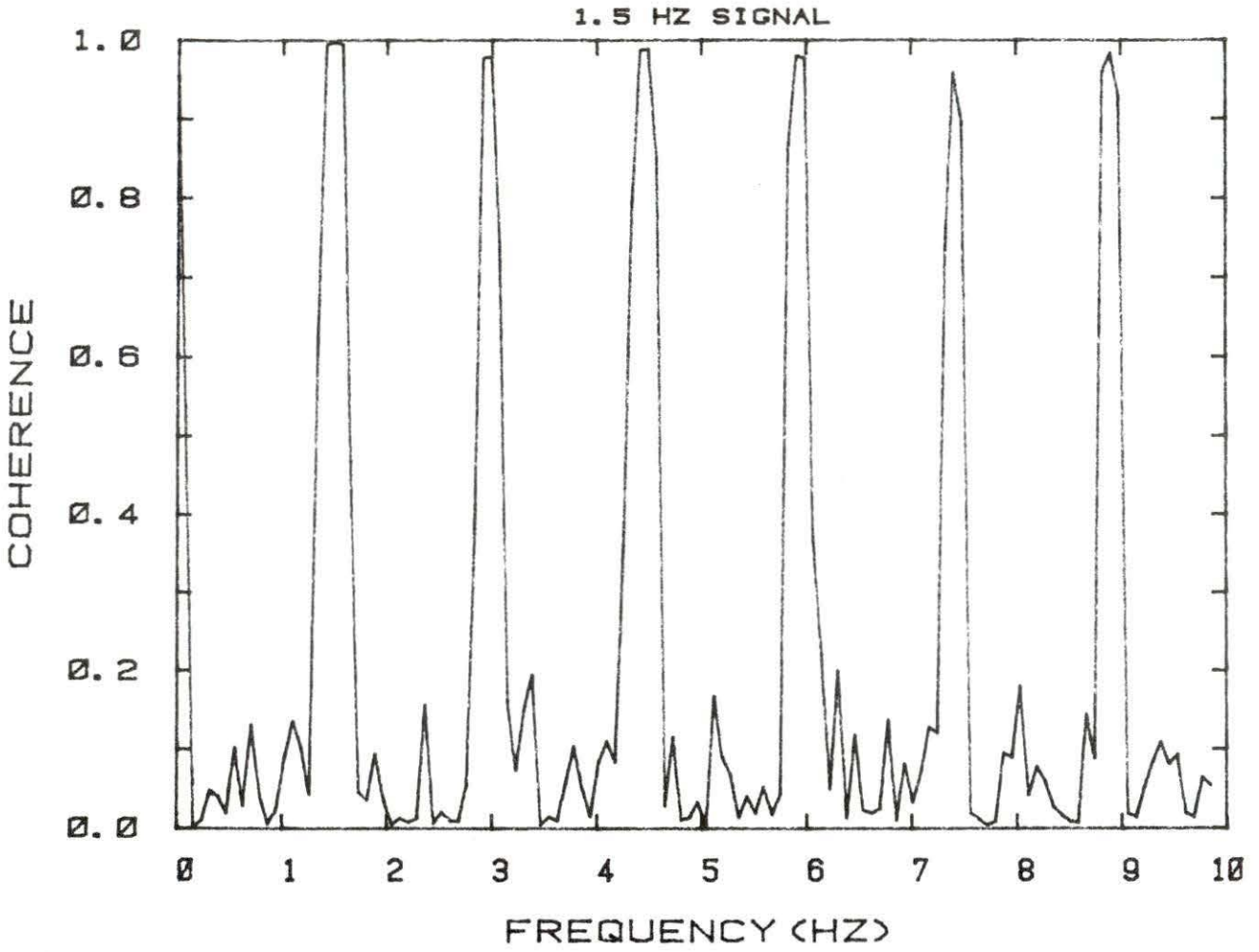

Figure 5.30 Detector 1 - LVDT coherence for periodic vibrating absorber motion

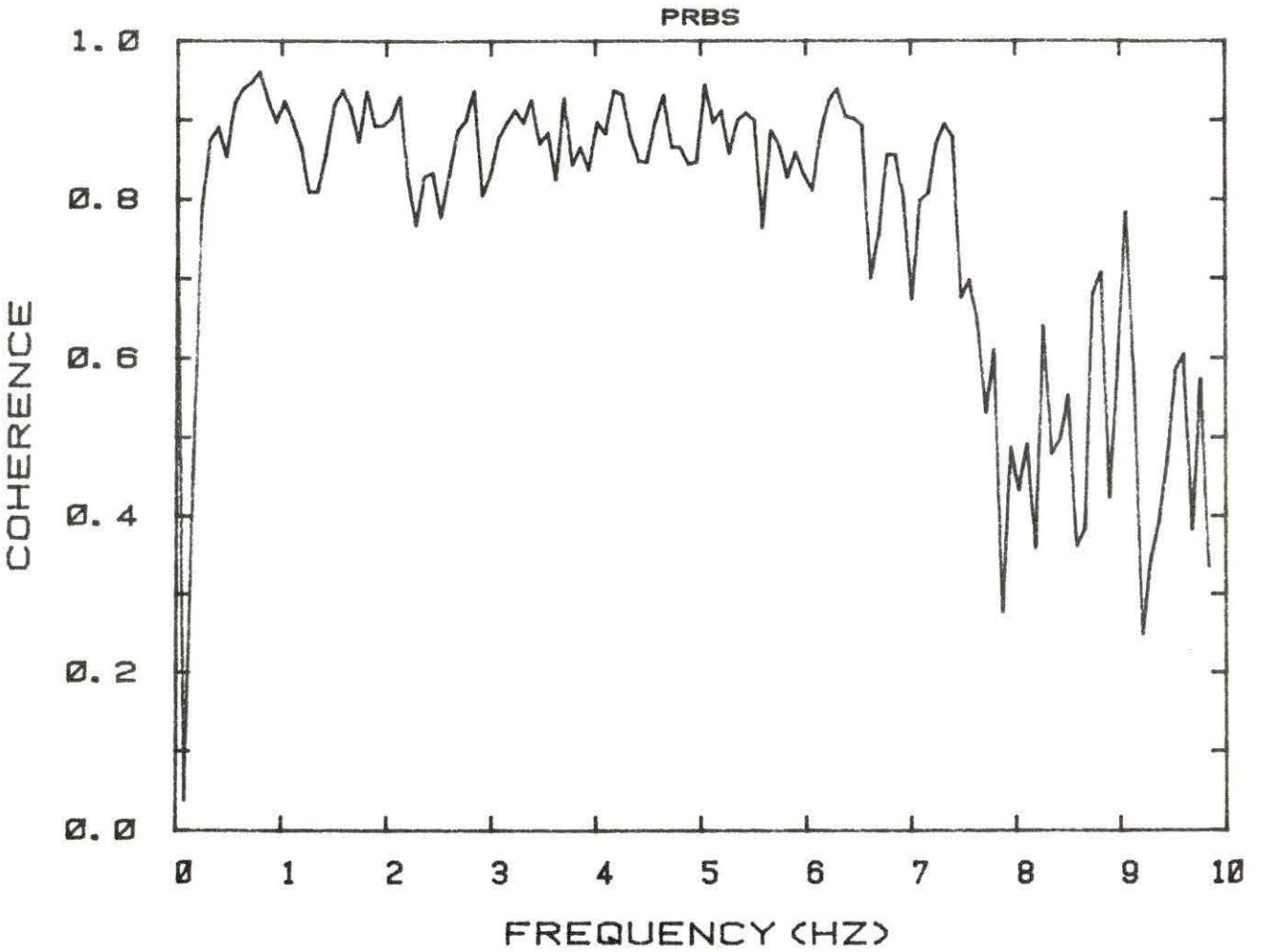

Figure 5.31 Detector 1 - LVDT coherence for PRBS vibrating absorber motion

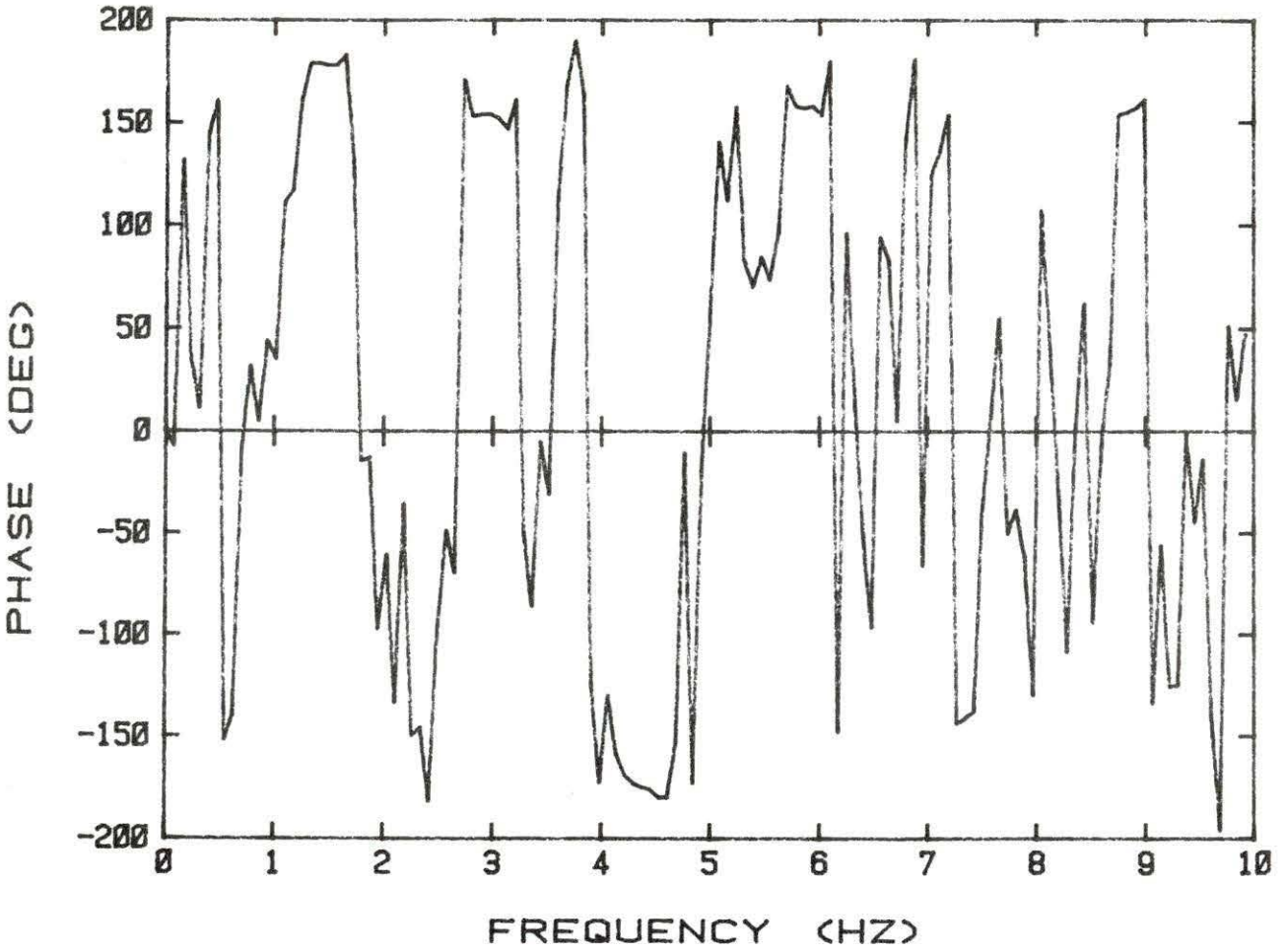

Figure 5.32 Detector 1 - LVDT phase for periodic vibrating absorber motion

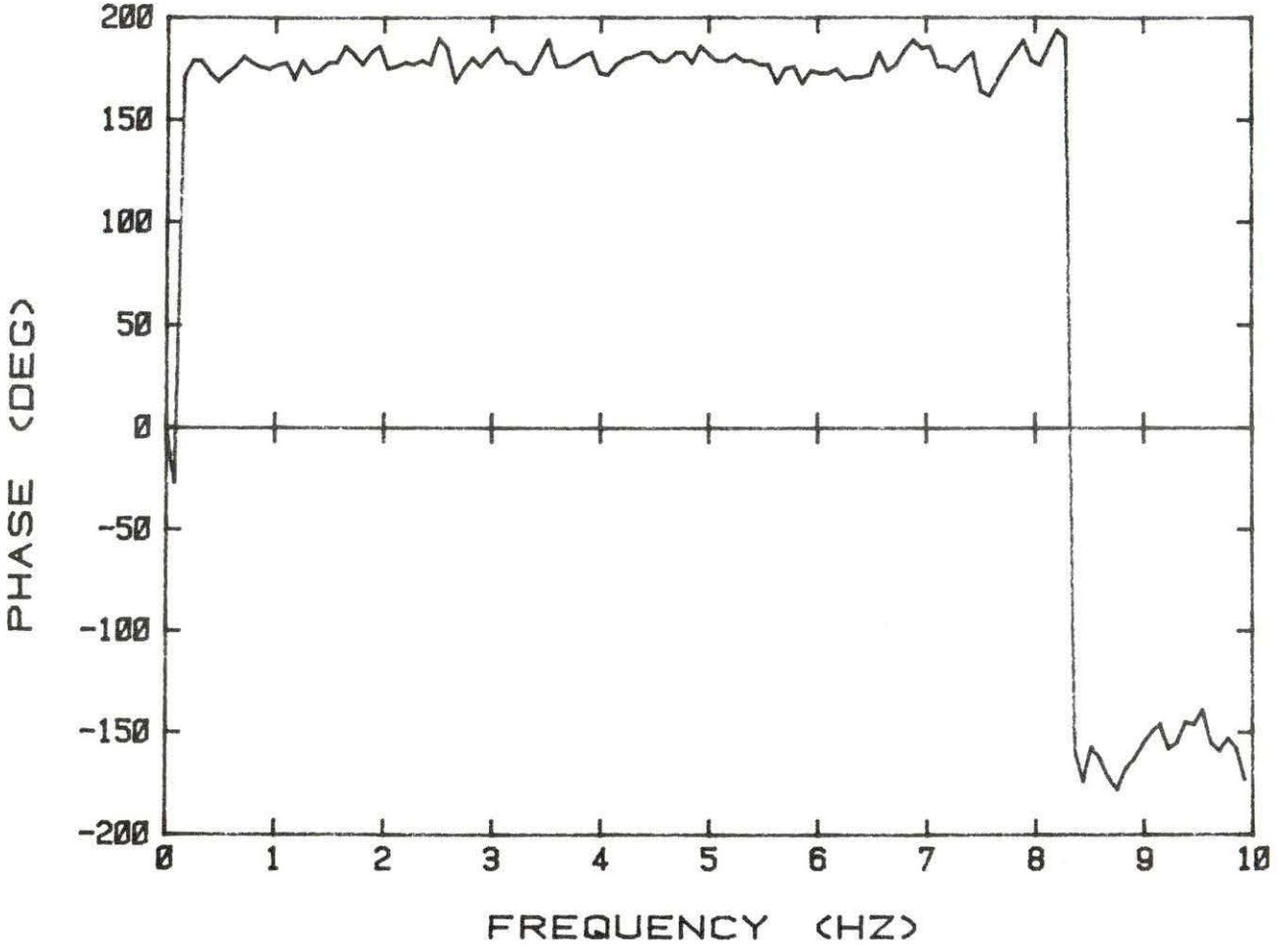

Figure 5.33 Detector 1 - LVDT phase for random vibrating absorber motion

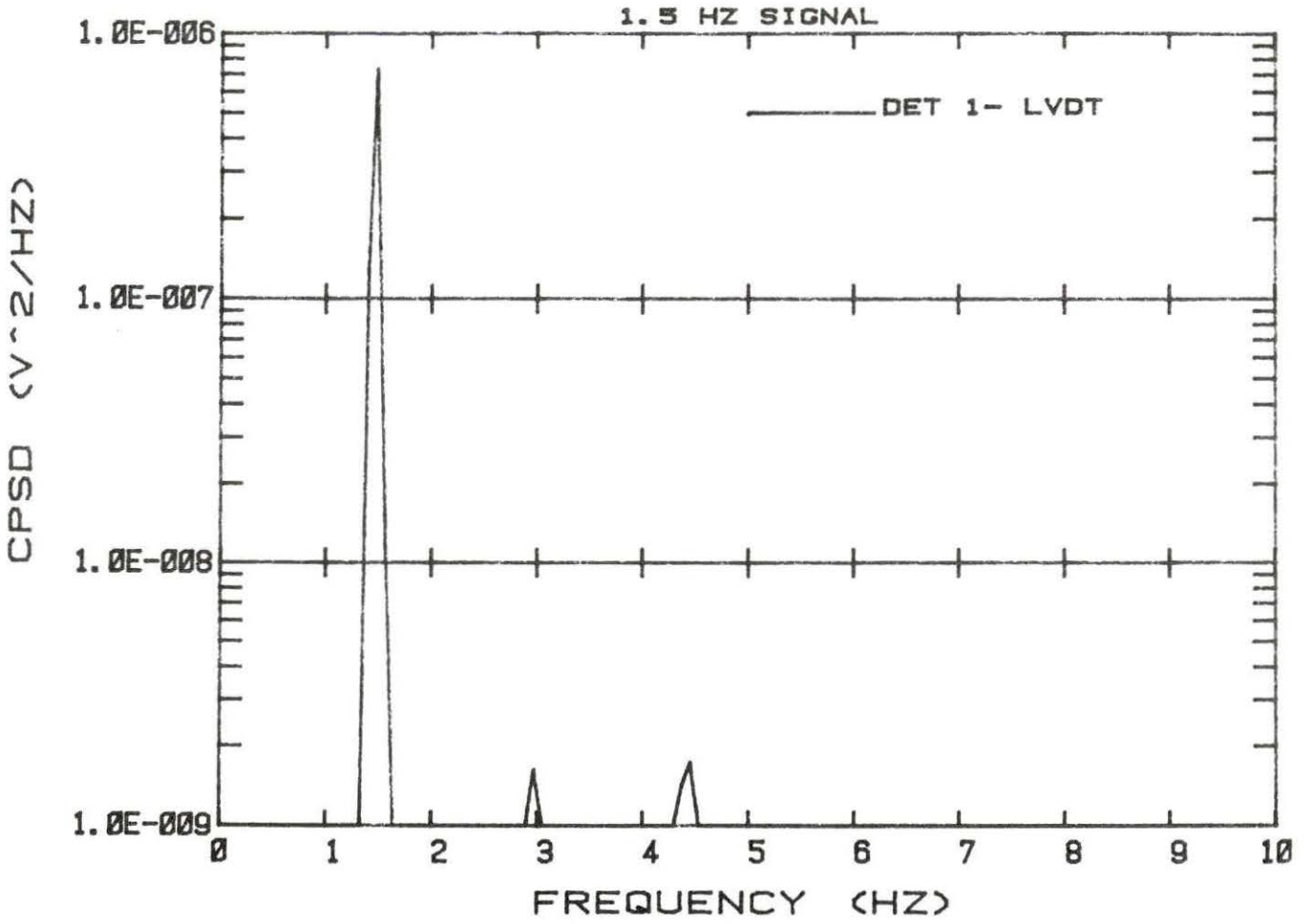

Figure 5.34 Detector 1 - LVDT CPSD for periodic vibrating absorber motion

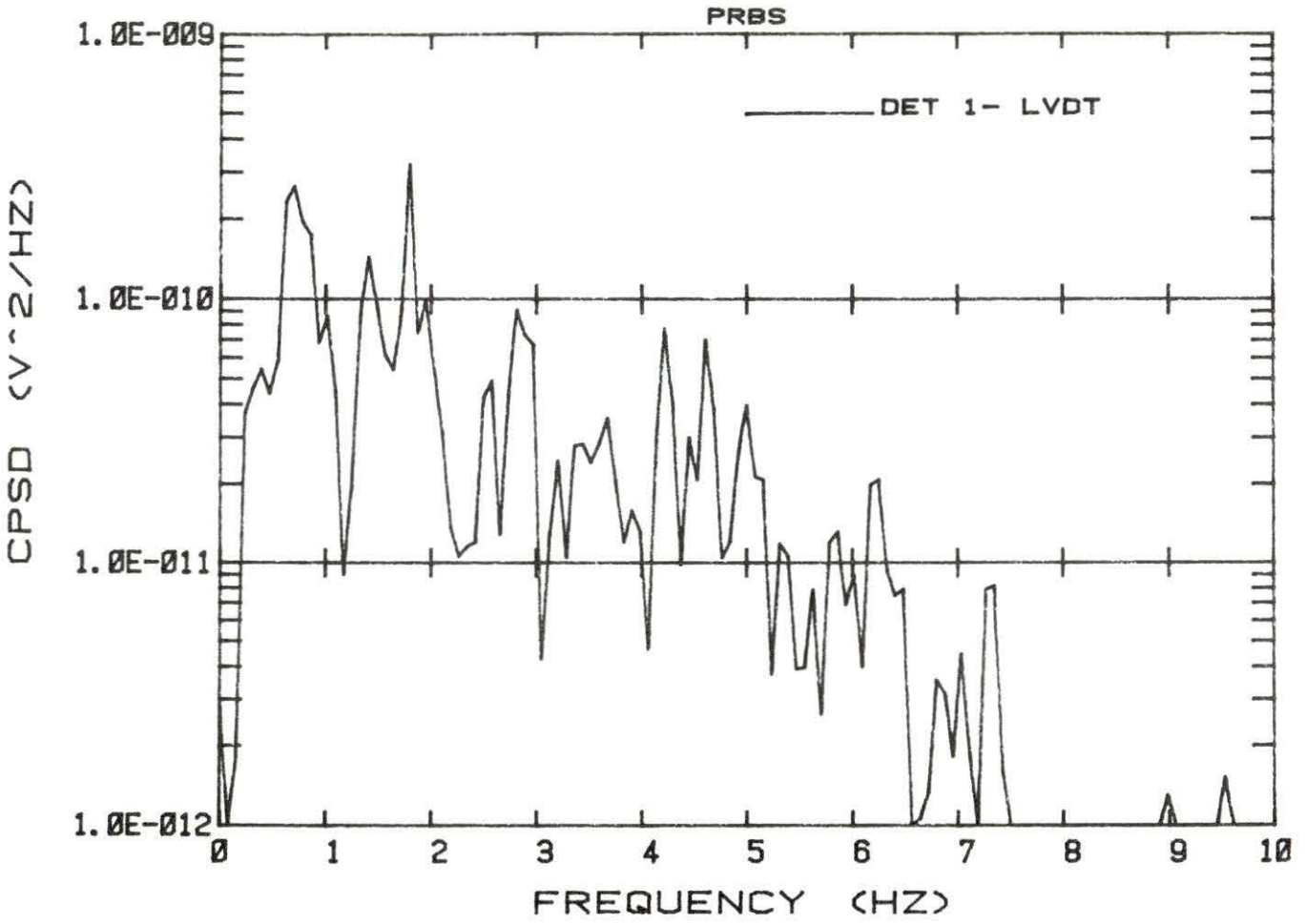

Figure 5.35 Detector 1 - LVDT CPSD for PRBS vibrating absorber motion

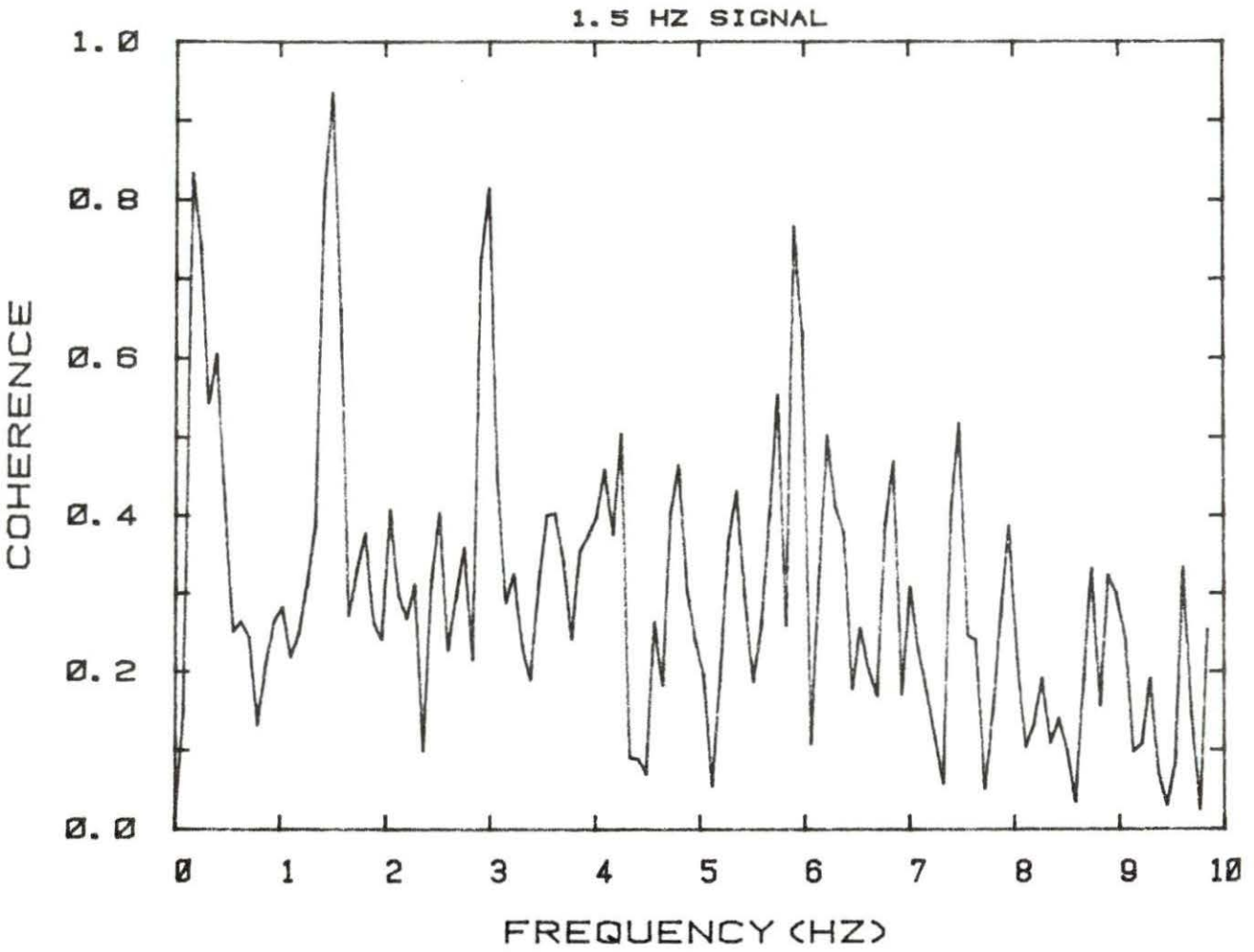

Figure 5.36 Detector 2 - CIC detector coherence for periodic vibrating absorber motion

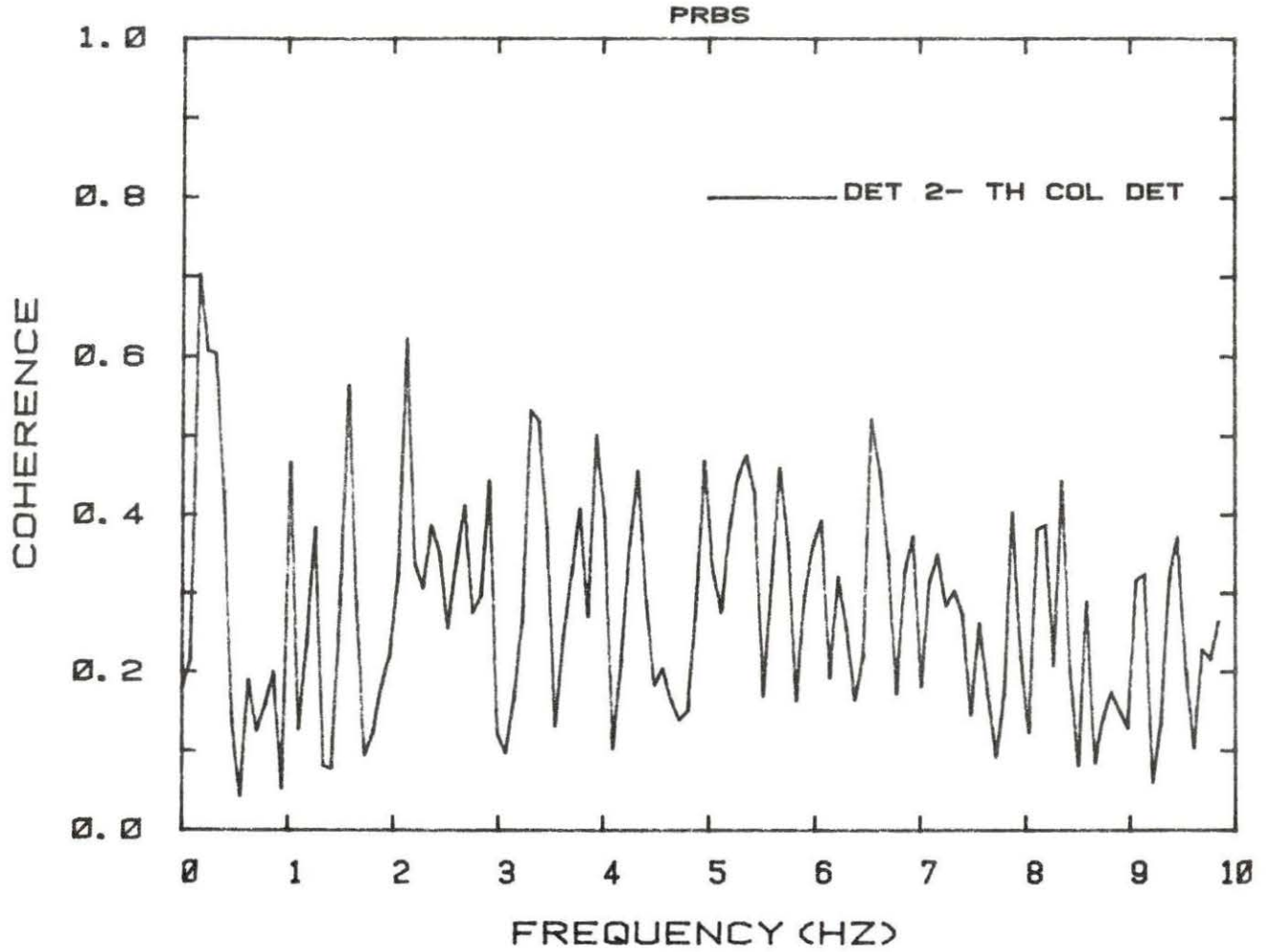

Figure 5.37 Detector 2 - CIC detector coherence for PRBS vibrating absorber motion

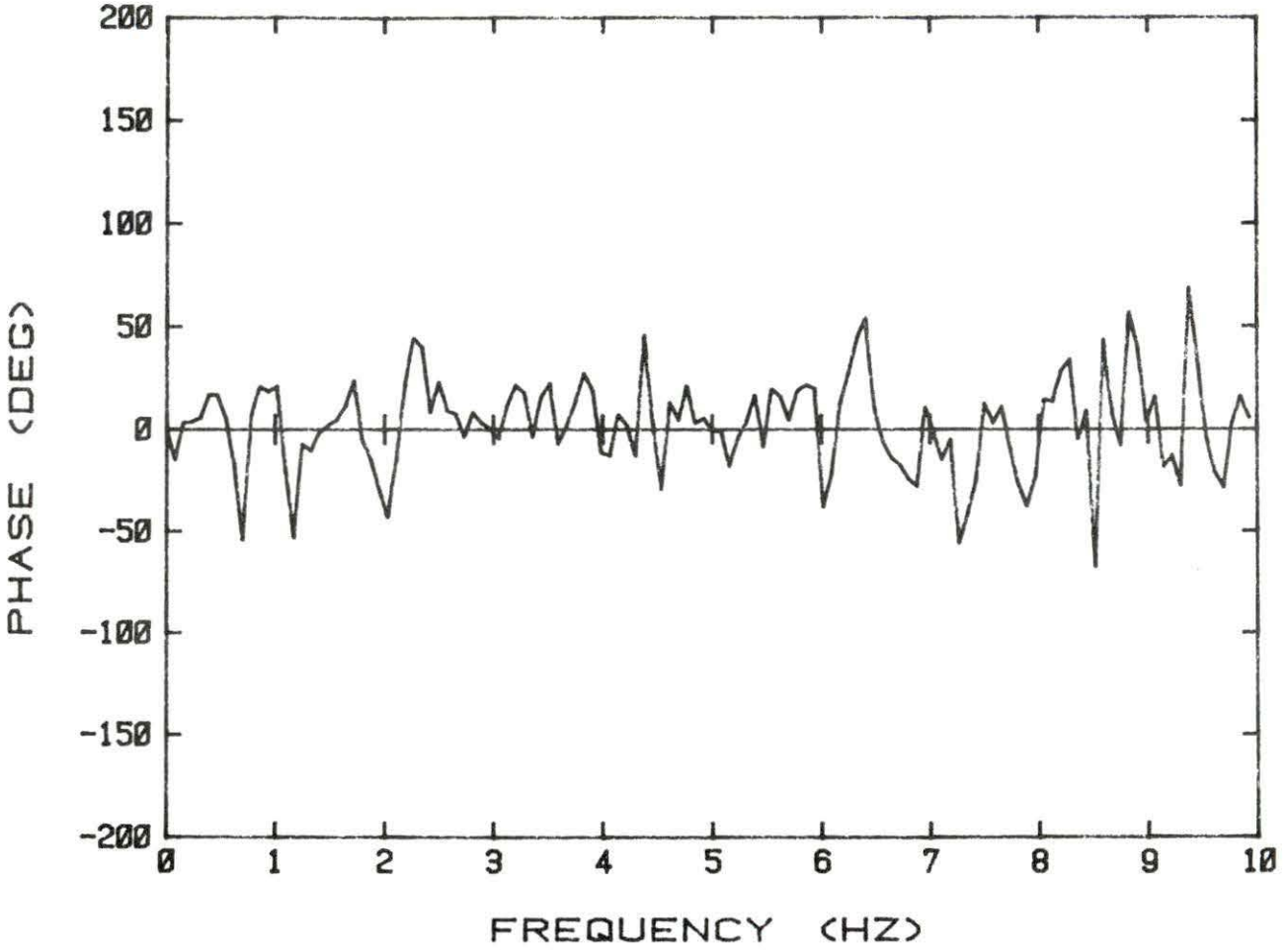

Figure 5.38 Detector 2 - CIC detector phase for periodic vibrating absorber motion

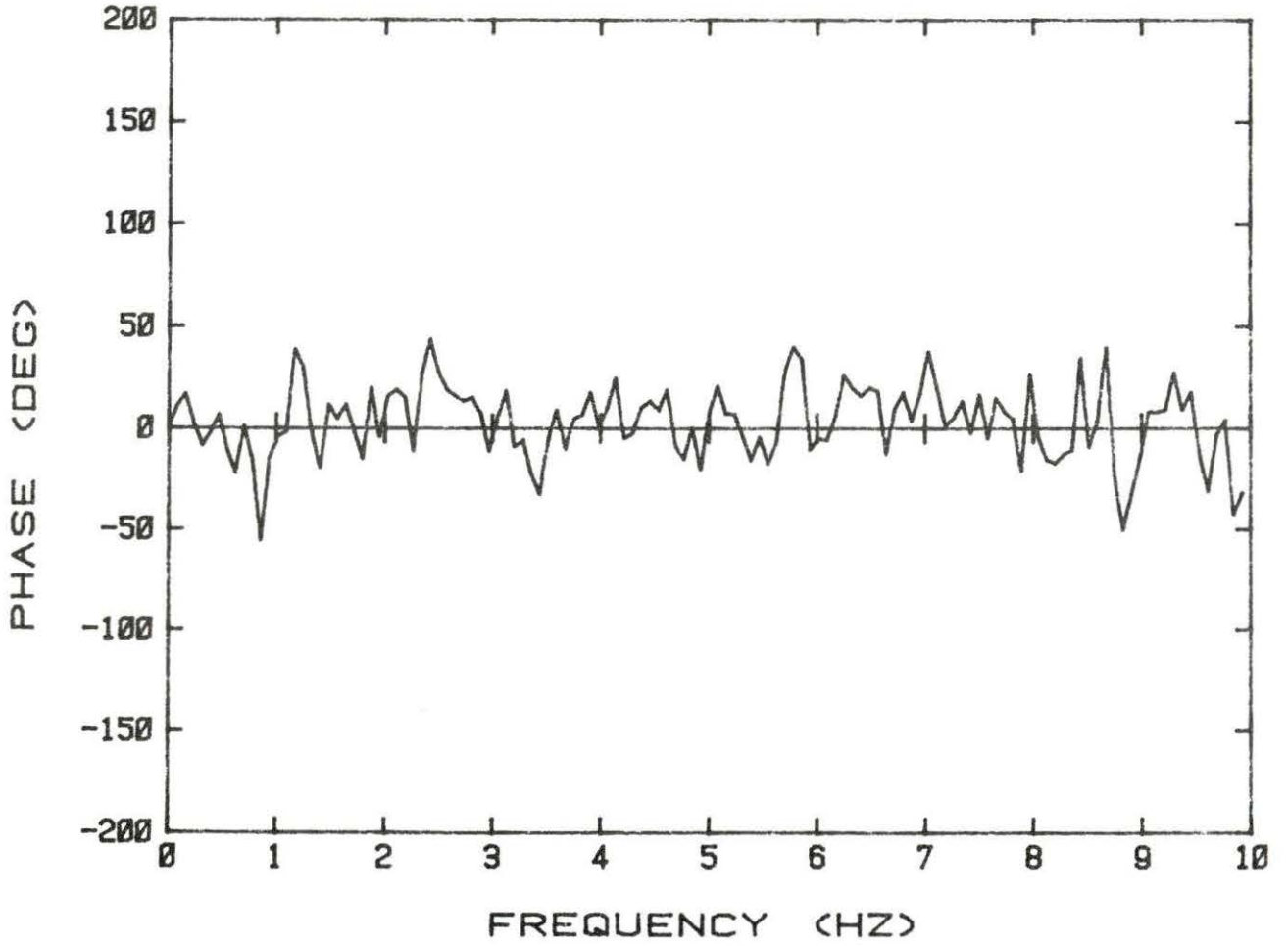

Figure 5.39 Detector 2 - CIC detector phase for PRBS vibrating absorber motion

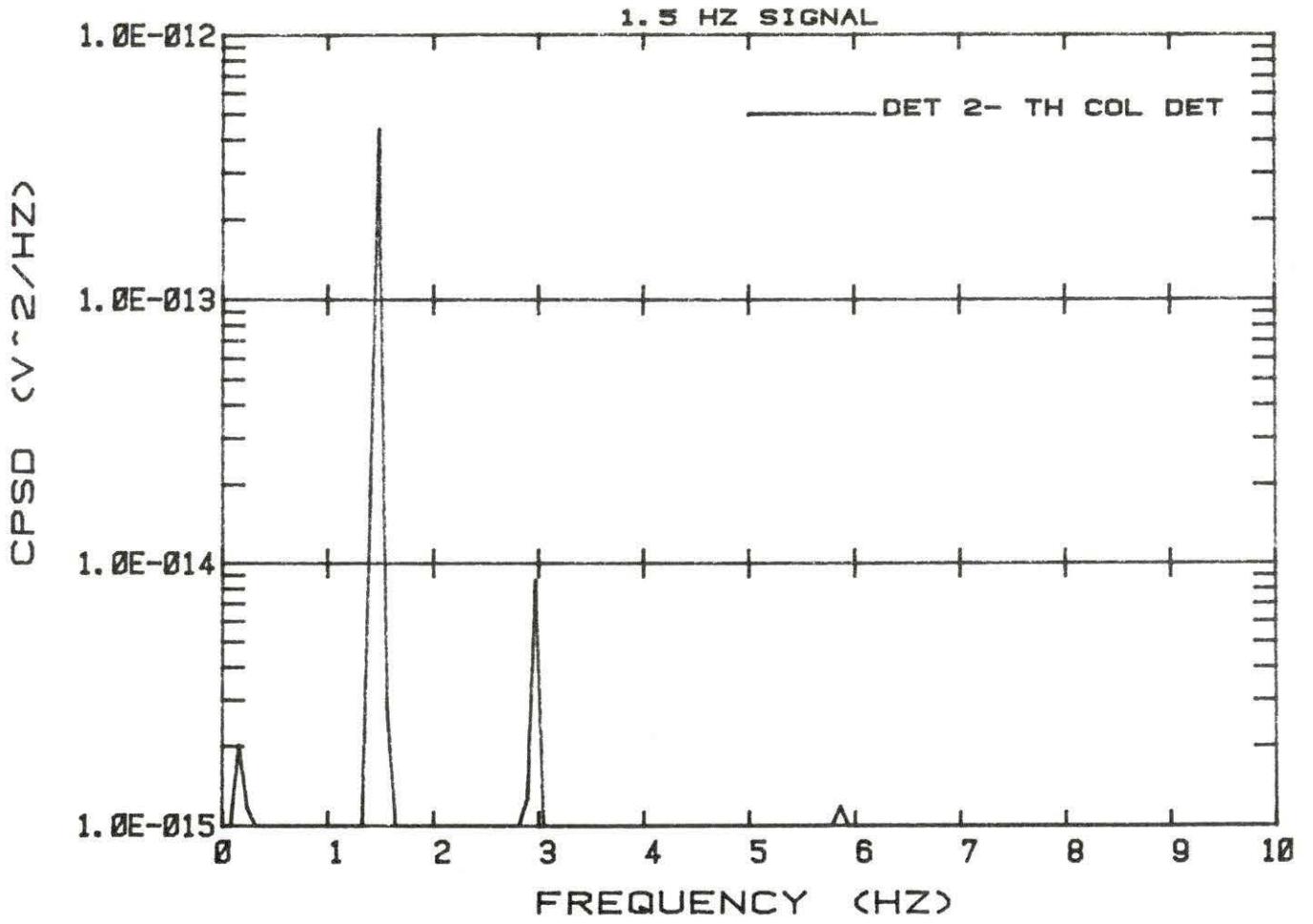

Figure 5.40 Detector 2 - CIC detector CPSD for periodic vibrating absorber motion

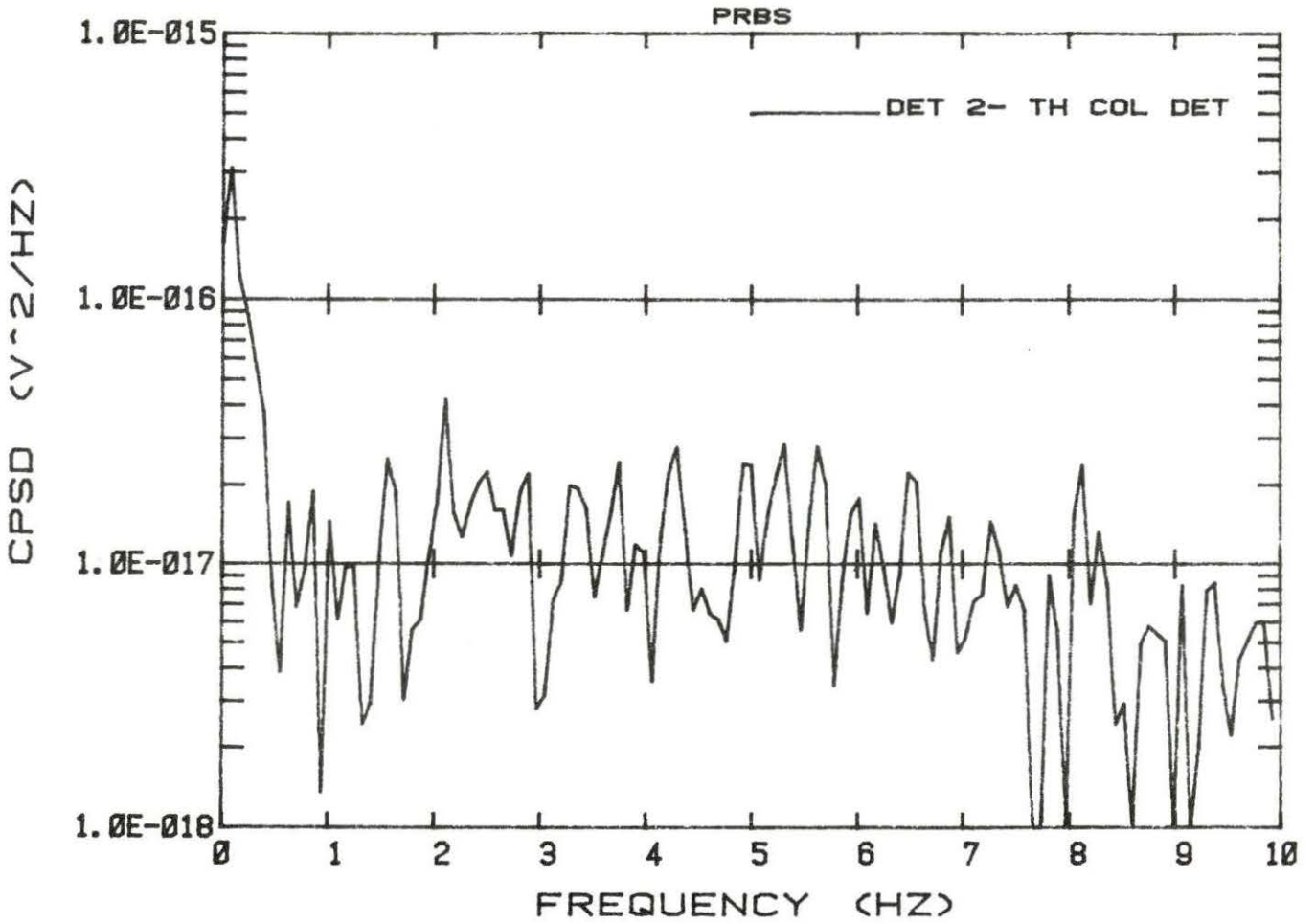

Figure 5.41 Detector 2 - CIC detector CPSD for PRBS vibrating absorber motion

PRBS phase plots (Figures 5.38 and 5.39) indicate the response at the CIC and detector 2 are in phase. Since both detectors see only the global response, this is as expected. The CPSD for the PRBS (Figure 5.41) shows a small common response.

Figures 5.42 to 5.47 show the signal combinations for detector 2 and the LVDT. As can be seen in Figures 5.42 and 5.43, the coherence is strong for the periodic signal, but the PRBS signal shows little commonality. Although it shows considerable scatter, the periodic signal seems to show about zero phase shift (Figure 5.44). This is what is expected. More averages are needed in this plot to smooth out the curve. The PRBS phase (Figure 5.45) also shows scatter and is probably meaningless, as indicated by the low coherence. The CPSD of the detector 2 - LVDT combination (Figure 5.46) shows a strong peak at the fundamental frequency, but the PRBS plot (Figure 5.47) is again quite low. The reason it has as high a magnitude as it does is due to the powerful contribution of the LVDT signal.

The final set of graphs in the set, Figures 5.48 through 5.53, are of the thermal column CIC detector and the LVDT. These graphs show good correlation (Figures 5.48 and 5.49), phase information (Figures 5.50 and 5.51), and CPSD plots (Figures 5.52 and 5.53) for both the periodic and PRBS signals. The reason the CIC appears to see a larger response to the vibrating absorber than detector 2, even though it is farther away from the absorber, is because it is a larger detector and has a higher efficiency.

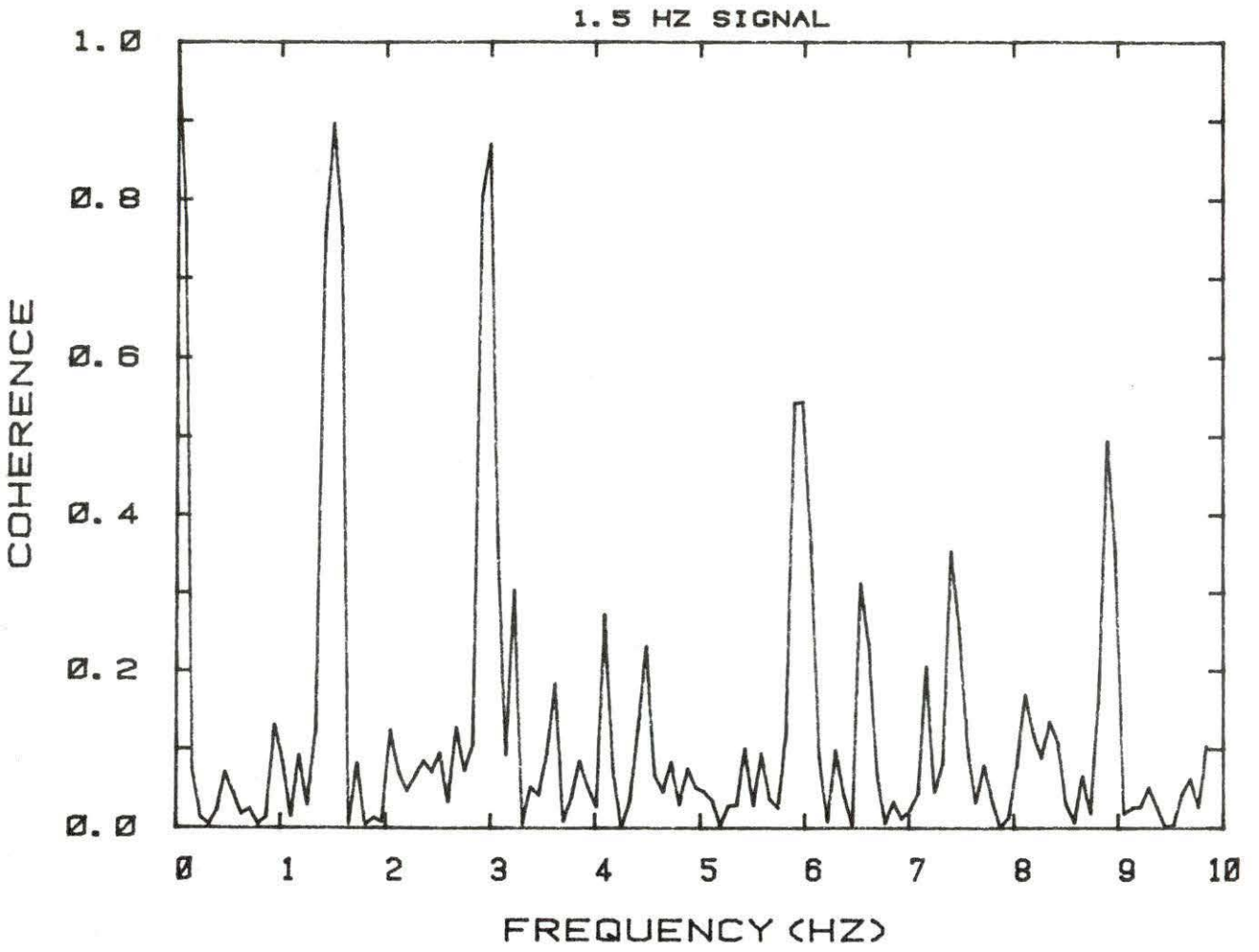

Figure 5.42 Detector 2 - LVDT coherence for periodic vibrating absorber motion

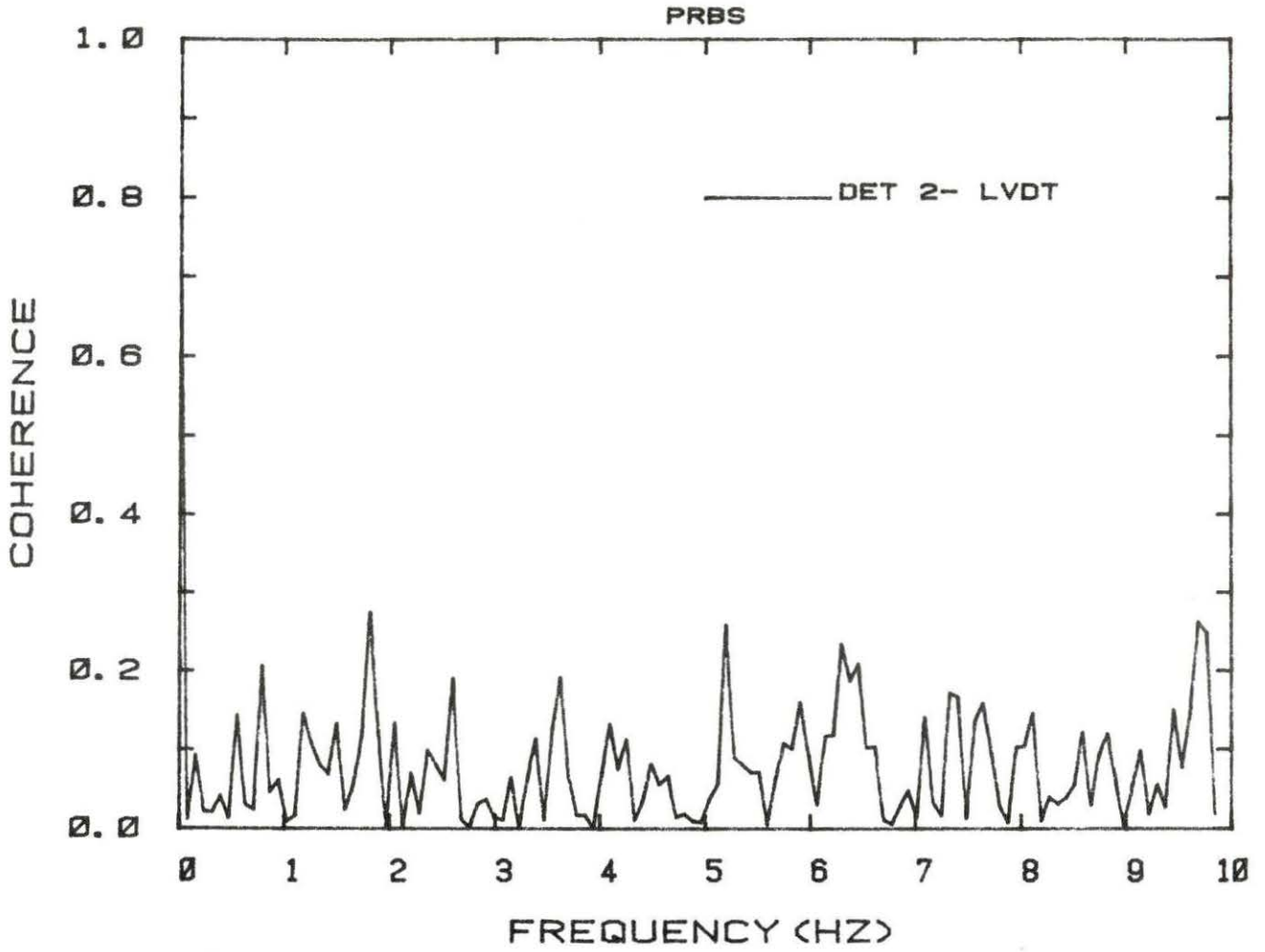

Figure 5.43 Detector 2 - LVDT coherence for random vibrating absorber motion

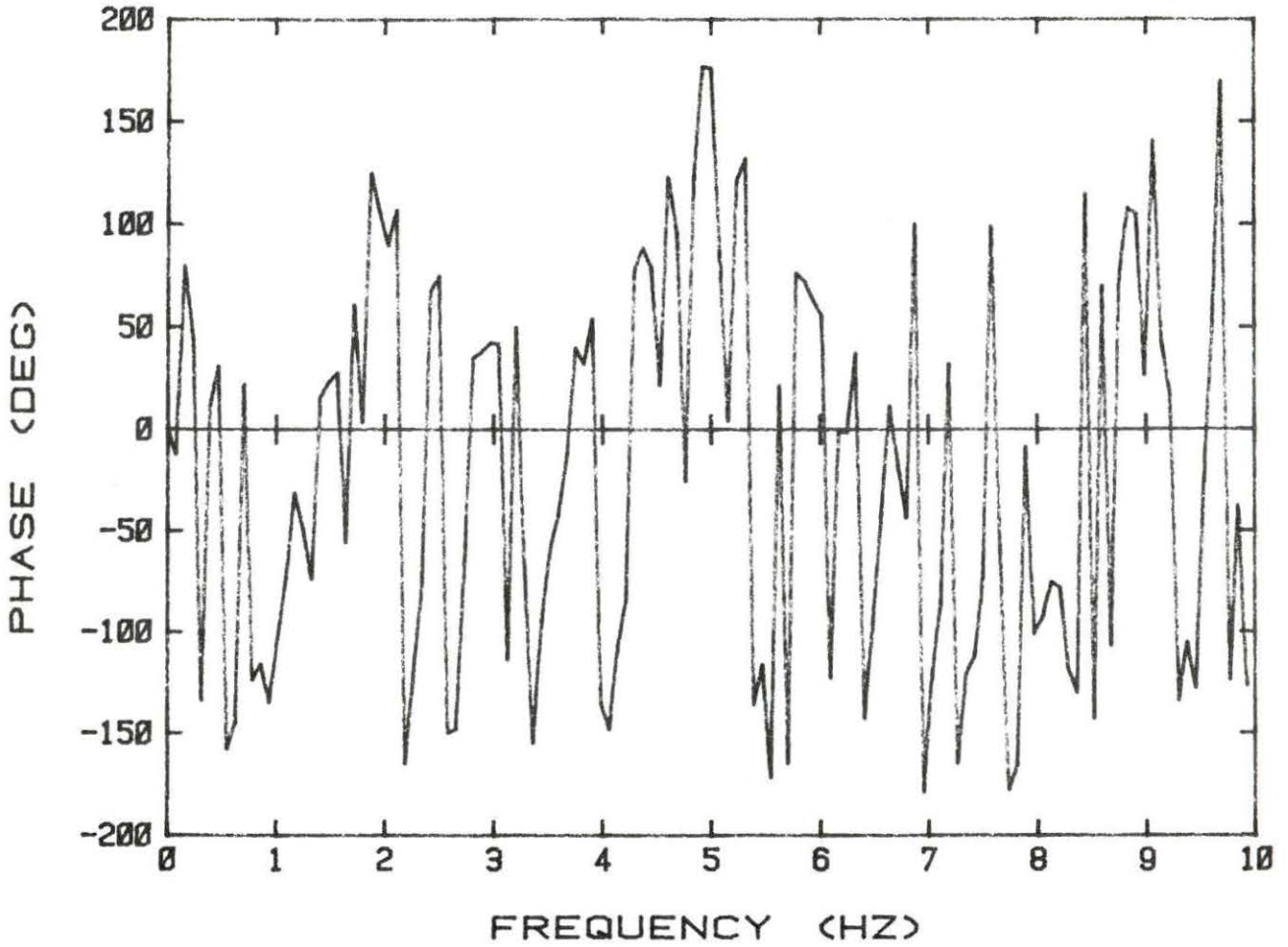

Figure 5.44 Detector 2 - LVDT phase for periodic vibrating absorber motion

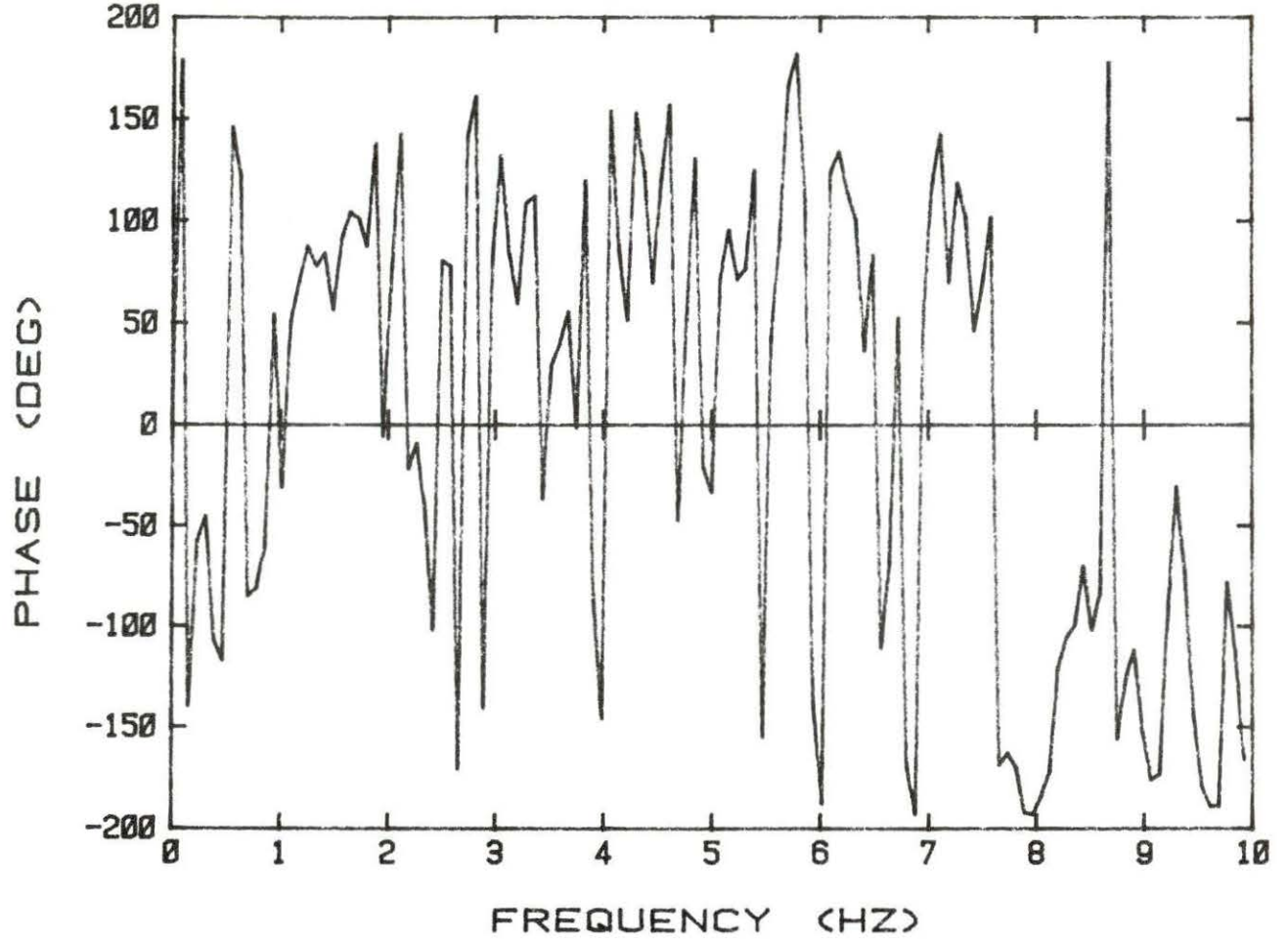

Figure 5.45 Detector 2 - LVDT phase for PRBS vibrating absorber motion

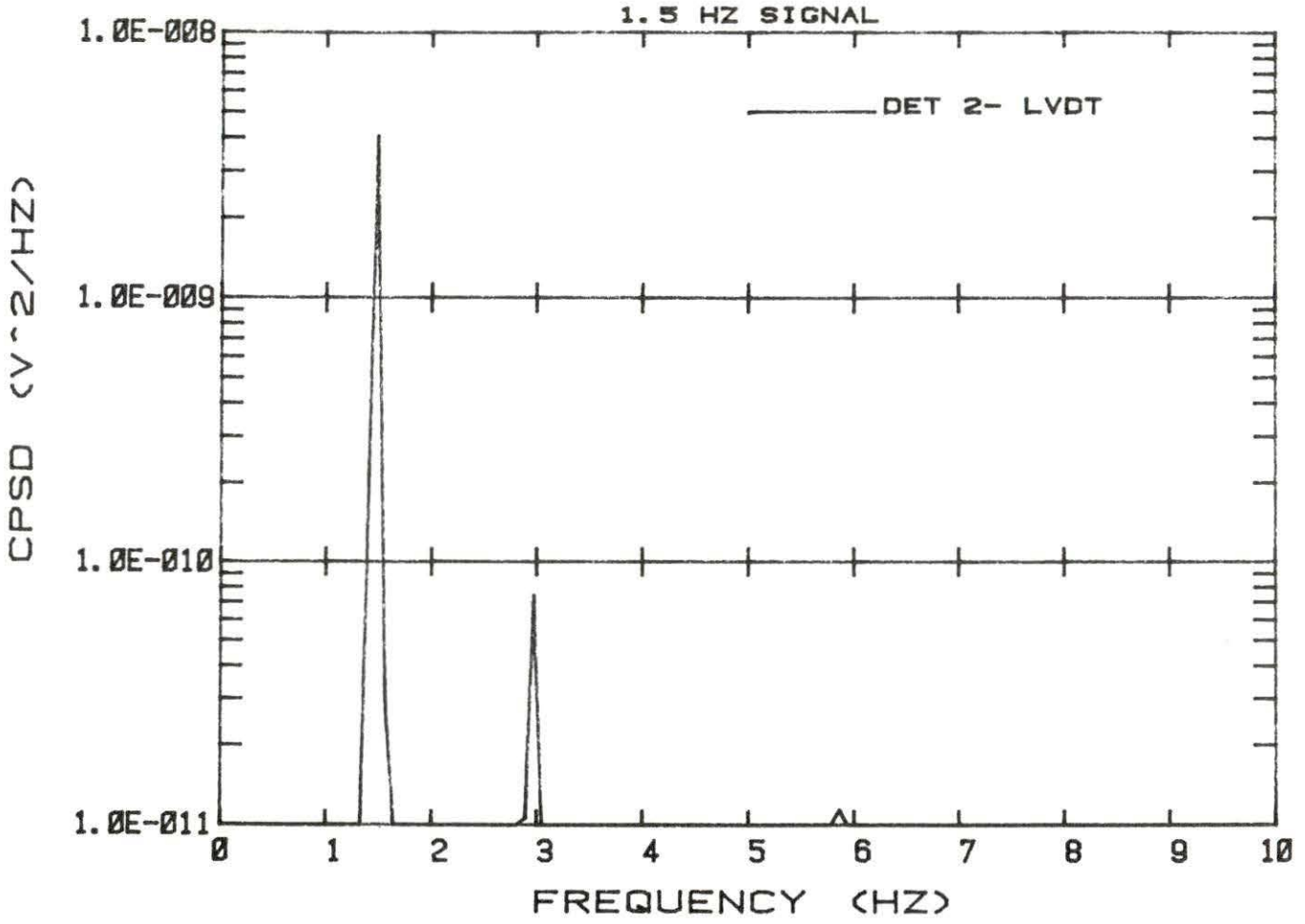

Figure 5.46 Detector 2 - LVDT CPSD for periodic vibrating absorber motion

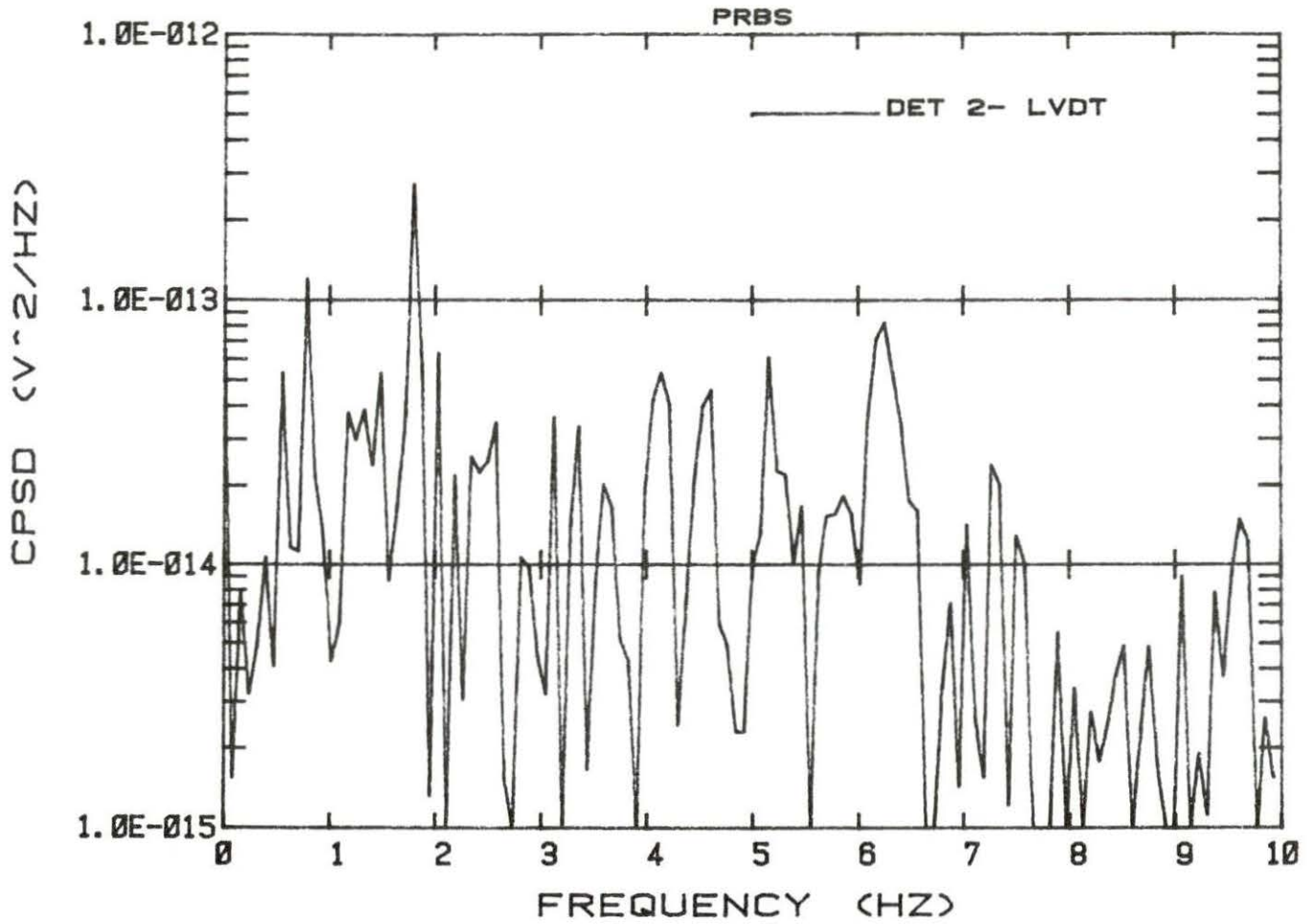

Figure 5.47 Detector 2 - LVDT CPSD for PRBS vibrating absorber motion

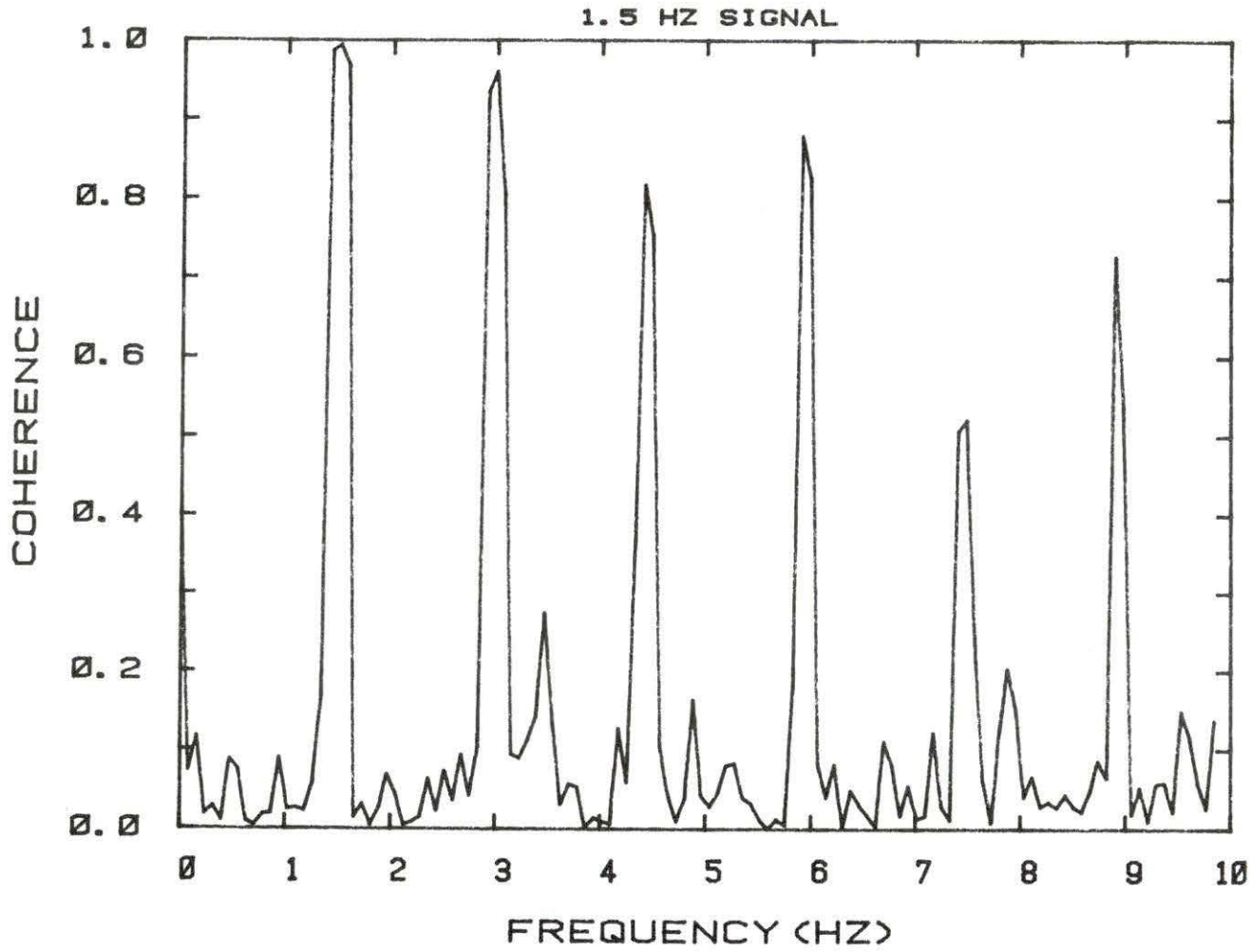

Figure 5.48 CIC detector - LVDT coherence for periodic vibrating absorber motion

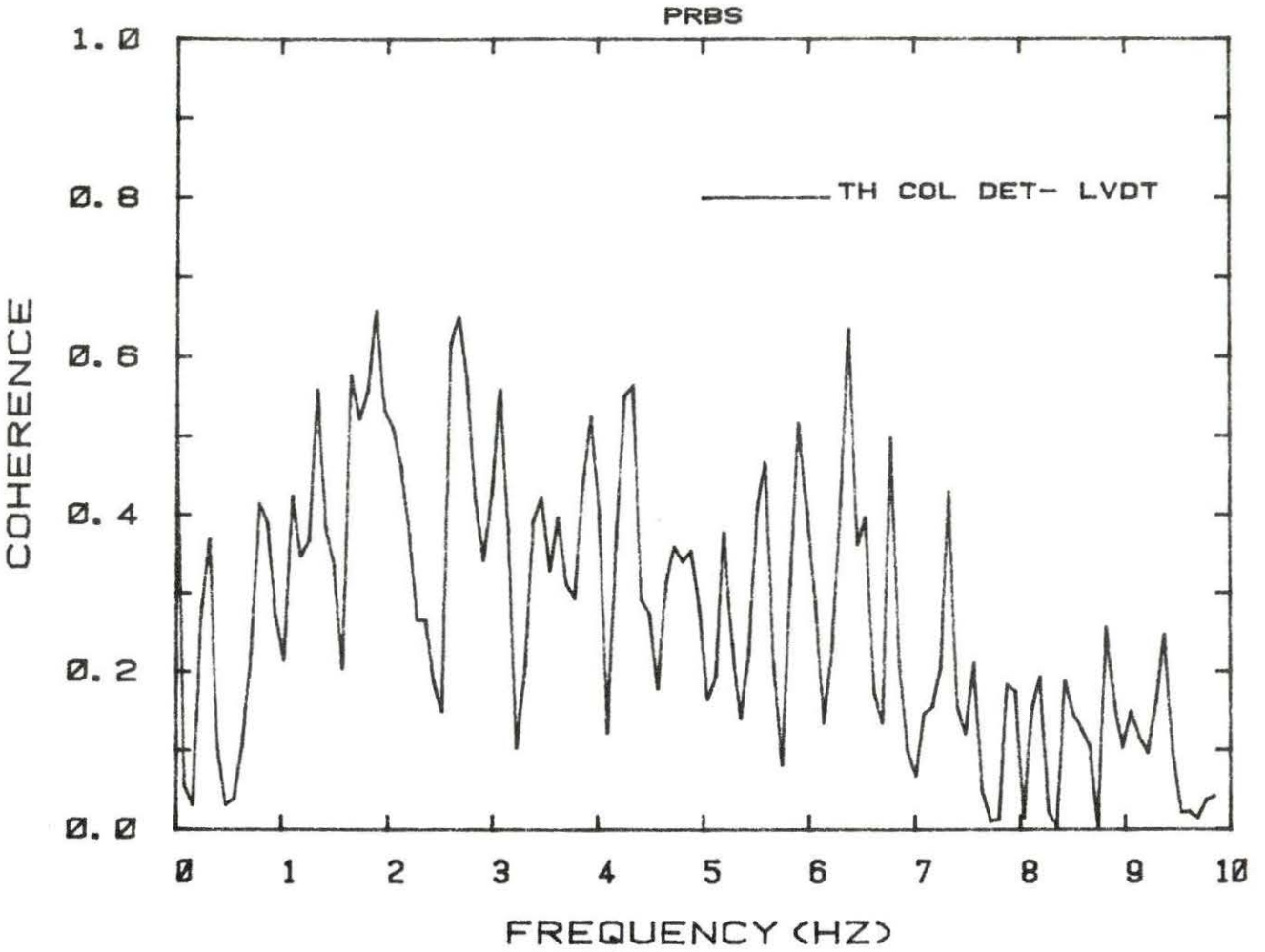

Figure 5.49 CIC detector - LVDT coherence for PRBS vibrating absorber motion

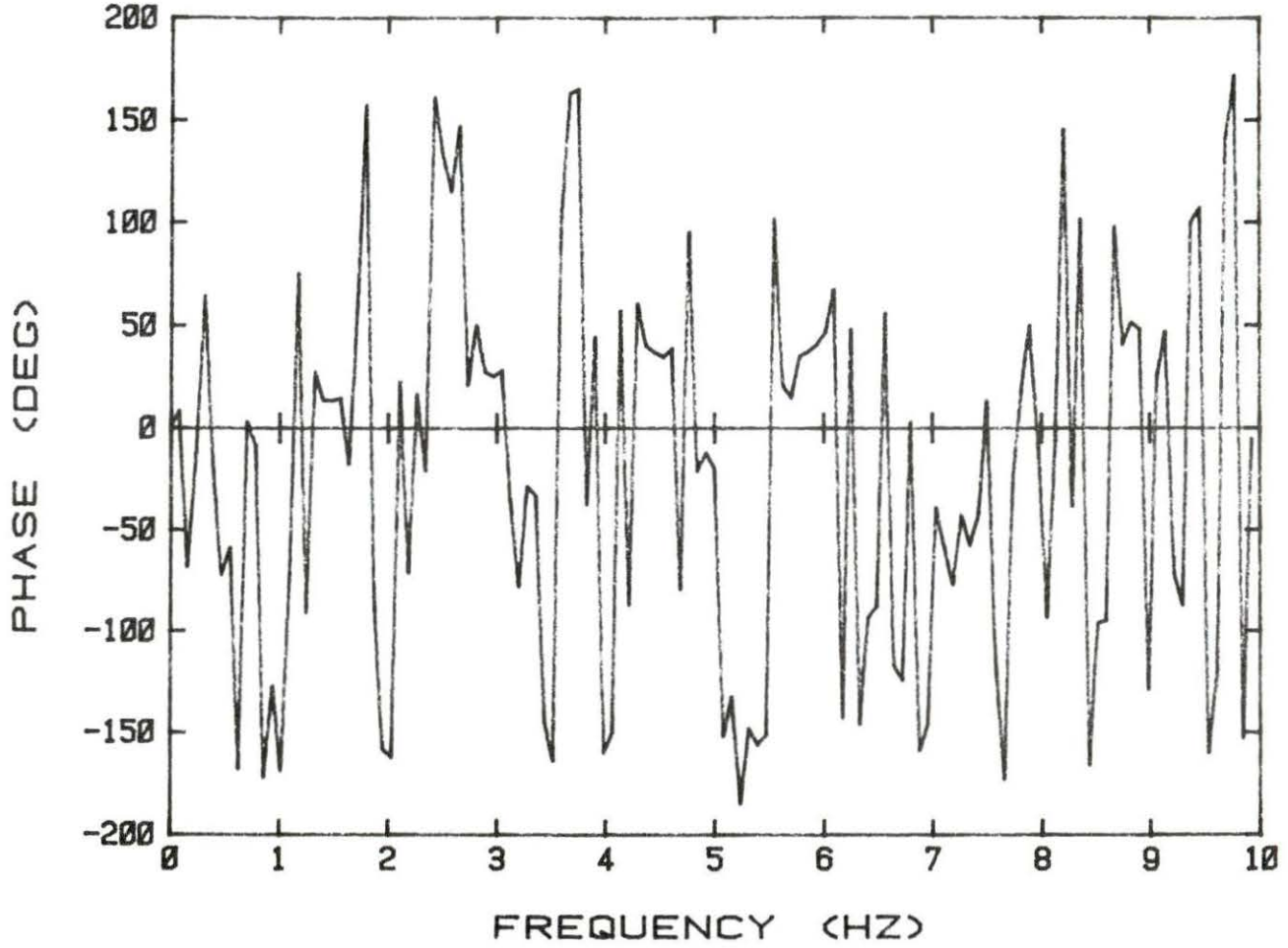

Figure 5.50 CIC detector - LVDT phase for periodic vibrating absorber motion

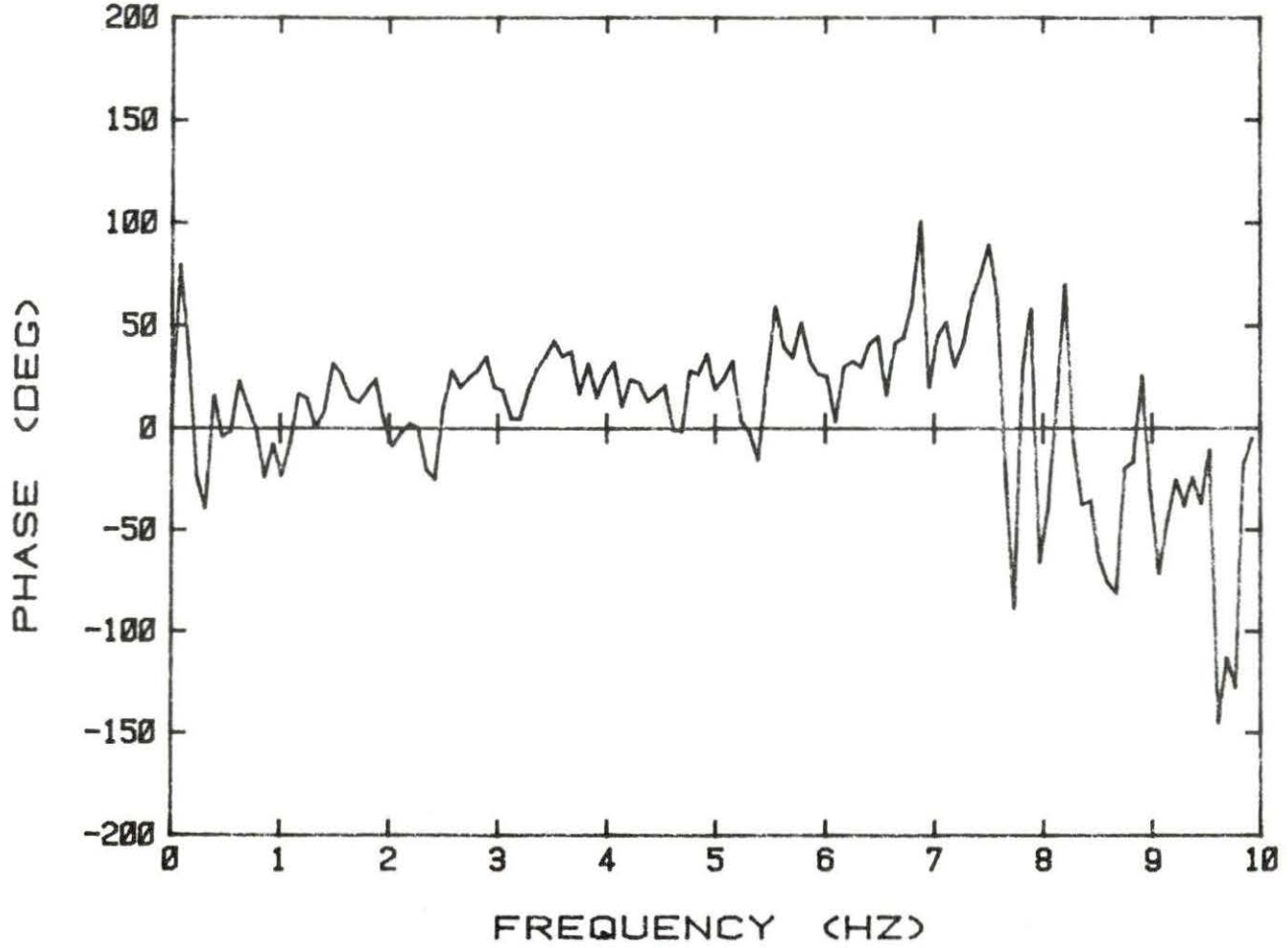

Figure 5.51 CIC detector - LVDT phase for PRBS vibrating absorber motion

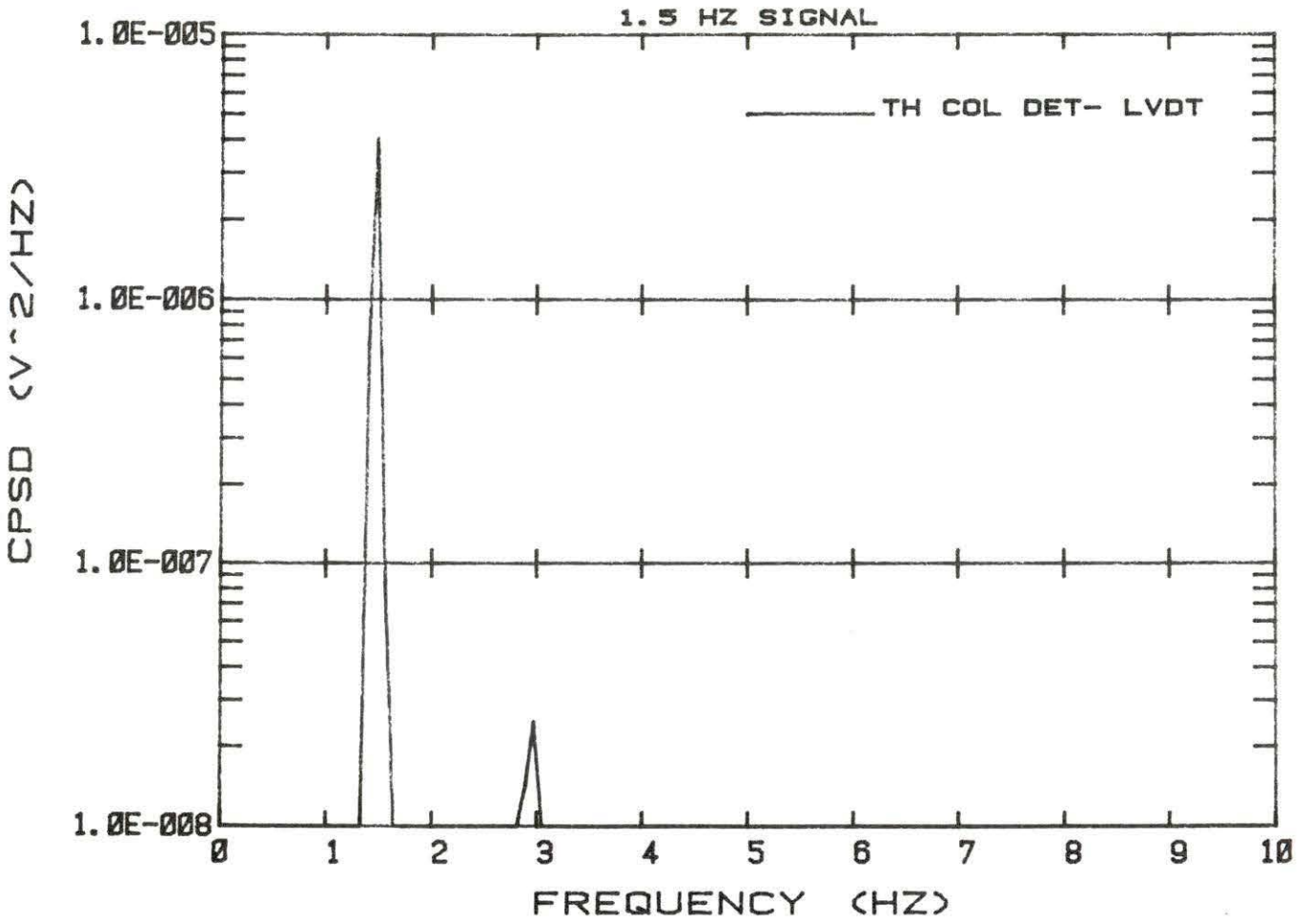

Figure 5.52 CIC detector - LVDT CPSD for periodic vibrating absorber motion

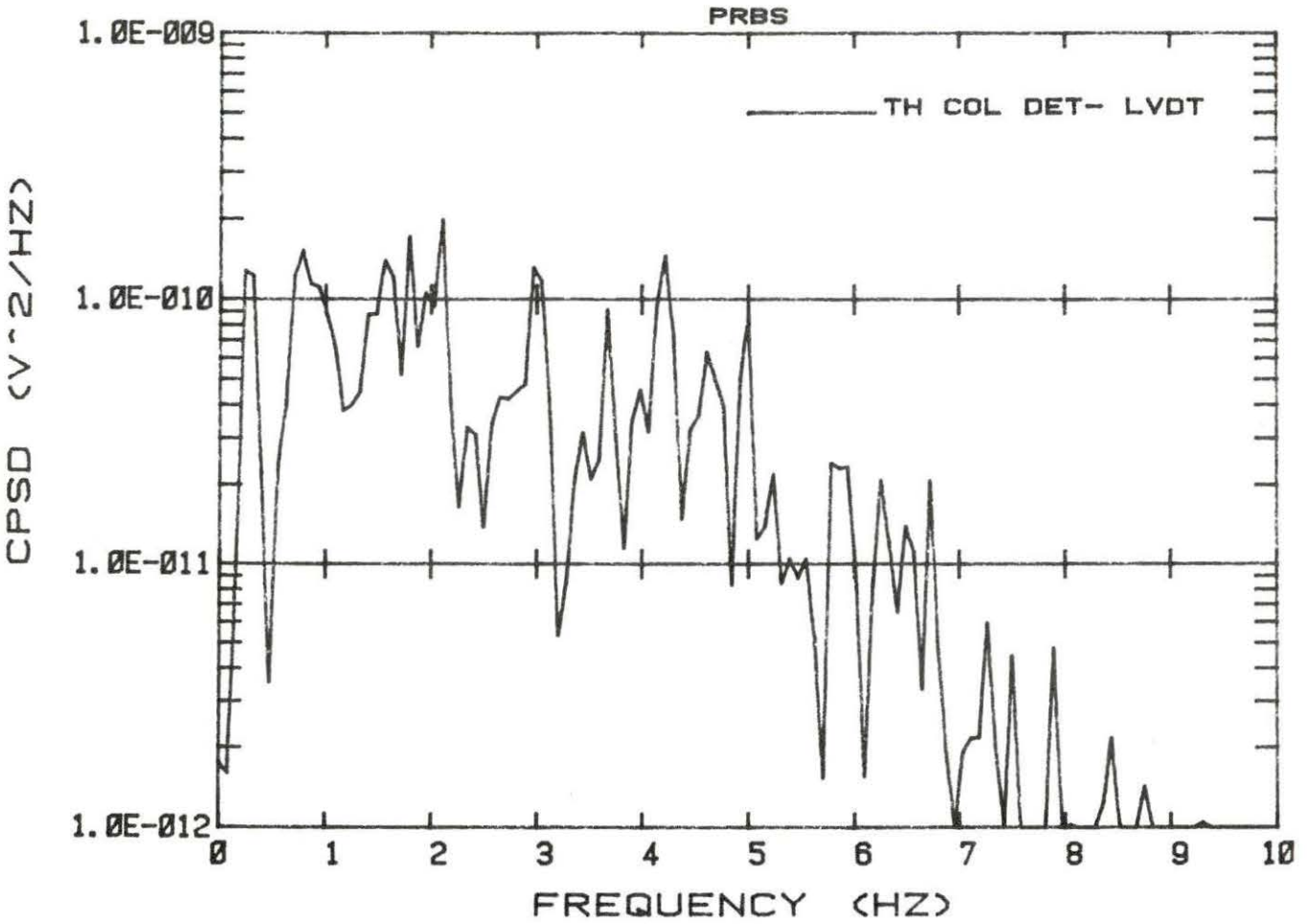

Figure 5.53 CIC detector - LVDT CPSD for PRBS vibrating absorber motion

VI. COMPARISON OF EXPERIMENTAL RESULTS WITH THE THEORETICAL MODEL

The ratio of the responses of detector 1 and 2 was calculated from Equation 2.40 using the results from the theoretical model. As reported in Table 1, this ratio is 8.59 based on a separation between the vibrator and detectors that is equal to the centerline to centerline distance. When the distance from the vibrator to detector 1 was changed to the distance from the vibrator centerline to the near edge of the detector, this ratio was found to be 10.6. The measurements were also used to obtain the response ratio. From the plots of the detector 1 and 2 APSDs for periodic motion (Figures 5.11 and 5.13), the actual flux ratio corresponding to the calculated ratio is given by the ratio of peak APSD values at 1.5 Hz.

$$\text{Ratio} = (\text{APSD}_{\text{det1}})^{1/2}/(\text{APSD}_{\text{det2}})^{1/2}.$$

Recall that the computer program calculated the square root of the APSD. The ratio of response is found to be

$$(3.61 \times 10^{-6})^{1/2}/(4.62 \times 10^{-8})^{1/2} = 9.07$$

This measured ratio falls between the two calculated values given in Table 1. As pointed out in Chapter IV, the calculated ratio of responses is sensitive to the assumed location of the near detector to the vibrator. In the model, the vibrator is assumed not to displace graphite, whereas in the actual reactor there is an air void. This will affect the rate at which the response drops.

This might be accounted for by using an effective separation distance for the calculated response. These results serve to indicate that an appropriate effective spacing falls between the centerline to centerline spacing and centerline to detector edge spacing.

Comparisons of theory and measurements of a qualitative nature can also be made. The theoretical model predicts that the response will drop off rapidly with distance between the detector and vibrator. The results of the measurements support this calculation. The model fails, however, to predict the 180^{o} phase change between the two detectors in the internal reflector. This phase shift would appear as a change in sign between the two detector responses. There may be several aspects of the model which contribute to this failure to model the phase correctly. Among other points; (1) the flux gradient at the vibrator location may not be correctly predicted (the dG/dy term), (2) the fuel regions are not correctly modeled at the edges, and (3) additional modes may improve the convergence resulting in better agreement between theory and experiment.

VII. CONCLUSIONS AND SUGGESTIONS FOR FURTHER RESEARCH

Since the actual reactor flux response ratio measured by the experiment and presented in Chapter VI falls in the range of the ratios predicted by the computer programs and presented in Chapter IV, it is concluded that the Green's function model of the UTR-10 reactor represents a reasonable first step in a theoretical development. Refinements can be made in the model to make it more consistent with experimental results. These refinements include reviewing the cross sections and other reactor parameters used in the model, and devising a way to add more modes to the solutions. The present value of 21 modes is restricted by problems in the library subroutines. These problems stem from the inability of the computer to handle the ill-conditioned matrices encountered in the higher mode solutions of matrix A. Adding modes to the solutions could improve the calculated value of the Green's functions. It would also be desirable to improve the calculation of dG/dy_o. In addition, it would be interesting to develop a model which accounted for the graphite regions at the ends of the fuel tanks.

Another conclusion which can be made from the experiment is that the phases between the detector signals and the absorber motion were consistent with the local-global interpretation of the response. The global response of detectors was readily identifiable from the phase shift associated with the reactor transfer function, e.g. detector 2 and the thermal column detector. The coherence function was found to

be a useful indicator of the commonality of signals for the purpose of phase shift measurements. When the coherence function was greater than 0.2, meaningful phase information was obtained (Figure 5.25 and 5.27).

VIII. REFERENCES

1. Hugo Van Dam, Neutron Noise in Boiling Water Reactors, Atomkernenergie 27, No. 1, 8 (1976).

2. I. Pazsit, Two Group Theory of Noise in Reflected Reactors with Application to Vibrating Absorbers, Annals of Nuclear Energy 5, 185 (1978).

3. I. Pazsit and G. Th. Analytis, Theoretical Investigation of the Neutron Noise Diagonistics of Two-Dimensional Control Rod Vibrations in a PWR, Annals of Nuclear Energy 7, 171 (1980).

4. W. C. Nodean, The Response of a Coupled Core Reactor to a Localized Oscillation of the Absorption Cross Section, PhD Dissertation, Department of Nuclear Engineering, Iowa State University, 1969 (unpublished).

5. M. A. Al-Ammar, Use of Local-Global Ratio in Detecting Component Vibration in Reactors, PhD Dissertation, Department of Nuclear Engineering, Iowa State University, 1981 (unpublished).

6. R. J. Borland, Effects of Neutron Flux Gradient and Detector-Vibrator Geometry on the Local-Global Responses of the UTR-10 Reactor, MS Thesis, Department of Nuclear Engineering, Iowa State University, 1982 (unpublished).

7. P. M. Morse and H. Feshbach, Methods in Theoretical Physics, (McGraw-Hill, New York, 1953), p. 820.

8. R. F. Barry, LEOPARD - A Spectrum Dependent Non-Spatial Depletion Code for the IBM-7094, WCAP-3269-26, (1983).

9. F. B. Hildebrand, Methods of Applied Mathematics (Prentice-Hall, Inc., Englewood Cliffs, NJ, 1965), p. 228.

10. M. Salih, Response of an In-Core Neutron Detector to a Vibrating Absorber Based on the Detector Adjoint Function, MS Thesis, Department of Nuclear Engineering, Iowa State University, 1971 (unpublished).

11. T. B. Fowler, M. L. Tobias, D. R. Vondy, EXTERMINATOR - A Multigroup Code for Solving Neutron Diffusion Equations in One and Two Dimensions, ORNL-TM-842, (1966).

IX. ACKNOWLEDGEMENTS

The author is very grateful to his major professor, Dr. Richard Danofsky, for his guidance, suggestions, and help in completing this research. Also, the author wishes to express his gratitude to his friends, Elden Plettner, John Sankoorikal, and Masoud Feiz for their freely given help during the experimental portion of this work and to Ms. Jo Sedore for her typing and assistance in completing the process. Finally, special thanks are extended to the author's parents, Joseph and Dorothy Hennessy, and to Felicia Plesic, for their encouragement and support during this period.

X. APPENDIX A: LISTING OF COMPUTER PROGRAMS

This appendix contains listings of the computer programs used in the Green's function modeling of the UTR-10 reactor. The first program, GFP-20, uses the criticality equations to calculate the determinant of matrix A.

```
1.      //C300  JOB  U3780,WJH
2.      //STEP1  EXEC  WATFIV,REGION=192K,LIB='SYS2.WATFIV.IMSL.DOUBLE'
3.      //GO.SYSIN  DD  *
4.      $JOB              'WJH',TIME=5,PAGES=10
5.      C      THIS PROGRAM IS GFP20-IT CALCS. DET A FOR 2 GROUPS
6.      C      THE PROGRAM IS USED TO LOCATE THE VALUE OF Z WHICH RESULTS
7.      C          IN A ZERO DETERMINANT OF MATRIX A
8.             DOUBLE PRECISION PI,SIGA0M,SIGAFL,DF1L,DF2L,A1,B1,B2,B3,B4,B5
9.             DOUBLE PRECISION Y0,SRM,SRFL,SFL,SFR,NUL,MUL,A2,QL,RL,NU2L,MU2L
10.            DOUBLE PRECISION BTFL,BT2FL,BK,SAM,SAFL,DM1,DM2,BETA
11.            DOUBLE PRECISION DEXP,DSQRT,FISL,BZ,DABS,DSIN,DCOS
12.            DOUBLE PRECISION BTM,BT2M,ALFL,AFL,ALM,AL2M,STEP,Z
13.            DOUBLE PRECISION SIGAFR,DF1R,DF2R,SAFR,SRFR,BT2FR,BTFR
14.            DOUBLE PRECISION ALFR,AFR,FISR,MU2R,MUR,NU2R,NUR,QR,RR
15.            REAL A(20,20),B(20),G1(100),G(100),WKAREA(700),D1,D2,DET
16.            INTEGER I,J,K,L,M,N,IA,IDGT,IER,IJOB,P
17.            PI=3.141592654
18.     C      THESE ARE THE TWO GROUP PARAMETERS
19.            SIGA0M=0.00030661
20.            SIGAFL=0.055405
21.            SIGAFR=0.055719
22.            DF1L=1.421447
23.            DF1R=1.421447
24.            DF2L=0.231576
25.            DF2R=0.231576
26.            DM1=1.152864
27.            DM2=0.991810
28.            BETA=0.0065
29.            SAFL=0.002076
30.            SAFR=0.002082
31.            SAM=0.5326368D-07
32.            SFL=0.08233
33.            SFR=0.08397
34.            SRFL=0.03364
35.            SRFR=0.03447
36.            SRM=0.00287363
37.            Y0=22.65
38.            B5=32.36
39.            B4=16.11
40.            B3=22.65
41.            B2=16.11
42.            B1=32.36
43.            B3=Y0+B3
44.     C      THIS IS THE ESTIMATED VALUE OF Z
45.            Z=67.
46.            A1=111.760
47.     C      THIS IS THE STEP SIZE BY WHICH Z IS INCREMENTED IN THE SEARCH
48.            STEP=0.1
49.     C      THE MAIN LOOP CALCULATES A NEW DET A FOR EACH Z
50.            DO 20 K=1,100
51.            Z=Z+STEP
52.            BZ=(PI/Z)**2.
53.            IJOB=4
54.            N=20
55.            IA=20
56.     C      THE ELEMENTS OF A ARE INITIALLY SET=0. FOR EACH STEP
57.            DO 10 I=1,20
58.            B(I)=0.
59.            DO 11 J=1,20
60.            A(I,J)=0.
```

```
   11    CONTINUE
   10    CONTINUE
         D1=0.
C        THESE STEPS CALCULATE THE SOLUTION EQUATION PARAMETERS
         BK=(PI/A1)**2.
         BT2M=BK+(SIGAOM/DM2)+BZ
         BTM=DSQRT(BT2M)
         BT2FL=BK+(SIGAFL/DF2L)+BZ
         BT2FR=BK+(SIGAFR/DF2R)+BZ
         BTFL=DSQRT(BT2FL)
         BTFR=DSQRT(BT2FR)
         AL2M=BK+(SAM+SRM)/DM1+BZ
         ALM=DSQRT(AL2M)
         AFL=BK+(SAFL+SRFL)/DF1L+BZ
         AFR=BK+(SAFR+SRFR)/DF1R+BZ
         ALFL=DSQRT(AFL)
         ALFR=DSQRT(AFR)
         A2=(SRM/DM2)/(AL2M-BT2M)
         FISL=(SFL*SRFL)/(DF1L*DF2L)
         FISR=(SFR*SRFR)/(DF1R*DF2R)
         MU2L=(AFL+BT2FL)/2.+DSQRT((AFL+BT2FL)**2.-4*(BT2FL*AFL-FISL))/2.
         MU2R=(AFR+BT2FR)/2.+DSQRT((AFR+BT2FR)**2.-4*(BT2FR*AFR-FISR))/2.
         MUL=DSQRT(MU2L)
         MUR=DSQRT(MU2R)
         NU2L=(AFL+BT2FL)/2.-DSQRT((AFL+BT2FL)**2.-4*(BT2FL*AFL-FISL))/2.
         NU2R=(AFR+BT2FR)/2.-DSQRT((AFR+BT2FR)**2.-4*(BT2FR*AFR-FISR))/2.
         NUL=DSQRT(DABS(NU2L))
         NUR=DSQRT(DABS(NU2R))
         QL=(SRFL/DF2L)/(MU2L-BT2FL)
         QR=(SRFR/DF2R)/(MU2R-BT2FR)
         RL=-(SRFL/DF2L)/(NU2L+BT2FL)
         RR=-(SRFR/DF2R)/(NU2R+BT2FR)
C        MATRIX A IS LOADED HERE
         A(1,1)=1.
         A(1,2)=1.
         A(2,3)=1.
         A(2,4)=1.
         A(3,1)=DEXP(-ALM*B1)
         A(3,2)=DEXP(ALM*B1)
         A(3,5)=-1.
         A(3,6)=-1.
         A(3,7)=-1.
         A(3,8)=0.
         A(4,1)=-A2*DEXP(-ALM*B1)
         A(4,2)=-A2*DEXP(ALM*B1)
         A(4,3)=DEXP(-BTM*B1)
         A(4,4)=DEXP(BTM*B1)
         A(4,5)=QL
         A(4,6)=QL
         A(4,7)=RL
         A(4,8)=0.
         A(5,1)=-DM1*ALM*DEXP(-ALM*B1)
         A(5,2)=DM1*ALM*DEXP(ALM*B1)
         A(5,5)=DF1L*MUL
         A(5,6)=-DF1L*MUL
         A(5,7)=0.
         A(5,8)=-DF1L*NUL
         A(6,1)=DM2*A2*ALM*DEXP(-ALM*B1)
         A(6,2)=-DM2*A2*ALM*DEXP(ALM*B1)
         A(6,3)=-DM2*BTM*DEXP(-BTM*B1)
```

```
121.            A(6,4)=DM2*BTM*DEXP(BTM*B1)
122.            A(6,5)=-DF2L*QL*MUL
123.            A(6,6)=DF2L*QL*MUL
124.            A(6,7)=0.
125.            A(6,8)=DF2L*RL*NUL
126.            A(7,5)=DEXP(-MUL*B2)
127.            A(7,6)=DEXP(MUL*B2)
128.            A(7,7)=DCOS(NUL*B2)
129.            A(7,8)=DSIN(NUL*B2)
130.            A(7,9)=-1.
131.            A(7,10)=-1.
132.            A(8,5)=-QL*DEXP(-MUL*B2)
133.            A(8,6)=-QL*DEXP(MUL*B2)
134.            A(8,7)=-RL*DCOS(NUL*B2)
135.            A(8,8)=-RL*DSIN(NUL*B2)
136.            A(8,9)=A2
137.            A(8,10)=A2
138.            A(8,11)=-1.
139.            A(8,12)=-1.
140.            A(9,5)=-DF1L*MUL*DEXP(-MUL*B2)
141.            A(9,6)=DF1L*MUL*DEXP(MUL*B2)
142.            A(9,7)=-DF1L*NUL*DSIN(NUL*B2)
143.            A(9,8)=DF1L*NUL*DCOS(NUL*B2)
144.            A(9,9)=DM1*ALM
145.            A(9,10)=-DM1*ALM
146.            A(10,5)=DF2L*QL*MUL*DEXP(-MUL*B2)
147.            A(10,6)=-DF2L*QL*MUL*DEXP(MUL*B2)
148.            A(10,7)=DF2L*RL*NUL*DSIN(NUL*B2)
149.            A(10,8)=-DF2L*RL*NUL*DCOS(NUL*B2)
150.            A(10,9)=-DM2*A2*ALM
151.            A(10,10)=DM2*A2*ALM
152.            A(10,11)=DM2*BTM
153.            A(10,12)=-DM2*BTM
154.            A(11,9)=DEXP(-ALM*B3)
155.            A(11,10)=DEXP(ALM*B3)
156.            A(11,13)=-1.
157.            A(11,14)=-1.
158.            A(11,15)=-1.
159.            A(11,16)=0.
160.            A(12,9)=-A2*DEXP(-ALM*B3)
161.            A(12,10)=-A2*DEXP(ALM*B3)
162.            A(12,11)=DEXP(-BTM*B3)
163.            A(12,12)=DEXP(BTM*B3)
164.            A(12,13)=QR
165.            A(12,14)=QR
166.            A(12,15)=RR
167.            A(12,16)=0.
168.            A(13,9)=-DM1*ALM*DEXP(-ALM*B3)
169.            A(13,10)=DM1*ALM*DEXP(ALM*B3)
170.            A(13,13)=DF1R*MUR
171.            A(13,14)=-DF1R*MUR
172.            A(13,15)=0.
173.            A(13,16)=-DF1R*NUR
174.            A(14,9)=DM2*A2*ALM*DEXP(-ALM*B3)
175.            A(14,10)=-DM2*A2*ALM*DEXP(ALM*B3)
176.            A(14,11)=-DM2*BTM*DEXP(-BTM*B3)
177.            A(14,12)=DM2*BTM*DEXP(BTM*B3)
178.            A(14,13)=-DF2R*QR*MUR
179.            A(14,14)=DF2R*QR*MUR
180.            A(14,15)=0.
```

```
181.            A(14,16)=DF2R*RR*NUR
182.            A(15,13)=DEXP(-MUR*B4)
183.            A(15,14)=DEXP(MUR*E4)
184.            A(15,15)=DCOS(NUR*B4)
185.            A(15,16)=DSIN(NUR*B4)
186.            A(15,17)=-1.
187.            A(15,18)=-1.
188.            A(16,13)=-QR*DEXP(-MUR*B4)
189.            A(16,14)=-QR*DEXP(MUR*B4)
190.            A(16,15)=-RR*DCOS(NUR*B4)
191.            A(16,16)=-RR*DSIN(NUR*B4)
192.            A(16,17)=A2
193.            A(16,18)=A2
194.            A(16,19)=-1.
195.            A(16,20)=-1.
196.            A(17,13)=-DF1R*MUR*DEXP(-MUR*B4)
197.            A(17,14)=DF1R*MUR*DEXP(MUR*B4)
198.            A(17,15)=-DF1R*NUR*DSIN(NUR*B4)
199.            A(17,16)=DF1R*NUR*DCOS(NUR*B4)
200.            A(17,17)=DM1*ALM
201.            A(17,18)=-DM1*ALM
202.            A(18,13)=DF2R*QR*MUR*DEXP(-MUR*B4)
203.            A(18,14)=-DF2R*QR*MUR*DEXP(MUR*B4)
204.            A(18,15)=DF2R*RR*NUR*DSIN(NUR*B4)
205.            A(18,16)=-DF2R*RR*NUR*DCOS(NUR*B4)
206.            A(18,17)=-DM2*A2*ALM
207.            A(18,18)=DM2*A2*ALM
208.            A(18,19)=DM2*BTM
209.            A(18,20)=-DM2*BTM
210.            A(19,17)=DEXP(-ALM*B5)
211.            A(19,18)=DEXP(ALM*B5)
212.            A(20,17)=-A2*DEXP(-ALM*B5)
213.            A(20,18)=-A2*DEXP(ALM*B5)
214.            A(20,19)=DEXP(-BTM*B5)
215.            A(20,20)=DEXP(BTM*B5)
216.      C     THE SUBROUTINE LINV3F IS USED TO CALCULATE DET A
217.            CALL LINV3F (A,B,IJOB,N,1A,D1,D2,WKAREA,IER)
218.      C     THE PROGRAM STOPS IF A TERMINAL ERROR IS RECIEVED FROM THE
219.      C         SUBROUTINE.  THE TERMINAL ERROR INDICATES THAT THE
220.      C         DETERMINANT IS NEAR ZERO.
221.            IF (IER.EQ.130) GO TO 25
222.            DET=D1*2.**D2
223.            WRITE (6,12) DET,Z
224.      12    FORMAT (' THE DETERMINANT IS ',E12.5,' AT Z= ',F8.5)
225.      20    CONTINUE
226.      25    STOP
227.            END
228.      $ENTRY
```

The next program, GFP-24, calculates the Green's functions, G.

```
1.      //C300   JOB   U3780,WJH
2.      //STEP1   EXEC   FORTGCG,REGION=300K,TIME=(,40),LIB='SYS1.IMSL.DOUBLE'
3.      //FORT.SYSIN   DD   *
4.      C       THIS PROGRAM IS GFP24PL-IT CALCS./PLOTS THE G.F. FOR 2 GROUPS
5.              DOUBLE PRECISION PI,SIGA0M,SIGAFL,DF1L,DF2L,A1,B1,B2,B3,B4,B5
6.              DOUBLE PRECISION Y0,SRM,SRFL,SFL,SFR,NUL,MUL,A2,QL,RL,NU2L,MU2L
7.              DOUBLE PRECISION BTFL,BT2FL,BK,SAM,SAFL,DM1,DM2,BETA
8.              DOUBLE PRECISION DEXP,DSQRT,FISL,BZ,DABS,DSIN,DCOS
9.              DOUBLE PRECISION BTM,BT2M,ALFL,AFL,ALM,AL2M,STEP,Z
10.             DOUBLE PRECISION SIGAFR,DF1R,DF2R,SAFR,SRFR,BT2FR,BTFR
11.             DOUBLE PRECISION ALFR,AFR,FISR,MU2R,MUR,NU2R,NUR,QR,RR
12.             DOUBLE PRECISION Y2K1,Y2K2,Y2K3,Y2K4,Y2K5,Y2K6
13.             DOUBLE PRECISION Y3,X0,Y,BB,YB,X1,G1
14.             REAL A(24,24),B(24),WKAREA(700),D1,D2,X(100),G(100),G3(100)
15.             INTEGER I,J,K,L,M,IA,IDGT,IER,IJOB,Y1
16.             PI=3.141592654
17.     C       THESE ARE THE TWO GROUP PARAMETERS
18.             SIGA0M=0.00030661
19.             SIGAFL=0.055405
20.             SIGAFR=0.055719
21.             DF1L=1.421447
22.             DF1R=1.421447
23.             DF2L=0.231576
24.             DF2R=0.231576
25.             DM1=1.152864
26.             DM2=0.991810
27.             BETA=0.0065
28.             SAFL=0.002076
29.             SAFR=0.002082
30.             SAM=0.5326368D-07
31.             SFL=0.08233
32.             SFR=0.08397
33.             SRFL=0.03364
34.             SRFR=0.03447
35.             SRM=0.00287363
36.             Y0=22.65
37.             B5=32.36
38.             B4=16.11
39.             B3=22.65
40.             B2=16.11
41.             B1=32.36
42.             Z=68.32755
43.             Y1=61
44.             A1=111.760
45.     C       STEP IS THE SIZE OF THE INCREMENTS IN Y ACROSS THE CORE
46.             STEP=142.24/60.
47.             X0=55.88
48.             X1=55.88
49.             Y=0.
50.             BZ=(PI/Z)**2.
51.             IJOB=2
52.             N=24
53.             IA=24
54.     C       THIS STARTS THE MAIN LOOP WHICH CALCULATES THE GREENS
55.     C           FUNCTIONS AT EACH Y
56.             DO 50 L=1,Y1
57.             X(L)=Y
58.             G(L)=0.
59.     C       THIS IS THE MODE LOOP- THE LIBRARY SUBROUTINE RETURNS
60.     C           A TERMINAL ERROR MESSAGE FOR K>13
```

```
      DO 20 K=1,13
C     INITIALLY THE ELEMENTS OF A AND B ARE SET=0.
      DO 10 I=1,24
      B(I)=0.
      DO 11 J=1,24
      A(I,J)=0.
11    CONTINUE
10    CONTINUE
      B(14)=1.
      D1=0.
C     THESE STEPS CALCULATE THE SOLUTION EQUATION PARAMETERS
      BK=(K*PI/A1)**2.
      BT2M=BK+(SIGA0M/DM2)+BZ
      BTM=DSQRT(BT2M)
      BT2FL=BK+(SIGAFL/DF2L)+BZ
      BT2FR=BK+(SIGAFR/DF2R)+BZ
      BTFL=DSQRT(BT2FL)
      BTFR=DSQRT(BT2FR)
      AL2M=BK+(SAM+SRM)/DM1+BZ
      ALM=DSQRT(AL2M)
      AFL=BK+(SAFL+SRFL)/DF1L+BZ
      AFR=BK+(SAFR+SRFR)/DF1R+BZ
      ALFL=DSQRT(AFL)
      ALFR=DSQRT(AFR)
      A2=(SRM/DM2)/(AL2M-BT2M)
      FISL=((1.-BETA)*SFL*SRFL)/(DF1L*DF2L)
      FISR=((1.-BETA)*SFR*SRFR)/(DF1R*DF2R)
      MU2L=(AFL+BT2FL)/2.+DSQRT((AFL+BT2FL)**2.-4*(BT2FL*AFL-FISL))/2.
      MU2R=(AFR+BT2FR)/2.+DSQRT((AFR+BT2FR)**2.-4*(BT2FR*AFR-FISR))/2.
      MUL=DSQRT(MU2L)
      MUR=DSQRT(MU2R)
      NU2L=(AFL+BT2FL)/2.-DSQRT((AFL+BT2FL)**2.-4*(BT2FL*AFL-FISL))/2.
      NU2R=(AFR+BT2FR)/2.-DSQRT((AFR+BT2FR)**2.-4*(BT2FR*AFR-FISR))/2.
      NUL=DSQRT(DABS(NU2L))
      NUR=DSQRT(DABS(NU2R))
      QL=(SRFL/DF2L)/(MU2L-BT2FL)
      QR=(SRFR/DF2R)/(MU2R-BT2FR)
      RL=-(SRFL/DF2L)/(NU2L+BT2FL)
      RR=-(SRFR/DF2R)/(NU2R+BT2FR)
      IF (NU2L.LT.0.) GO TO 40
      RL=(SRFL/DF2L)/(NU2L-BT2FL)
40    IF (NU2R.LT.0.) GO TO 41
      RR=(SRFR/DF2R)/(NU2R-BT2FR)
C     LOAD MATRIX A HERE
41    A(1,1)=1.
      A(1,2)=1.
      A(2,3)=1.
      A(2,4)=1.
      A(3,1)=DEXP(-ALM*B1)
      A(3,2)=DEXP(ALM*B1)
      A(3,5)=-1.
      A(3,6)=-1.
      A(3,7)=-1.
      A(3,8)=0.
      A(4,1)=-A2*DEXP(-ALM*B1)
      A(4,2)=-A2*DEXP(ALM*B1)
      A(4,3)=DEXP(-BTM*B1)
      A(4,4)=DEXP(BTM*B1)
      A(4,5)=QL
      A(4,6)=QL
```

```
121.            A(4,7)=RL
122.            A(4,8)=0.
123.            A(5,1)=-DM1*ALM*DEXP(-ALM*B1)
124.            A(5,2)=DM1*ALM*DEXP(ALM*B1)
125.            A(5,5)=DF1L*MUL
126.            A(5,6)=-DF1L*MUL
127.            A(5,7)=0.
128.            A(5,8)=-DF1L*NUL
129.            A(6,1)=DM2*A2*ALM*DEXP(-ALM*B1)
130.            A(6,2)=-DM2*A2*ALM*DEXP(ALM*B1)
131.            A(6,3)=-DM2*BTM*DEXP(-BTM*B1)
132.            A(6,4)=DM2*BTM*DEXP(BTM*B1)
133.            A(6,5)=-DF2L*QL*MUL
134.            A(6,6)=DF2L*QL*MUL
135.            A(6,7)=0.
136.            A(6,8)=DF2L*RL*NUL
137.            A(7,5)=DEXP(-MUL*B2)
138.            A(7,6)=DEXP(MUL*B2)
139.            A(7,7)=DCOS(NUL*B2)
140.            A(7,8)=DSIN(NUL*B2)
141.            A(7,9)=-1.
142.            A(7,10)=-1.
143.            A(8,5)=-QL*DEXP(-MUL*B2)
144.            A(8,6)=-QL*DEXP(MUL*B2)
145.            A(8,7)=-RL*DCOS(NUL*B2)
146.            A(8,8)=-RL*DSIN(NUL*B2)
147.            A(8,9)=A2
148.            A(8,10)=A2
149.            A(8,11)=-1.
150.            A(8,12)=-1.
151.            A(9,5)=-DF1L*MUL*DEXP(-MUL*B2)
152.            A(9,5)=DF1L*MUL*DEXP(MUL*B2)
153.            A(9,7)=-DF1L*NUL*DSIN(NUL*B2)
154.            A(9,8)=DF1L*NUL*DCOS(NUL*B2)
155.            A(9,9)=DM1*ALM
156.            A(9,10)=-DM1*ALM
157.            A(10,5)=DF2L*QL*MUL*DEXP(-MUL*B2)
158.            A(10,6)=-DF2L*QL*MUL*DEXP(MUL*B2)
159.            A(10,7)=DF2L*RL*NUL*DSIN(NUL*B2)
160.            A(10,8)=-DF2L*FL*NUL*DCOS(NUL*B2)
161.            A(10,9)=-DM2*A2*ALM
162.            A(10,10)=DM2*A2*ALM
163.            A(10,11)=DM2*BTM
164.            A(10,12)=-DM2*BTM
165.            A(11,9)=DEXP(-ALM*Y0)
166.            A(11,10)=DEXP(ALM*Y0)
167.            A(11,13)=-1.
168.            A(11,14)=-1.
169.            A(12,9)=-A2*DEXP(-ALM*Y0)
170.            A(12,10)=-A2*DEXP(ALM*Y0)
171.            A(12,11)=DEXP(-BTM*Y0)
172.            A(12,12)=DEXP(BTM*Y0)
173.            A(12,13)=A2
174.            A(12,14)=A2
175.            A(12,15)=-1.
176.            A(12,16)=-1.
177.            A(13,9)=-DM1*ALM*DEXP(-ALM*Y0)
178.            A(13,10)=DM1*ALM*DEXP(ALM*Y0)
179.            A(13,13)=DM1*ALM
180.            A(13,14)=-DM1*ALM
```

```
181.          A(14,9)=A2*ALM*DEXP(-ALM*Y0)
182.          A(14,10)=-A2*ALM*DEXP(ALM*Y0)
183.          A(14,11)=-BTM*DEXP(-BTM*Y0)
184.          A(14,12)=BTM*DEXP(BTM*Y0)
185.          A(14,13)=-A2*ALM
186.          A(14,14)=A2*ALM
187.          A(14,15)=BTM
188.          A(14,16)=-BTM
189.          A(15,13)=DEXP(-ALM*B3)
190.          A(15,14)=DEXP(ALM*B3)
191.          A(15,17)=-1.
192.          A(15,18)=-1.
193.          A(15,19)=-1.
194.          A(15,20)=0.
195.          A(16,13)=-A2*DEXP(-ALM*B3)
196.          A(16,14)=-A2*DEXP(ALM*B3)
197.          A(16,15)=DEXP(-BTM*B3)
198.          A(16,16)=DEXP(BTM*B3)
199.          A(16,17)=QR
200.          A(16,18)=QR
201.          A(16,19)=RR
202.          A(16,20)=0.
203.          A(17,13)=-DM1*ALM*DEXP(-ALM*B3)
204.          A(17,14)=DM1*ALM*DEXP(ALM*B3)
205.          A(17,17)=DF1R*MUR
206.          A(17,18)=-DF1R*MUR
207.          A(17,19)=0.
208.          A(17,20)=-DF1R*NUR
209.          A(18,13)=DM2*A2*ALM*DEXP(-ALM*B3)
210.          A(18,14)=-DM2*A2*ALM*DEXP(ALM*B3)
211.          A(18,15)=-DM2*BTM*DEXP(-BTM*B3)
212.          A(18,16)=DM2*BTM*DEXP(BTM*B3)
213.          A(18,17)=-DF2R*QR*MUR
214.          A(18,18)=DF2R*QR*MUR
215.          A(18,19)=0.
216.          A(18,20)=DF2R*RR*NUR
217.          A(19,17)=DEXP(-MUR*B4)
218.          A(19,18)=DEXP(MUR*B4)
219.          A(19,19)=DCOS(NUR*B4)
220.          A(19,20)=DSIN(NUR*B4)
221.          A(19,21)=-1.
222.          A(19,22)=-1.
223.          A(20,17)=-QR*DEXP(-MUR*B4)
224.          A(20,18)=-QR*DEXP(MUR*B4)
225.          A(20,19)=-RR*DCOS(NUR*B4)
226.          A(20,20)=-RR*DSIN(NUR*B4)
227.          A(20,21)=A2
228.          A(20,22)=A2
229.          A(20,23)=-1.
230.          A(20,24)=-1.
231.          A(21,17)=-DF1R*MUR*DEXP(-MUR*B4)
232.          A(21,18)=DF1R*MUR*DEXP(MUR*B4)
233.          A(21,19)=-DF1R*NUR*DSIN(NUR*B4)
234.          A(21,20)=DF1R*NUR*DCOS(NUR*B4)
235.          A(21,21)=DM1*ALM
236.          A(21,22)=-DM1*ALM
237.          A(22,17)=DF2R*QR*MUR*DEXP(-MUR*B4)
238.          A(22,18)=-DF2R*QR*MUR*DEXP(MUR*B4)
239.          A(22,19)=DF2R*RR*NUR*DSIN(NUR*B4)
240.          A(22,20)=-DF2R*RR*NUR*DCOS(NUR*B4)
```

```
241.            A(22,21)=-DM2*A2*ALM
242.            A(22,22)=DM2*A2*ALM
243.            A(22,23)=DM2*BTM
244.            A(22,24)=-DM2*BTM
245.            A(23,21)=DEXP(-ALM*B5)
246.            A(23,22)=DEXP(ALM*B5)
247.            A(24,21)=-A2*DEXP(-ALM*B5)
248.            A(24,22)=-A2*DEXP(ALM*B5)
249.            A(24,23)=DEXP(-BTM*B5)
250.            A(24,24)=DEXP(BTM*B5)
251.      C     THESE ELEMENTS OF A HAVE DIFFERENT VALUES DEPENDING ON THE
252.      C          SIGN OF NU2L
253.            IF (NU2L.LT.0.) GO TO 30
254.            A(3,8)=-1.
255.            A(4,8)=PL
256.            A(5,7)=DF1L*NUL
257.            A(6,7)=-DF2L*RL*NUL
258.            A(7,7)=DEXP(-NUL*B2)
259.            A(7,8)=DEXP(NUL*B2)
260.            A(8,7)=-RL*DEXP(-NUL*B2)
261.            A(8,8)=-RL*DEXP(NUL*B2)
262.            A(9,7)=-DF1L*NUL*DEXP(-NUL*B2)
263.            A(9,8)=DF1L*NUL*DEXP(NUL*B2)
264.            A(10,7)=DF2L*RL*NUL*DEXP(-NUL*B2)
265.            A(10,8)=-DF2L*RL*NUL*DEXP(NUL*B2)
266.            IF (NU2R.LT.0.) GO TO 30
267.            A(15,20)=-1.
268.            A(16,20)=RR
269.            A(17,19)=DF1R*NUR
270.            A(18,19)=-DF2R*RR*NUR
271.            A(19,19)=DEXP(-NUR*B4)
272.            A(19,20)=DEXP(NUR*B4)
273.            A(20,19)=-RR*DEXP(-NUR*B4)
274.            A(20,20)=-RR*DEXP(NUR*B4)
275.            A(21,19)=-DF1R*NUR*DEXP(-NUR*B4)
276.            A(21,20)=DF1R*NUR*DEXP(NUR*B4)
277.            A(22,19)=DF2R*RR*NUR*DEXP(-NUR*B4)
278.            A(22,20)=-DF2R*RR*NUR*DEXP(NUR*B4)
279.      C     THE LIBRARY SUBROUTINE LINV3F IS CALLED TO SOLVE FOR X IN A*X=B
280.      30    CALL LINV3F (A,B,IJOB,N,IA,D1,D2,WKAREA,IER)
281.      C     THESE STEPS CALCULATE THE GREENS FUNCTIONS FOR EACH MODE-
282.      C          THE VALUE OF Y DETERMINES WHICH EQUATION IS TO BE USED.
283.            IF (IER.EQ.130) GO TO 25
284.            IF (Y.GT.B1) GO TO 60
285.            Y2K1=B(3)*DEXP(-BTM*Y)+B(4)*DEXP(BTM*Y)-A2*(B(1)*DEXP(-ALM*Y)
286.           &+B(2)*DEXP(ALM*Y))
287.            YB=Y2<1
288.            GO TO 69
289.      60    CONTINUE
290.            BB=B1+B2
291.            IF (Y.GT.BB) GO TO 61
292.            Y3=Y-(BB-B2)
293.            IF (NU2L.LT.0.) GO TO 65
294.            Y2K2=-QL*(B(5)*DEXP(-MUL*Y3)+B(6)*DEXP(MUL*Y3))-RL*(B(7)*DEX>
295.           &(-NUL*Y3)+B(8)*DEXP(NUL*Y3))
296.            YB=Y2<2
297.            GO TO 69
298.      65    CONTINUE
299.            Y2K2=-QL*(B(5)*DEXP(-MUL*Y3)+B(6)*DEXP(MUL*Y3))-RL*(B(7)*DCOS
300.           &(NUL*Y3)+B(8)*DSIN(NUL*Y3))
```

```
301.              YB=Y2K2
302.              GO TO 69
303.        61    CONTINUE
304.              BB=BB+Y0
305.              IF (Y.GT.BB) GO TO 62
306.              Y3=Y-(BB-Y0)
307.              Y2K3=B(11)*DEXP(-BTM*Y3)+B(12)*DEXP(BTM*Y3)-A2*(B(9)*DEXP
308.             &(-ALM*Y3)+B(10)*DEXP(ALM*Y3))
309.              YB=Y2K3
310.              GO TO 69
311.        62    CONTINUE
312.              BB=BB+B3
313.              IF (Y.GT.BB) GO TO 63
314.              Y3=Y-(BB-B3)
315.              Y2K4=B(15)*DEXP(-BTM*Y3)+B(16)*DEXP(BTM*Y3)-A2*(B(13)*DEXP
316.             &(-ALM*Y3)+B(14)*DEXP(ALM*Y3))
317.              YB=Y2K4
318.              GO TO 69
319.        63    CONTINUE
320.              BB=BB+B4
321.              IF (Y.GT.BB) GO TO 64
322.              Y3=Y-(BB-B4)
323.              IF (NU2R.LT.0.) GO TO 66
324.              Y2K5=-QR*(B(17)*DEXP(-MUR*Y3)+B(18)*DEXP(MUR*Y3))-RR*(B(19)
325.             &*DEXP(-NUR*Y3)+B(20)*DEXP(NUR*Y3))
326.              YB=Y2K5
327.              GO TO 69
328.        66    CONTINUE
329.              Y2K5=-QR*(B(17)*DEXP(-MUR*Y3)+B(18)*DEXP(MUR*Y3))-RR*(B(19)
330.             &*DCOS(NUR*Y3)+B(20)*DSIN(NUR*Y3))
331.              YB=Y2K5
332.              GO TO 69
333.        64    CONTINUE
334.              Y3=Y-BB
335.              Y2K6=B(23)*DEXP(-BTM*Y3)+B(24)*DEXP(BTM*Y3)-A2*(B(21)*DEXP
336.             &(-ALM*Y3)+B(22)*DEXP(ALM*Y3))
337.              YB=Y2K6
338.        69    CONTINUE
339.              G1=G(L)
340.        C     ALL THE GREENS FUNCTIONS ARE SUMMED AT EACH Y
341.              G(L)=2./A1*DSIN(BK*X0)*DSIN(BK*X1)*YB+G(L)
342.        20    CONTINUE
343.              IF (Y.LT.(B1+B2).OR.Y.GT.(B1+B2+B3+Y0)) GO TO 51
344.        C     THE SUBROUTINE CENT IS CALLED WHEN Y IS IN THE
345.        C         CENTRAL GRAPHITE REGION
346.              CALL CENT(G,L,Y,IER,Y0)
347.              IF (IER.EQ.130) GO TO 25
348.        51    Y=Y+STEP
349.        50    CONTINUE
350.        C     THESE STEPS PRINT AND PLOT THE RESULTS- ADDITIONAL STEPS MAY
351.        C         BE ADDED HERE WHICH PUNCH
352.              Y=0.
353.              DO 70 I=1,Y1
354.              WRITE (6,55) Y,G(I)
355.        55    FORMAT (' Y= ',F6.2,'  GREENS FUNCTION= ',D12.5)
356.              Y=Y+STEP
357.              G3(I)=ALOG10(G(I))
358.        70    CONTINUE
359.              CALL GRAPH (61,X,G3,11,1,10.0,-8.0,15.0,0.0,3.0,-3.0,
360.             &'Y, CM.;','GREENS FUNCTIONS;','GFP24PL;','X=CENTER;')
```

```
361.            GO TO 27
362.      25    WRITE (6,26) K,L
363.      26    FORMAT (' K= ',I2,' L= ',I2)
364.      27    STOP
365.            END
366.            SUBROUTINE CENT(G,L,Y,IER,Y0)
367.      C     THIS SUBROUTINE IS USED TO ADD 7 MORE MODES TO THE GREENS
368.      C         FUNCTION WHEN Y IS IN THE CENTRAL GRAPHITE REGION
369.            DOUBLE PRECISION PI,SIGA0M,A1,B1,B2,B3,Y0,SRM,A2,E
370.            DOUBLE PRECISION BK,SAM,DM1,DM2,DEXP,DSQRT,BZ
371.            DOUBLE PRECISION BTM,BT2M,ALM,AL2M,STEP,Z
372.            DOUBLE PRECISION Y3,X0,Y,BB,YB,X1,G1,Y2K3,Y2K4
373.            REAL A(8,8),B(8),WKAREA(700),D1,D2,DET,G(100)
374.            INTEGER I,J,K,L,M,N,IA,IDGT,IER,IJOB,P,Y1
375.            PI=3.141592654
376.            SIGA0M=0.00030661
377.            DM1=1.152864
378.            DM2=0.991810
379.            SAM=0.5326368D-07
380.            SRM=0.00287363
381.            B3=22.65
382.            B2=16.11
383.            B1=32.36
384.            Z=68.32755
385.            A1=111.760
386.            X0=55.88
387.            X1=55.88
388.            BZ=(PI/Z)**2.
389.            IJOB=2
390.            DO 75 K=14,21
391.            BK=(K*PI/A1)**2.
392.            BT2M=BK+(SIGA0M/DM2)+BZ
393.            BTM=DSQRT(BT2M)
394.            AL2M=BK+(SAM+SRM)/DM1+BZ
395.            ALM=DSQRT(AL2M)
396.            A2=(SRM/DM2)/(AL2M-BT2M)
397.            N=8
398.            IA=8
399.            DO 76 I=1,8
400.            B(I)=0.
401.            DO 77 J=1,8
402.            A(I,J)=0.
403.      77    CONTINUE
404.      76    CONTINUE
405.            B(6)=1.
406.            A(1,1)=1.
407.            A(1,2)=1.
408.            A(2,1)=-A2
409.            A(2,2)=-A2
410.            A(2,3)=1.
411.            A(2,4)=1.
412.            A(3,1)=DEXP(-ALM*Y0)
413.            A(3,2)=DEXP(ALM*Y0)
414.            A(3,3)=-1.
415.            A(3,4)=-1.
416.            A(4,1)=-A2*DEXP(-ALM*Y0)
417.            A(4,2)=-A2*DEXP(ALM*Y0)
418.            A(4,3)=DEXP(-BTM*Y0)
419.            A(4,4)=DEXP(BTM*Y0)
420.            A(4,5)=A2
```

```
421.            A(4,6)=A2
422.            A(4,7)=-1.
423.            A(4,8)=-1.
424.            A(5,1)=-DM1*ALM*DEXP(-ALM*Y0)
425.            A(5,2)=DM1*ALM*DEXP(ALM*Y0)
426.            A(5,5)=DM1*ALM
427.            A(5,6)=-DM1*ALM
428.            A(6,1)=A2*ALM*DEXP(-ALM*Y0)
429.            A(6,2)=-A2*ALM*DEXP(ALM*Y0)
430.            A(6,3)=-BTM*DEXP(-BTM*Y0)
431.            A(6,4)=BTM*DEXP(BTM*Y0)
432.            A(6,5)=-A2*ALM
433.            A(6,6)=A2*ALM
434.            A(6,7)=BTM
435.            A(6,8)=-BTM
436.            A(7,5)=DEXP(-ALM*B3)
437.            A(7,6)=DEXP(ALM*B3)
438.            A(8,5)=-A2*DEXP(-ALM*B3)
439.            A(8,6)=-A2*DEXP(ALM*B3)
440.            A(8,7)=DEXP(-BTM*B3)
441.            A(8,8)=DEXP(BTM*B3)
442.            CALL LINV3F (A,B,IJOB,N,IA,D1,D2,WKAREA,IER)
443.            IF (IER.EQ.130) GO TO 85
444.            BB=B1+B2+Y0
445.            IF (Y.GT.BB) GO TO 72
446.            Y3=Y-(BB-Y0)
447.            Y2K3=B(3)*DEXP(-BTM*Y3)+B(4)*DEXP(BTM*Y3)-A2*(B(1)*DEXP
448.           &(-ALM*Y3)+B(2)*DEXP(ALM*Y3))
449.            YB=Y2K3
450.            GO TO 73
451.      72    BB=BB+B3
452.            Y3=Y-(BB-B3)
453.            Y2K4=B(7)*DEXP(-BTM*Y3)+B(8)*DEXP(BTM*Y3)-A2*(B(5)*DEXP
454.           &(-ALM*Y3)+B(6)*DEXP(ALM*Y3))
455.            YB=Y2K4
456.      73    CONTINUE
457.            G(L)=2./A1*DSIN(BK*X0)*DSIN(BK*X1)*YB+G(L)
458.      75    CONTINUE
459.            GO TO 87
460.      85    WRITE (6,86) K,L
461.      86    FORMAT (' IN THE SUBROUTINE CENT IER=130 AT K= ',I2,' L=',I2)
462.      87    RETURN
463.            END
464.      //GO.SYSIN  DD  *
465.      //GO.FT14F001  DD  DSNAME=&SM,UNIT=SCRTCH,DISP=(NEW,PASS),
466.      //  SPACE=(800,(120,15)),DCB=(RECFM=VBS,LRECL=796,BLKSIZE=800)
467.      //SMPLTTR  EXEC  PLOT,PLOTTER=PRINTER
```

```
1.      //C300  JOB  U3780,WJH
2.      //STEP1  EXEC  FORTGCG,REGION=320K,TIME=1,LIB='SYS1.IMSL.DOUBLE'
3.      //FORT.SYSIN  DD  *
4.      C      THIS PROGRAM IS GFP25PL-IT CALCS. DEL G/DEL Y0 FOR 2 GROUPS
5.      C      THE PROGRAM WILL ALSO PLOT OR PUNCH THE RESULTS
6.             DOUBLE PRECISION PI,SIGA0M,SIGAFL,DF1L,DF2L,A1,B1,B2,B3,B4,B5
7.             DOUBLE PRECISION Y0,SRM,SRFL,SFL,SFR,NUL,MUL,A2,QL,RL,NU2L,MU2L
8.             DOUBLE PRECISION BTFL,BT2FL,BK,SAM,SAFL,DM1,DM2,BETA
9.             DOUBLE PRECISION DEXP,DSQRT,FISL,BZ,DABS,DSIN,DCOS
10.            DOUBLE PRECISION BTM,BT2M,ALFL,AFL,ALM,AL2M,STEP,Z,STEP1
11.            DOUBLE PRECISION SIGAFR,DF1R,DF2R,SAFR,SRFR,BT2FR,BTFR
12.            DOUBLE PRECISION ALFR,AFR,FISR,MU2R,MUR,NU2R,NUR,QR,RR
13.            DOUBLE PRECISION Y2K1,Y2K2,Y2K3,Y2K4,Y2K5,Y2K6
14.            DOUBLE PRECISION Y3,X0,Y,BB,YB,X1,G1(100),G2(100)
15.            REAL A(24,24),B(24),WKAREA(700),D1,D2,X(100),G(100)
16.            INTEGER I,J,K,L,M,N,IA,IDGT,IER,IJOB,P,Y1
17.            PI=3.141592654
18.     C      THESE ARE THE TWO GROUP PARAMETERS FOR EACH FUEL REGION
19.            SIGA0M=0.00030661
20.            SIGAFL=0.055405
21.            SIGAFR=0.055719
22.            DF1L=1.421447
23.            DF1R=1.421447
24.            DF2L=0.231576
25.            DF2R=0.231576
26.            DM1=1.152864
27.            DM2=0.991810
28.            BETA=0.0065
29.            SAFL=0.002076
30.            SAFR=0.002082
31.            SAM=0.5326368D-07
32.            SFL=0.08233
33.            SFR=0.08397
34.            SRFL=0.03364
35.            SRFR=0.03447
36.            SRM=0.00287363
37.            B5=32.36
38.            B4=15.11
39.            B3=22.65
40.            B2=16.11
41.            B1=32.36
42.            Z=68.32755
43.            Y1=2
44.            A1=111.760
45.     C      STEP IS THE SIZE OF DEL Y0
46.            STEP=1.28/100.
47.            Y0=22.65
48.     C      STEP1 IS THE NUMBER OF POINTS IN THE Y DIRECTION
49.            STEP1=142.24/60.
50.            X0=55.88
51.            X1=55.88
52.            BZ=(PI/Z)**2.
53.            IJOB=2
54.            N=24
55.            IA=24
56.     C      THIS LOOP LOADS VALUES OF DEL G INTO G1 OR G2
57.            DO 50 L=1,Y1
58.            Y=0.0
59.            IF (L.EQ.1) GO TO 52
60.            Y0=22.65+STEP
```

```
      C     THIS BEGINS THE MAIN LOOP FOR MOVING ACROSS THE CORE, Y DIRECTION
   52 DO 51 M=1,61
      X(M)=Y
      G(M)=0.
      C     THE LIBRARY SUBROUTINE WILL NOT CONVERGE FOR K>13 FOR THIS MATRIX
      DO 20 K=1,13
      C     ALL ELEMENTS OF A & B ARE SET=0. FOR EACH MODE
      DO 10 I=1,24
      B(I)=0.
      DO 11 J=1,24
      A(I,J)=0.
   11 CONTINUE
   10 CONTINUE
      B(14)=1.
      D1=0.
      C     THESE STEPS CALCULATE THE NEW SOLUTION EQUATION PARAMETERS
      C         FOR EACH MODE
      BK=(K*PI/A1)**2.
      BT2M=BK+(SIGA0M/DM2)+BZ
      BTM=DSQRT(BT2M)
      BT2FL=BK+(SIGAFL/DF2L)+BZ
      BT2FR=BK+(SIGAFR/DF2R)+BZ
      BTFL=DSQRT(BT2FL)
      BTFR=DSQRT(BT2FR)
      AL2M=BK+(SAM+SRM)/DM1+BZ
      ALM=DSQRT(AL2M)
      AFL=BK+(SAFL+SRFL)/DF1L+BZ
      AFR=BK+(SAFR+SRFR)/DF1R+BZ
      ALFL=DSQRT(AFL)
      ALFR=DSQRT(AFR)
      A2=(SRM/DM2)/(AL2M-BT2M)
      FISL=((1.-BETA)*SFL*SRFL)/(DF1L*DF2L)
      FISR=((1.-BETA)*SFR*SRFR)/(DF1R*DF2R)
      MU2L=(AFL+BT2FL)/2.+DSQRT((AFL+BT2FL)**2.-4*(BT2FL*AFL-FISL))/2.
      MU2R=(AFR+BT2FR)/2.+DSQRT((AFR+BT2FR)**2.-4*(BT2FR*AFR-FISR))/2.
      MUL=DSQRT(MU2L)
      MUR=DSQRT(MU2R)
      NU2L=(AFL+BT2FL)/2.-DSQRT((AFL+BT2FL)**2.-4*(BT2FL*AFL-FISL))/2.
      NU2R=(AFR+BT2FR)/2.-DSQRT((AFR+BT2FR)**2.-4*(BT2FR*AFR-FISR))/2.
      NUL=DSQRT(DABS(NU2L))
      NUR=DSQRT(DABS(NU2R))
      QL=(SRFL/DF2L)/(MU2L-BT2FL)
      QR=(SRFR/DF2R)/(MU2R-BT2FR)
      RL=-(SRFL/DF2L)/(NU2L+BT2FL)
      RR=-(SRFR/DF2R)/(NU2R+BT2FR)
      IF (NU2L.LT.0.) GO TO 40
      RL=(SRFL/DF2L)/(NU2L-BT2FL)
   40 IF (NU2R.LT.0.) GO TO 41
      RR=(SRFR/DF2R)/(NU2R-BT2FR)
      C     MATRIX A IS LOADED HERE
   41 A(1,1)=1.
      A(1,2)=1.
      A(2,3)=1.
      A(2,4)=1.
      A(3,1)=DEXP(-ALM*B1)
      A(3,2)=DEXP(ALM*B1)
      A(3,5)=-1.
      A(3,6)=-1.
      A(3,7)=-1.
      A(3,8)=0.
```

```
121.            A(4,1)=-A2*DEXP(-ALM*B1)
122.            A(4,2)=-A2*DEXP(ALM*B1)
123.            A(4,3)=DEXP(-BTM*B1)
124.            A(4,4)=DEXP(BTM*B1)
125.            A(4,5)=QL
126.            A(4,6)=QL
127.            A(4,7)=RL
128.            A(4,8)=0.
129.            A(5,1)=-DM1*ALM*DEXP(-ALM*B1)
130.            A(5,2)=DM1*ALM*DEXP(ALM*B1)
131.            A(5,5)=DF1L*MUL
132.            A(5,6)=-DF1L*MUL
133.            A(5,7)=0.
134.            A(5,8)=-DF1L*NUL
135.            A(6,1)=DM2*A2*ALM*DEXP(-ALM*B1)
136.            A(6,2)=-DM2*A2*ALM*DEXP(ALM*B1)
137.            A(6,3)=-DM2*BTM*DEXP(-BTM*B1)
138.            A(6,4)=DM2*BTM*DEXP(BTM*B1)
139.            A(6,5)=-DF2L*QL*MUL
140.            A(6,6)=DF2L*QL*MUL
141.            A(6,7)=0.
142.            A(6,8)=DF2L*RL*NUL
143.            A(7,5)=DEXP(-MUL*B2)
144.            A(7,6)=DEXP(MUL*B2)
145.            A(7,7)=DCOS(NUL*B2)
146.            A(7,8)=DSIN(NUL*B2)
147.            A(7,9)=-1.
148.            A(7,10)=-1.
149.            A(8,5)=-QL*DEXP(-MUL*B2)
150.            A(8,6)=-QL*DEXP(MUL*B2)
151.            A(8,7)=-RL*DCOS(NUL*B2)
152.            A(8,8)=-RL*DSIN(NUL*B2)
153.            A(8,9)=A2
154.            A(8,10)=A2
155.            A(8,11)=-1.
156.            A(8,12)=-1.
157.            A(9,5)=-DF1L*MUL*DEXP(-MUL*B2)
158.            A(9,6)=DF1L*MUL*DEXP(MUL*B2)
159.            A(9,7)=-DF1L*NUL*DSIN(NUL*B2)
160.            A(9,8)=DF1L*NUL*DCOS(NUL*B2)
161.            A(9,9)=DM1*ALM
162.            A(9,10)=-DM1*ALM
163.            A(10,5)=DF2L*QL*MUL*DEXP(-MUL*B2)
164.            A(10,6)=-DF2L*QL*MUL*DEXP(MUL*B2)
165.            A(10,7)=DF2L*RL*NUL*DSIN(NUL*B2)
166.            A(10,8)=-DF2L*RL*NUL*DCOS(NUL*B2)
167.            A(10,9)=-DM2*A2*ALM
168.            A(10,10)=DM2*A2*ALM
169.            A(10,11)=DM2*BTM
170.            A(10,12)=-DM2*BTM
171.            A(11,9)=DEXP(-ALM*Y0)
172.            A(11,10)=DEXP(ALM*Y0)
173.            A(11,13)=-1.
174.            A(11,14)=-1.
175.            A(12,9)=-A2*DEXP(-ALM*Y0)
176.            A(12,10)=-A2*DEXP(ALM*Y0)
177.            A(12,11)=DEXP(-BTM*Y0)
178.            A(12,12)=DEXP(BTM*Y0)
179.            A(12,13)=A2
180.            A(12,14)=A2
```

```
181.            A(12,15)=-1.
182.            A(12,16)=-1.
183.            A(13,9)=-DM1*ALM*DEXP(-ALM*Y0)
184.            A(13,10)=DM1*ALM*DEXP(ALM*Y0)
185.            A(13,13)=DM1*ALM
186.            A(13,14)=-DM1*ALM
187.            A(14,9)=A2*ALM*DEXP(-ALM*Y0)
188.            A(14,10)=-A2*ALM*DEXP(ALM*Y0)
189.            A(14,11)=-BTM*DEXP(-BTM*Y0)
190.            A(14,12)=BTM*DEXP(BTM*Y0)
191.            A(14,13)=-A2*ALM
192.            A(14,14)=A2*ALM
193.            A(14,15)=BTM
194.            A(14,16)=-BTM
195.            A(15,13)=DEXP(-ALM*B3)
196.            A(15,14)=DEXP(ALM*B3)
197.            A(15,17)=-1.
198.            A(15,18)=-1.
199.            A(15,19)=-1.
200.            A(15,20)=0.
201.            A(16,13)=-A2*DEXP(-ALM*B3)
202.            A(16,14)=-A2*DEXP(ALM*B3)
203.            A(16,15)=DEXP(-BTM*B3)
204.            A(16,16)=DEXP(BTM*B3)
205.            A(16,17)=QR
206.            A(16,18)=QR
207.            A(16,19)=RR
208.            A(16,20)=0.
209.            A(17,13)=-DM1*ALM*DEXP(-ALM*B3)
210.            A(17,14)=DM1*ALM*DEXP(ALM*B3)
211.            A(17,17)=DF1R*MUR
212.            A(17,18)=-DF1R*MUR
213.            A(17,19)=0.
214.            A(17,20)=-DF1R*NUR
215.            A(18,13)=DM2*A2*ALM*DEXP(-ALM*B3)
216.            A(18,14)=-DM2*A2*ALM*DEXP(ALM*B3)
217.            A(18,15)=-DM2*BTM*DEXP(-BTM*B3)
218.            A(18,16)=DM2*BTM*DEXP(BTM*B3)
219.            A(18,17)=-DF2R*QR*MUR
220.            A(18,18)=DF2R*QR*MUR
221.            A(18,19)=0.
222.            A(18,20)=DF2R*RR*NUR
223.            A(19,17)=DEXP(-MUR*B4)
224.            A(19,18)=DEXP(MUR*B4)
225.            A(19,19)=DCOS(NUR*B4)
226.            A(19,20)=DSIN(NUR*B4)
227.            A(19,21)=-1.
228.            A(19,22)=-1.
229.            A(20,17)=-QR*DEXP(-MUR*B4)
230.            A(20,18)=-QR*DEXP(MUR*B4)
231.            A(20,19)=-RR*DCOS(NUR*B4)
232.            A(20,20)=-RR*DSIN(NUR*B4)
233.            A(20,21)=A2
234.            A(20,22)=A2
235.            A(20,23)=-1.
236.            A(20,24)=-1.
237.            A(21,17)=-DF1R*MUR*DEXP(-MUR*B4)
238.            A(21,18)=DF1R*MUR*DEXP(MUR*B4)
239.            A(21,19)=-DF1R*NUR*DSIN(NUR*B4)
240.            A(21,20)=DF1R*NUR*DCOS(NUR*B4)
```

```
241.            A(21,21)=DM1*ALM
242.            A(21,22)=-DM1*ALM
243.            A(22,17)=DF2R*QR*MUR*DEXP(-MUR*B4)
244.            A(22,18)=-DF2R*QR*MUR*DEXP(MUR*B4)
245.            A(22,19)=DF2R*RR*NUR*DSIN(NUR*B4)
246.            A(22,20)=-DF2R*RR*NUR*DCOS(NUR*B4)
247.            A(22,21)=-DM2*A2*ALM
248.            A(22,22)=DM2*A2*ALM
249.            A(22,23)=DM2*BTM
250.            A(22,24)=-DM2*BTM
251.            A(23,21)=DEXP(-ALM*B5)
252.            A(23,22)=DEXP(ALM*B5)
253.            A(24,21)=-A2*DEXP(-ALM*B5)
254.            A(24,22)=-A2*DEXP(ALM*B5)
255.            A(24,23)=DEXP(-BTM*B5)
256.            A(24,24)=DEXP(BTM*B5)
257.      C     THESE ELEMENTS ARE DIFFERENT DUE TO THE DIFFERENT SOLUTIONS
258.      C        TO THE DIFFERENTIAL EQUATIONS DEPENDING ON THE SIGN OF NU2L
259.            IF (NU2L.LT.0.) GO TO 30
260.            A(3,8)=-1.
261.            A(4,8)=RL
262.            A(5,7)=DF1L*NUL
263.            A(6,7)=-DF2L*RL*NUL
264.            A(7,7)=DEXP(-NUL*B2)
265.            A(7,8)=DEXP(NUL*B2)
266.            A(8,7)=-RL*DEXP(-NUL*B2)
267.            A(8,8)=-RL*DEXP(NUL*B2)
268.            A(9,7)=-DF1L*NUL*DEXP(-NUL*B2)
269.            A(9,8)=DF1L*NUL*DEXP(NUL*B2)
270.            A(10,7)=DF2L*RL*NUL*DEXP(-NUL*B2)
271.            A(10,8)=-DF2L*RL*NUL*DEXP(NUL*B2)
272.            IF (NU2R.LT.0.) GO TO 30
273.            A(15,20)=-1.
274.            A(16,20)=RR
275.            A(17,19)=DF1R*NUR
276.            A(18,19)=-DF2R*RR*NUR
277.            A(19,19)=DEXP(-NUR*B4)
278.            A(19,20)=DEXP(NUR*B4)
279.            A(20,19)=-RR*DEXP(-NUR*B4)
280.            A(20,20)=-RR*DEXP(NUR*B4)
281.            A(21,19)=-DF1R*NUR*DEXP(-NUR*B4)
282.            A(21,20)=DF1R*NUR*DEXP(NUR*B4)
283.            A(22,19)=DF2R*RR*NUR*DEXP(-NUR*B4)
284.            A(22,20)=-DF2R*RR*NUR*DEXP(NUR*B4)
285.      C     THE LIBRARY SUBROUTINE LINV3F SOLVES FOR X IN A*X=B
286.      30    CALL LINV3F (A,B,IJOB,N,IA,D1,D2,WKAREA,IER)
287.      C     THESE STEPS DETERMINE WHICH SOLUTION EQUATION IS APPROPIATE FOR
288.      C        THE CURRENT VALUE OF Y AND CALCULATE THE GREENS FUNCTIONS
289.            IF (IER.EQ.130) GO TO 25
290.            IF (Y.GT.B1) GO TO 60
291.            Y2K1=3(3)*DEXP(-BTM*Y)+B(4)*DEXP(BTM*Y)-A2*(B(1)*DEXP(-ALM*Y)
292.           &+B(2)*DEXP(ALM*Y))
293.            YB=Y2K1
294.            GO TO 69
295.      60    CONTINUE
296.            BB=B1+B2
297.            IF (Y.GT.BB) GO TO 61
298.            Y3=Y-(BB-B2)
299.            IF (NU2L.LT.0.) GO TO 65
300.            Y2K2=-QL*(B(5)*DEXP(-MUL*Y3)+B(6)*DEXP(MUL*Y3))-RL*(B(7)*DEXP
```

```
301.            &(-NUL*Y3)+B(8)*DEXP(NUL*Y3))
302.              YB=Y2K2
303.              GO TO 69
304.        65    CONTINUE
305.              Y2K2=-QL*(B(5)*DEXP(-MUL*Y3)+B(6)*DEXP(MUL*Y3))-RL*(B(7)*DCOS
306.            &(NUL*Y3)+B(8)*DSIN(NUL*Y3))
307.              YB=Y2K2
308.              GO TO 69
309.        61    CONTINUE
310.              BB=BB+Y0
311.              IF (Y.GT.BB) GO TO 62
312.              Y3=Y-(BB-Y0)
313.              Y2K3=B(11)*DEXP(-BTM*Y3)+B(12)*DEXP(BTM*Y3)-A2*(B(9)*DEXP
314.            &(-ALM*Y3)+B(10)*DEXP(ALM*Y3))
315.              YB=Y2K3
316.              GO TO 69
317.        62    CONTINUE
318.              BB=BB+B3
319.              IF (Y.GT.BB) GO TO 63
320.              Y3=Y-(BB-B3)
321.              Y2K4=B(15)*DEXP(-BTM*Y3)+B(16)*DEXP(BTM*Y3)-A2*(B(13)*DEXP
322.            &(-ALM*Y3)+B(14)*DEXP(ALM*Y3))
323.              YB=Y2K4
324.              GO TO 69
325.        63    CONTINUE
326.              BB=BB+B4
327.              IF (Y.GT.BB) GO TO 64
328.              Y3=Y-(BB-B4)
329.              IF (NU2R.LT.0.) GO TO 66
330.              Y2K5=-QR*(B(17)*DEXP(-MUR*Y3)+B(18)*DEXP(MUR*Y3))-RR*(B(19)
331.            &*DEXP(-NUR*Y3)+B(20)*DEXP(NUR*Y3))
332.              YB=Y2K5
333.              GO TO 69
334.        66    CONTINUE
335.              Y2K5=-QR*(B(17)*DEXP(-MUR*Y3)+B(18)*DEXP(MUR*Y3))-RR*(B(19)
336.            &*DCOS(NUR*Y3)+B(20)*DSIN(NUR*Y3))
337.              YB=Y2K5
338.              GO TO 69
339.        64    CONTINUE
340.              Y3=Y-BB
341.              Y2K6=B(23)*DEXP(-BTM*Y3)+B(24)*DEXP(BTM*Y3)-A2*(B(21)*DEXP
342.            &(-ALM*Y3)+B(22)*DEXP(ALM*Y3))
343.              YB=Y2K6
344.        69    CONTINUE
345.              G(M)=2./A1*DSIN(BK*X0)*DSIN(BK*X1)*YB+G(M)
346.        20    CONTINUE
347.              IF (Y.LT.(B1+B2).OR.Y.GT.(B1+B2+B3+Y0)) GO TO 53
348.        C     THE SUBROUTINE CENT IS CALLED IF Y IS IN THE CENTRAL GRAPHITE
349.        C         REGION TO FURTHER CONVERGE THE SOLUTIONS
350.              CALL CENT(G,M,Y,IER,Y0)
351.        53    IF (IER.EQ.130) GO TO 25
352.              IF (L.EQ.2) GO TO 54
353.              G1(M)=G(M)
354.        54    G2(M)=G(M)
355.              Y=Y+STEP1
356.        51    CONTINUE
357.        50    CONTINUE
358.        C     DEL G/DEL Y0 IS CALCULATED HERE.  ADDITIONAL STEPS MAY BE
359.        C         INSERTED HERE TO GENERATE PLOTS OR TO PUNCH CARDS
360.              DO 70 I=1,61
```

```
361.            G(I)=(G2(I)-G1(I))/STEP
362.            WRITE (6,55) G(I)
363.      55    FORMAT (E12.5)
364.      70    CONTINUE
365.            GO TO 27
366.      25    WRITE (6,26) K,L
367.      26    FORMAT (' K= ',I2,' L= ',I2)
368.      27    STOP
369.            END
370.            SUBROUTINE CENT(G,M,Y,IER,Y0)
371.      C     THIS SUBROUTINE ADDS 7 EXTRA MODES TO THE CALCULATION
372.      C         FOR THE CENTRAL GRAPHITE REGION
373.            DOUBLE PRECISION PI,SIGA0M,A1,B1,B2,B3,Y0,SRM,A2,E
374.            DOUBLE PRECISION BK,SAM,DM1,DM2,DEXP,DSQRT,BZ
375.            DOUBLE PRECISION BTM,BT2M,ALM,AL2M,STEP,Z
376.            DOUBLE PRECISION Y3,X0,Y,BB,YB,X1,G(100),Y2K3,Y2K4
377.            REAL A(8,8),B(8),WKAREA(700),D1,D2
378.            INTEGER I,J,K,L,M,N,IA,IDGT,IER,IJOB,P,Y1
379.            PI=3.141592654
380.            SIGA0M=0.00030661
381.            DM1=1.152864
382.            DM2=0.991810
383.            SAM=0.5326368D-07
384.            SRM=0.00287363
385.            B3=22.65
386.            B2=16.11
387.            B1=32.36
388.            Z=68.32755
389.            A1=111.760
390.            X0=55.88
391.            X1=55.88
392.            BZ=(PI/Z)**2.
393.            IJOB=2
394.      C     THE LIBRARY SUBROUTINE WILL NOT CONVERGE FOR K>21 FOR THIS MATRIX
395.            DO 75 K=14,21
396.            BK=(K*PI/A1)**2.
397.            BT2M=BK+(SIGA0M/DM2)+BZ
398.            BTM=DSQRT(BT2M)
399.            AL2M=BK+(SAM+SRM)/DM1+BZ
400.            ALM=DSQRT(AL2M)
401.            A2=(SRM/DM2)/(AL2M-BT2M)
402.            N=8
403.            IA=8
404.            DO 76 I=1,8
405.            B(I)=0.
406.            DO 77 J=1,8
407.            A(I,J)=0.
408.      77    CONTINUE
409.      76    CONTINUE
410.            B(6)=1.
411.            A(1,1)=1.
412.            A(1,2)=1.
413.            A(2,1)=-A2
414.            A(2,2)=-A2
415.            A(2,3)=1.
416.            A(2,4)=1.
417.            A(3,1)=DEXP(-ALM*Y0)
418.            A(3,2)=DEXP(ALM*Y0)
419.            A(3,3)=-1.
420.            A(3,4)=-1.
```

```
421.            A(4,1)=-A2*DEXP(-ALM*Y0)
422.            A(4,2)=-A2*DEXP(ALM*Y0)
423.            A(4,3)=DEXP(-BTM*Y0)
424.            A(4,4)=DEXP(BTM*Y0)
425.            A(4,5)=A2
426.            A(4,6)=A2
427.            A(4,7)=-1.
428.            A(4,8)=-1.
429.            A(5,1)=-DM1*ALM*DEXP(-ALM*Y0)
430.            A(5,2)=DM1*ALM*DEXP(ALM*Y0)
431.            A(5,5)=DM1*ALM
432.            A(5,6)=-DM1*ALM
433.            A(6,1)=A2*ALM*DEXP(-ALM*Y0)
434.            A(6,2)=-A2*ALM*DEXP(ALM*Y0)
435.            A(6,3)=-BTM*DEXP(-BTM*Y0)
436.            A(6,4)=BTM*DEXP(BTM*Y0)
437.            A(6,5)=-A2*ALM
438.            A(6,6)=A2*ALM
439.            A(6,7)=BTM
440.            A(6,8)=-BTM
441.            A(7,5)=DEXP(-ALM*B3)
442.            A(7,6)=DEXP(ALM*B3)
443.            A(8,5)=-A2*DEXP(-ALM*B3)
444.            A(8,6)=-A2*DEXP(ALM*B3)
445.            A(8,7)=DEXP(-BTM*B3)
446.            A(8,8)=DEXP(BTM*B3)
447.            CALL LINV3F (A,B,IJOB,N,IA,D1,D2,WKAREA,IER)
448.            IF (IER.EQ.130) GO TO 85
449.            BB=B1+B2+Y0
450.            IF (Y.GT.BB) GO TO 72
451.            Y3=Y-(BB-Y0)
452.            Y2K3=B(3)*DEXP(-BTM*Y3)+B(4)*DEXP(BTM*Y3)-A2*(B(1)*DEXP
453.           &(-ALM*Y3)+B(2)*DEXP(ALM*Y3))
454.            YB=Y2K3
455.            GO TO 73
456.     72     BB=BB+B3
457.            Y3=Y-(BB-B3)
458.            Y2K4=B(7)*DEXP(-BTM*Y3)+B(8)*DEXP(BTM*Y3)-A2*(B(5)*DEXP
459.           &(-ALM*Y3)+B(6)*DEXP(ALM*Y3))
460.            YB=Y2K4
461.     73     CONTINUE
462.            G(M)=2./A1*DSIN(BK*X0)*DSIN(BK*X1)*YB+G(M)
463.     75     CONTINUE
464.            GO TO 87
465.     85     WRITE (6,86) K,L
466.     86     FORMAT (' IN THE SUBROUTINE CENT IER=130 AT K= ',I2,' L=',I2)
467.     87     RETURN
468.            END
469.     //GO.SYSIN  DD  *
```

GFP-27 calculates the thermal fluxes, $\phi 2$.

```
1.      //C300   JOB   U3780,WJH
2.      //STEP1  EXEC  WATFIV,REGION=192K,LIB='SYS2.WATFIV.IMSL.DOUBLE'
3.      //GO.SYSIN  DD  *
4.      $JOB                 'WJH',TIME=5,PAGES=10
5.      C       THIS PROGRAM IS GFP27PL-IT CALCS./PLOTS FLUXES FOR 2 GROUPS
6.              DOUBLE PRECISION PI,SIGA0M,SIGAFL,DF1L,DF2L,A1,B1,B2,B3,B4,B5
7.              DOUBLE PRECISION Y0,SRM,SRFL,SFL,SFR,NUL,MUL,A2,QL,RL,NU2L,MU2L
8.              DOUBLE PRECISION BTFL,BT2FL,BK,SAM,SAFL,DM1,DM2,BETA,X0
9.              DOUBLE PRECISION DEXP,DSQRT,FISL,BZ,DABS,DSIN,DCOS,BB,Y,Y3,YB
10.             DOUBLE PRECISION BTM,BT2M,ALFL,AFL,ALM,AL2M,STEP,Z1
11.             DOUBLE PRECISION SIGAFR,DF1R,DF2R,SAFR,SRFR,BT2FR,BTFR
12.             DOUBLE PRECISION ALFR,AFR,FISR,MU2R,MUR,NU2R,NUR,QR,RR
13.             REAL A(20,20),B(20),G(100),WK(700),D1,D2,X(100)
14.             INTEGER I,J,K,L,M,N,IA,IDGT,IER,IJOB,P,IZ
15.             COMPLEX W(20),Z(20,20)
16.             PI=3.141592654
17.     C       THESE ARE THE 2 GROUP PARAMETERS
18.             SIGA0M=0.00030661
19.             SIGAFL=0.055405
20.             SIGAFR=0.055719
21.             DF1L=1.421447
22.             DF1R=1.421447
23.             DF2L=0.231576
24.             DF2R=0.231576
25.             DM1=1.152864
26.             DM2=0.991810
27.             BETA=0.0065
28.             SAFL=0.002076
29.             SAFR=0.002082
30.             X0=55.88
31.             SAM=0.5326368D-07
32.             SFL=0.08233
33.             SFR=0.08397
34.             SRFL=0.03364
35.             SRFR=0.03447
36.             SRM=0.00287363
37.             Y0=22.65
38.             B5=32.36
39.             B4=15.11
40.             B3=22.65
41.             B2=15.11
42.             B1=32.36
43.             B3=Y0+B3
44.             Z1=68.32755
45.             A1=111.760
46.             BZ=(PI/Z1)**2.
47.             IJOB=2
48.             N=20
49.             IA=20
50.             IZ=20
51.     C       ALL ELEMENTS OF A ARE INITIALLY SET=0.
52.             DO 10 I=1,20
53.             DO 11 J=1,20
54.             A(I,J)=0.
55.     11      CONTINUE
56.     10      CONTINUE
57.             D1=0.
58.     C       THESE STEPS CALCULATE THE SOLUTION EQUATION PARAMETERS
59.             BK=(PI/A1)**2.
60.             BT2M=BK+(SIGA0M/DM2)+BZ
```

```
      BTM=DSQRT(BT2M)
      BT2FL=BK+(SIGAFL/DF2L)+BZ
      BT2FR=BK+(SIGAFR/DF2R)+BZ
      BTFL=DSQRT(BT2FL)
      BTFR=DSQRT(BT2FR)
      AL2M=BK+(SAM+SRM)/DM1+BZ
      ALM=DSQRT(AL2M)
      AFL=BK+(SAFL+SRFL)/DF1L+BZ
      AFR=BK+(SAFR+SRFR)/DF1R+BZ
      ALFL=DSQRT(AFL)
      ALFR=DSQRT(AFR)
      A2=(SRM/DM2)/(AL2M-BT2M)
      FISL=(SFL*SRFL)/(DF1L*DF2L)
      FISR=(SFR*SRFR)/(DF1R*DF2R)
      MU2L=(AFL+BT2FL)/2.+DSQRT((AFL+BT2FL)**2.-4*(BT2FL*AFL-FISL))/2.
      MU2R=(AFR+BT2FR)/2.+DSQRT((AFR+BT2FR)**2.-4*(BT2FR*AFR-FISR))/2.
      MUL=DSQRT(MU2L)
      MUR=DSQRT(MU2R)
      NU2L=(AFL+BT2FL)/2.-DSQRT((AFL+BT2FL)**2.-4*(BT2FL*AFL-FISL))/2.
      NU2R=(AFR+BT2FR)/2.-DSQRT((AFR+BT2FR)**2.-4*(BT2FR*AFR-FISR))/2.
      NUL=DSQRT(DABS(NU2L))
      NUR=DSQRT(DABS(NU2R))
      QL=(SRFL/DF2L)/(MU2L-BT2FL)
      QR=(SRFR/DF2R)/(MU2R-BT2FR)
      RL=-(SRFL/DF2L)/(NU2L+BT2FL)
      RR=-(SRFR/DF2R)/(NU2R+BT2FR)
C     THESE STEPS LOAD MATRIX A
      A(1,1)=1.
      A(1,2)=1.
      A(2,3)=1.
      A(2,4)=1.
      A(3,1)=DEXP(-ALM*B1)
      A(3,2)=DEXP(ALM*B1)
      A(3,5)=-1.
      A(3,6)=-1.
      A(3,7)=-1.
      A(3,8)=0.
      A(4,1)=-A2*DEXP(-ALM*B1)
      A(4,2)=-A2*DEXP(ALM*B1)
      A(4,3)=DEXP(-BTM*B1)
      A(4,4)=DEXP(BTM*B1)
      A(4,5)=QL
      A(4,6)=QL
      A(4,7)=RL
      A(4,8)=0.
      A(5,1)=-DM1*ALM*DEXP(-ALM*B1)
      A(5,2)=DM1*ALM*DEXP(ALM*B1)
      A(5,5)=DF1L*MUL
      A(5,6)=-DF1L*MLL
      A(5,7)=0.
      A(5,8)=-DF1L*NUL
      A(6,1)=DM2*A2*ALM*DEXP(-ALM*B1)
      A(6,2)=-DM2*A2*ALM*DEXP(ALM*B1)
      A(6,3)=-DM2*BTM*DEXP(-BTM*B1)
      A(6,4)=DM2*BTM*DEXP(BTM*B1)
      A(6,5)=-DF2L*QL*MUL
      A(6,6)=DF2L*QL*MUL
      A(6,7)=0.
      A(6,8)=DF2L*RL*NUL
      A(7,5)=DEXP(-MUL*B2)
```

```
121.            A(7,6)=DEXP(MUL*B2)
122.            A(7,7)=DCOS(NUL*B2)
123.            A(7,8)=DSIN(NUL*B2)
124.            A(7,9)=-1.
125.            A(7,10)=-1.
126.            A(8,5)=-QL*DEXP(-MUL*B2)
127.            A(8,6)=-QL*DEXP(MUL*B2)
128.            A(8,7)=-RL*DCOS(NUL*B2)
129.            A(8,8)=-RL*DSIN(NUL*B2)
130.            A(8,9)=A2
131.            A(8,10)=A2
132.            A(8,11)=-1.
133.            A(8,12)=-1.
134.            A(9,5)=-DF1L*MUL*DEXP(-MUL*B2)
135.            A(9,6)=DF1L*MUL*DEXP(MUL*B2)
136.            A(9,7)=-DF1L*NUL*DSIN(NUL*B2)
137.            A(9,8)=DF1L*NUL*DCOS(NUL*B2)
138.            A(9,9)=DM1*ALM
139.            A(9,10)=-DM1*ALM
140.            A(10,5)=DF2L*QL*MUL*DEXP(-MUL*B2)
141.            A(10,6)=-DF2L*QL*MUL*DEXP(MUL*B2)
142.            A(10,7)=DF2L*RL*NUL*DSIN(NUL*B2)
143.            A(10,8)=-DF2L*RL*NUL*DCOS(NUL*B2)
144.            A(10,9)=-DM2*A2*ALM
145.            A(10,10)=DM2*A2*ALM
146.            A(10,11)=DM2*BTM
147.            A(10,12)=-DM2*BTM
148.            A(11,9)=DEXP(-ALM*B3)
149.            A(11,10)=DEXP(ALM*B3)
150.            A(11,13)=-1.
151.            A(11,14)=-1.
152.            A(11,15)=-1.
153.            A(11,16)=0.
154.            A(12,9)=-A2*DEXP(-ALM*B3)
155.            A(12,10)=-A2*DEXP(ALM*B3)
156.            A(12,11)=DEXP(-BTM*B3)
157.            A(12,12)=DEXP(BTM*B3)
158.            A(12,13)=QR
159.            A(12,14)=QR
160.            A(12,15)=RR
161.            A(12,16)=0.
162.            A(13,9)=-DM1*ALM*DEXP(-ALM*B3)
163.            A(13,10)=DM1*ALM*DEXP(ALM*B3)
164.            A(13,13)=DF1R*MUR
165.            A(13,14)=-DF1R*MUR
166.            A(13,15)=0.
167.            A(13,16)=-DF1R*NUR
168.            A(14,9)=DM2*A2*ALM*DEXP(-ALM*B3)
169.            A(14,10)=-DM2*A2*ALM*DEXP(ALM*B3)
170.            A(14,11)=-DM2*BTM*DEXP(-BTM*B3)
171.            A(14,12)=DM2*BTM*DEXP(BTM*B3)
172.            A(14,13)=-DF2R*QR*MUR
173.            A(14,14)=DF2R*QR*MUR
174.            A(14,15)=0.
175.            A(14,16)=DF2R*RR*NUR
176.            A(15,13)=DEXP(-MUR*B4)
177.            A(15,14)=DEXP(MUR*B4)
178.            A(15,15)=DCOS(NUR*B4)
179.            A(15,16)=DSIN(NUR*B4)
180.            A(15,17)=-1.
```

```
181.            A(15,18)=-1.
182.            A(16,13)=-QR*DEXP(-MUR*B4)
183.            A(16,14)=-QR*DEXP(MUR*B4)
184.            A(16,15)=-RR*DCOS(NUR*B4)
185.            A(16,16)=-RR*DSIN(NUR*B4)
186.            A(16,17)=A2
187.            A(16,18)=A2
188.            A(16,19)=-1.
189.            A(16,20)=-1.
190.            A(17,13)=-DF1R*MUR*DEXP(-MUR*B4)
191.            A(17,14)=DF1R*MUR*DEXP(MUR*B4)
192.            A(17,15)=-DF1R*NUR*DSIN(NUR*B4)
193.            A(17,16)=DF1R*NUR*DCOS(NUR*B4)
194.            A(17,17)=DM1*ALM
195.            A(17,18)=-DM1*ALM
196.            A(18,13)=DF2R*QR*MUR*DEXP(-MUR*B4)
197.            A(18,14)=-DF2R*QR*MUR*DEXP(MUR*B4)
198.            A(18,15)=DF2R*RR*NUR*DSIN(NUR*B4)
199.            A(18,16)=-DF2R*RR*NUR*DCOS(NUR*B4)
200.            A(18,17)=-DM2*A2*ALM
201.            A(18,18)=DM2*A2*ALM
202.            A(18,19)=DM2*BTM
203.            A(18,20)=-DM2*BTM
204.            A(19,17)=DEXP(-ALM*B5)
205.            A(19,18)=DEXP(ALM*B5)
206.            A(20,17)=-A2*DEXP(-ALM*B5)
207.            A(20,18)=-A2*DEXP(ALM*B5)
208.            A(20,19)=DEXP(-BTM*B5)
209.            A(20,20)=DEXP(BTM*B5)
210.      C     THE IDENTITY MATRIX IS ADDED TO A
211.            DO 40 I=1,20
212.            A(I,I)=A(I,I)+1.
213.      40    CONTINUE
214.      C     THE LIBRARY SUBROUTINE EIGRF DETERMINES THE EIGENVALUES
215.      C         AND ASSOCIATED EIGENVECTORS OF MATRIX A
216.            CALL EIGRF (A,N,IA,IJOB,W,Z,IZ,WK,IER)
217.      C     THE EIGENVECTORS ASSOCIATED WITH EIGENVALUE=1. ARE
218.      C         LOCATED IN Z(I,20); THEY ARE THE COEFFICIENTS OF THE
219.      C         FLUX SOLUTION EQUATIONS
220.            DO 42 I=1,20
221.            B(I)=REAL(Z(I,20))
222.      42    CONTINUE
223.            IF (IER.EQ.130) GO TO 25
224.            Y=0.
225.      C     THIS IS THE STEP SIZE IN THE Y DIRECTION
226.            STEP=142.24/60.
227.      C     THIS LOOP CALCULATES THE FLUXES ACROSS THE CORE
228.            DO 20 K=1,61
229.            X(K)=Y
230.            BB=0.
231.            IF (Y.GT.B1) GO TO 60
232.            Y2K1=B(3)*DEXP(-BTM*Y)+B(4)*DEXP(BTM*Y)-A2*(B(1)*DEXP(-ALM*Y)
233.           &+B(2)*DEXP(ALM*Y))
234.            YB=Y2K1
235.            GO TO 69
236.      60    CONTINUE
237.            BB=B1+B2
238.            IF (Y.GT.BB) GO TO 61
239.            Y3=Y-(BB-B2)
240.            Y2K2=-QL*(B(5)*DEXP(-MUL*Y3)+B(6)*DEXP(MUL*Y3))-RL*(B(7)*DCOS
```

```
241.            &(NUL*Y3)+B(8)*DSIN(NUL*Y3))
242.              YB=Y2K2
243.              GO TO 69
244.        61    CONTINUE
245.              BB=BB+B3
246.              IF (Y.GT.BB) GO TO 63
247.              Y3=Y-(BB-B3)
248.              Y2K4=B(11)*DEXP(-BTM*Y3)+B(12)*DEXP(BTM*Y3)-A2*(B(9)*DEXP
249.            &(-ALM*Y3)+B(10)*DEXP(ALM*Y3))
250.              YB=Y2K4
251.              GO TO 69
252.        63    CONTINUE
253.              BB=BB+B4
254.              IF (Y.GT.BB) GO TO 64
255.              Y3=Y-(BB-B4)
256.              Y2K5=-QR*(B(13)*DEXP(-MUR*Y3)+B(14)*DEXP(MUR*Y3))-RR*(B(15)
257.            &*DCOS(NUR*Y3)+B(16)*DSIN(NUR*Y3))
258.              YB=Y2K5
259.              GO TO 69
260.        64    CONTINUE
261.              Y3=Y-BB
262.              Y2K6=B(19)*DEXP(-BTM*Y3)+B(20)*DEXP(BTM*Y3)-A2*(B(17)*DEXP(-ALM
263.            &*Y3)+B(18)*DEXP(ALM*Y3))
264.              YB=Y2K6
265.        69    CONTINUE
266.              G(K)=DSIN(X0*PI/A1)*YB
267.              Y=Y+STEP
268.        20    CONTINUE
269.        C     THIS LOOP PUNCHES THE FLUXES; OTHER STEPS MAY BE INSERTED
270.        C         HERE TO PRINT OR GRAPH THE FLUXES
271.              DO 50 I=1,61
272.              WRITE (7,51)G(I)
273.        51    FORMAT (E12.5)
274.        50    CONTINUE
275.        25    STOP
276.              END
277.        $ENTRY
```

The last program, GFP-28, calculates $d\phi/dy$.

```
1.      //C300  JOB  U3780,WJH
2.      //STEP1  EXEC  FORTGCG,REGION=192K,LIB='SYS1.IMSL.DOUBLE'
3.      //FORT.SYSIN  DD  *
4.      C      THIS PROGRAM IS GFP28-IT CALCS. D PHI/D Y FOR 2 GROUPS
5.      C          AT THE POINT Y0 ONLY
6.            DOUBLE PRECISION PI,SIGA0M,SIGAFL,DF1L,DF2L,A1,B1,B2,B3,B4,B5
7.            DOUBLE PRECISION Y0,SRM,SRFL,SFL,SFR,NUL,MUL,A2,QL,RL,NU2L,MU2L
8.            DOUBLE PRECISION BTFL,BT2FL,BK,SAM,SAFL,DM1,DM2,BETA,X0
9.            DOUBLE PRECISION DEXP,DSQRT,FISL,BZ,DABS,DSIN,DCOS,BB,Y,Y3,Y8
10.           DOUBLE PRECISION BTM,BT2M,ALFL,AFL,ALM,AL2M,STEP,Z1
11.           DOUBLE PRECISION SIGAFR,DF1R,DF2R,SAFR,SRFR,BT2FR,BTFR
12.           DOUBLE PRECISION ALFR,AFR,FISR,MU2R,MUR,NU2R,NUR,QR,RR
13.           REAL A(20,20),B(20),G1(10),G(10),WK(700),D1,D2,DET,G2
14.           INTEGER I,J,K,L,M,N,IA,IDGT,IER,IJOB,P,IZ
15.           COMPLEX W(20),Z(20,20)
16.           PI=3.141592654
17.     C     THESE ARE THE TWO GROUP PARAMETERS
18.           SIGA0M=0.00030661
19.           SIGAFL=0.055405
20.           SIGAFR=0.055719
21.           DF1L=1.421447
22.           DF1R=1.421447
23.           DF2L=0.231576
24.           DF2R=0.231576
25.           DM1=1.152864
26.           DM2=0.991810
27.           BETA=0.0065
28.           SAFL=0.002076
29.           SAFR=0.002082
30.           X0=55.88
31.           SAM=0.5326368D-07
32.           SFL=0.08233
33.           SFR=0.08397
34.           SRFL=0.03364
35.           SRFR=0.03447
36.           SRM=0.00287363
37.           Y0=22.65
38.           B5=32.36
39.           B4=16.11
40.           B3=22.65
41.           B2=16.11
42.           B1=32.36
43.           B3=Y0+B3
44.           Z1=68.32755
45.           A1=111.760
46.           BZ=(PI/Z1)**2.
47.           IJOB=2
48.           N=20
49.           IA=20
50.           IZ=20
51.           G(1)=0.
52.           Y=B1+B2+Y0
53.           STEP=1.28/100.
54.           Y=Y-STEP
55.     C     THE FLUX IS CALCULATED THREE TIMES AT Y0-STEP,Y0,AND
56.     C         Y0+STEP, AND DEL PHI/DEL Y IS DETERMINED FROM
57.     C         ((PHI+STEP)-PHI)/STEP
58.           DO 20 K=1,3
59.     C     THE ELEMENTS OF A ARE INITIALLY SET=0.
60.           DO 10 I=1,20
```

```
      DO 11 J=1,20
      A(I,J)=0.
11    CONTINUE
10    CONTINUE
      D1=0.
C     THE SOLUTION EQUATION PARAMETERS ARE CALCULATED HERE
      BK=(PI/A1)**2.
      BT2M=BK+(SIGA0M/DM2)+BZ
      BTM=DSQRT(BT2M)
      BT2FL=BK+(SIGAFL/DF2L)+BZ
      BT2FR=BK+(SIGAFR/DF2R)+BZ
      BTFL=DSQRT(BT2FL)
      BTFR=DSQRT(BT2FR)
      AL2M=BK+(SAM+SRM)/DM1+BZ
      ALM=DSQRT(AL2M)
      AFL=BK+(SAFL+SRFL)/DF1L+BZ
      AFR=BK+(SAFR+SRFR)/DF1R+BZ
      ALFL=DSQRT(AFL)
      ALFR=DSQRT(AFR)
      A2=(SRM/DM2)/(AL2M-BT2M)
      FISL=(SFL*SRFL)/(DF1L*DF2L)
      FISR=(SFR*SRFR)/(DF1R*DF2R)
      MU2L=(AFL+BT2FL)/2.+DSQRT((AFL+BT2FL)**2.-4*(BT2FL*AFL-FISL))/2.
      MU2R=(AFR+BT2FR)/2.+DSQRT((AFR+BT2FR)**2.-4*(BT2FR*AFR-FISR))/2.
      MUL=DSQRT(MU2L)
      MUR=DSQRT(MU2R)
      NU2L=(AFL+BT2FL)/2.-DSQRT((AFL+BT2FL)**2.-4*(BT2FL*AFL-FISL))/2.
      NU2R=(AFR+BT2FR)/2.-DSQRT((AFR+BT2FR)**2.-4*(BT2FR*AFR-FISR))/2.
      NUL=DSQRT(DABS(NU2L))
      NUR=DSQRT(DABS(NU2R))
      QL=(SRFL/DF2L)/(MU2L-BT2FL)
      QR=(SRFR/DF2R)/(MU2R-BT2FR)
      RL=-(SRFL/DF2L)/(NU2L+BT2FL)
      RR=-(SRFR/DF2R)/(NU2R+BT2FR)
C     MATRIX A IS LOADED HERE
      A(1,1)=1.
      A(1,2)=1.
      A(2,3)=1.
      A(2,4)=1.
      A(3,1)=DEXP(-ALM*B1)
      A(3,2)=DEXP(ALM*B1)
      A(3,5)=-1.
      A(3,6)=-1.
      A(3,7)=-1.
      A(3,8)=0.
      A(4,1)=-A2*DEXP(-ALM*B1)
      A(4,2)=-A2*DEXP(ALM*B1)
      A(4,3)=DEXP(-BTM*B1)
      A(4,4)=DEXP(BTM*B1)
      A(4,5)=QL
      A(4,6)=QL
      A(4,7)=RL
      A(4,8)=0.
      A(5,1)=-DM1*ALM*DEXP(-ALM*B1)
      A(5,2)=DM1*ALM*DEXP(ALM*B1)
      A(5,5)=DF1L*MUL
      A(5,6)=-DF1L*MUL
      A(5,7)=0.
      A(5,8)=-DF1L*NUL
      A(6,1)=DM2*A2*ALM*DEXP(-ALM*B1)
```

```
121.            A(6,2)=-DM2*A2*ALM*DEXP(ALM*B1)
122.            A(6,3)=-DM2*BTM*DEXP(-BTM*B1)
123.            A(6,4)=DM2*BTM*DEXP(BTM*B1)
124.            A(6,5)=-DF2L*QL*MUL
125.            A(6,6)=DF2L*QL*MUL
126.            A(6,7)=0.
127.            A(6,8)=DF2L*RL*NUL
128.            A(7,5)=DEXP(-MUL*B2)
129.            A(7,6)=DEXP(MUL*B2)
130.            A(7,7)=DCOS(NUL*B2)
131.            A(7,8)=DSIN(NUL*B2)
132.            A(7,9)=-1.
133.            A(7,10)=-1.
134.            A(8,5)=-QL*DEXP(-MUL*B2)
135.            A(8,6)=-QL*DEXP(MUL*B2)
136.            A(8,7)=-RL*DCOS(NUL*B2)
137.            A(8,8)=-RL*DSIN(NUL*B2)
138.            A(8,9)=A2
139.            A(8,10)=A2
140.            A(8,11)=-1.
141.            A(8,12)=-1.
142.            A(9,5)=-DF1L*MUL*DEXP(-MUL*B2)
143.            A(9,6)=DF1L*MUL*DEXP(MUL*B2)
144.            A(9,7)=-DF1L*NUL*DSIN(NUL*B2)
145.            A(9,8)=DF1L*NUL*DCOS(NUL*B2)
146.            A(9,9)=DM1*ALM
147.            A(9,10)=-DM1*ALM
148.            A(10,5)=DF2L*QL*MUL*DEXP(-MUL*B2)
149.            A(10,6)=-DF2L*QL*MUL*DEXP(MUL*B2)
150.            A(10,7)=DF2L*RL*NUL*DSIN(NUL*B2)
151.            A(10,8)=-DF2L*RL*NUL*DCOS(NUL*B2)
152.            A(10,9)=-DM2*A2*ALM
153.            A(10,10)=DM2*A2*ALM
154.            A(10,11)=DM2*BTM
155.            A(10,12)=-DM2*BTM
156.            A(11,9)=DEXP(-ALM*B3)
157.            A(11,10)=DEXP(ALM*B3)
158.            A(11,13)=-1.
159.            A(11,14)=-1.
160.            A(11,15)=-1.
161.            A(11,16)=0.
162.            A(12,9)=-A2*DEXP(-ALM*B3)
163.            A(12,10)=-A2*DEXP(ALM*B3)
164.            A(12,11)=DEXP(-BTM*B3)
165.            A(12,12)=DEXP(BTM*B3)
166.            A(12,13)=QR
167.            A(12,14)=QR
168.            A(12,15)=RR
169.            A(12,16)=0.
170.            A(13,9)=-DM1*ALM*DEXP(-ALM*B3)
171.            A(13,10)=DM1*ALM*DEXP(ALM*B3)
172.            A(13,13)=DF1R*MUR
173.            A(13,14)=-DF1R*MUR
174.            A(13,15)=0.
175.            A(13,16)=-DF1R*NUR
176.            A(14,9)=DM2*A2*ALM*DEXP(-ALM*B3)
177.            A(14,10)=-DM2*A2*ALM*DEXP(ALM*B3)
178.            A(14,11)=-DM2*BTM*DEXP(-BTM*B3)
179.            A(14,12)=DM2*BTM*DEXP(BTM*B3)
180.            A(14,13)=-DF2R*QR*MUR
```

```
181.            A(14,14)=DF2R*GR*MUR
182.            A(14,15)=0.
183.            A(14,16)=DF2R*RR*NUR
184.            A(15,13)=DEXP(-MUR*B4)
185.            A(15,14)=DEXP(MUR*B4)
186.            A(15,15)=DCOS(NUR*B4)
187.            A(15,16)=DSIN(NUR*B4)
188.            A(15,17)=-1.
189.            A(15,18)=-1.
190.            A(16,13)=-QR*DEXP(-MUR*B4)
191.            A(16,14)=-QR*DEXP(MUR*B4)
192.            A(16,15)=-RR*DCOS(NUR*B4)
193.            A(16,16)=-RR*DSIN(NUR*B4)
194.            A(16,17)=A2
195.            A(16,18)=A2
196.            A(16,19)=-1.
197.            A(16,20)=-1.
198.            A(17,13)=-DF1R*MUR*DEXP(-MUR*B4)
199.            A(17,14)=DF1R*MUR*DEXP(MUR*B4)
200.            A(17,15)=-DF1R*NUR*DSIN(NUR*B4)
201.            A(17,16)=DF1R*NUR*DCOS(NUR*B4)
202.            A(17,17)=DM1*ALM
203.            A(17,18)=-DM1*ALM
204.            A(18,13)=DF2R*QR*MUR*DEXP(-MUR*B4)
205.            A(18,14)=-DF2R*QR*MUR*DEXP(MUR*B4)
206.            A(18,15)=DF2R*RR*NUR*DSIN(NUR*B4)
207.            A(18,16)=-DF2R*RR*NUR*DCOS(NUR*B4)
208.            A(18,17)=-DM2*A2*ALM
209.            A(18,18)=DM2*A2*ALM
210.            A(18,19)=DM2*BTM
211.            A(18,20)=-DM2*BTM
212.            A(19,17)=DEXP(-ALM*B5)
213.            A(19,18)=DEXP(ALM*B5)
214.            A(20,17)=-A2*DEXP(-ALM*B5)
215.            A(20,18)=-A2*DEXP(ALM*B5)
216.            A(20,19)=DEXP(-BTM*B5)
217.            A(20,20)=DEXP(BTM*B5)
218.      C     THE IDENTITY MATRIX IS ADDED TO A HERE
219.            DO 40 I=1,20
220.            A(I,I)=A(I,I)+1.
221.      40    CONTINUE
222.      C     THE LIBRARY SUBROUTINE EIGRF IS USED TO CALCULATE THE
223.      C         EIGENVALUES AND ASSOCIATED EIGENVECTORS OF MATRIX A
224.            CALL EIGRF (A,N,IA,IJOB,W,Z,IZ,WK,IER)
225.      C     THE FUNDAMENTAL EIGENVECTOR IS LOCATED IN Z(I,20)
226.            DO 42 I=1,20
227.            B(I)=REAL(Z(I,20))
228.      42    CONTINUE
229.            IF (IER.EQ.130) GO TO 25
230.      C     THESE STEPS DETERMINE WHICH SOLUTION EQUATION IS USED FOR THE
231.      C         IS USED FOR THE VALUE OF Y- IN THIS CASE ONLY THE CENTRAL
232.      C         EQUATIONS, Y2K3 AND Y2K4, ARE USED.
233.            BB=0.
234.            IF (Y.GT.B1) GO TO 60
235.            Y2K1=B(3)*DEXP(-BTM*Y)+B(4)*DEXP(BTM*Y)-A2*(B(1)*DEXP(-ALM*Y)
236.           &+B(2)*DEXP(ALM*Y))
237.            YB=Y2K1
238.            GO TO 69
239.      60    CONTINUE
240.            BB=B1+B2
```

```
241.            IF (Y.GT.BB) GO TO 61
242.            Y3=Y-(BB-B2)
243.            Y2K2=-QL*(B(5)*DEXP(-MUL*Y3)+B(6)*DEXP(MUL*Y3))-RL*(B(7)*DCOS
244.           &(NUL*Y3)+B(8)*DSIN(NUL*Y3))
245.            YB=Y2K2
246.            GO TO 69
247.      61    CONTINUE
248.            BB=BB+B3
249.            IF (Y.GT.BB) GO TO 63
250.            Y3=Y-(BB-B3)
251.            Y2K4=B(11)*DEXP(-BTM*Y3)+B(12)*DEXP(BTM*Y3)-A2*(B(9)*DEXP
252.           &(-ALM*Y3)+B(10)*DEXP(ALM*Y3))
253.            YB=Y2K4
254.            GO TO 69
255.      63    CONTINUE
256.            BB=BB+B4
257.            IF (Y.GT.BB) GO TO 64
258.            Y3=Y-(BB-B4)
259.            Y2K5=-QR*(B(13)*DEXP(-MUR*Y3)+B(14)*DEXP(MUR*Y3))-RR*(B(15)
260.           &*DCOS(NUR*Y3)+B(16)*DSIN(NUR*Y3))
261.            YB=Y2K5
262.            GO TO 69
263.      64    CONTINUE
264.            Y3=Y-BB
265.            Y2K6=B(19)*DEXP(-BTM*Y3)+B(20)*DEXP(BTM*Y3)-A2*(B(17)*DEXP(-ALM
266.           &*Y3)+B(18)*DEXP(ALM*Y3))
267.            YB=Y2K6
268.      69    CONTINUE
269.      C     THESE STEPS CALCULATE DEL PHI/DEL Y
270.            IF (K.EQ.1) GO TO 70
271.            L=K-1
272.            G2=G(L)
273.            GO TO 71
274.      70    G2=G(K)
275.      71    G(K)=DSIN(X0*PI/A1)*YB
276.            G1(K)=(G(K)-G2)/STEP
277.            WRITE (6,98) K,G(K),G2,G1(K)
278.      98    FORMAT (' K=',I2,'G(K)=',D12.5,'G2=',D12.5,'G1(K)=',D12.5)
279.            Y=Y+STEP
280.      20    CONTINUE
281.            Y=B1+B2+Y0-STEP/2.
282.      C     THESE STEPS PRINT AND PUNCH THE RESULTS
283.            DO 30 K=2,3
284.            WRITE (6,32) Y,G1(K)
285.      32    FORMAT (' AT Y= ',F8.3,' D PHI/D X = ',D12.5)
286.            Y=Y+STEP
287.      30    CONTINUE
288.            WRITE (7,45) G1(3)
289.      45    FORMAT (E12.5)
290.      25    STOP
291.            END
292.      //GO.SYSIN  DD  *
```

```
1.      //C300  JOB  U3780,WJH
2.      //STEP1  EXEC  FORTGCG,REGION=192K
3.      //FORT.SYSIN  DD  *
4.      C      THIS PROGRAM IS PLOT- IT PLOTS THE DETECTOR RESPONSE
5.      C      THE VALUES OF ALL INPUT ARE ALSO PRINTED
6.      C      THE INPUT COMES FROM GFP24, GFP25, GFP27, AND GFP28
7.             REAL PHI(100),G1(100),G2(100),G3(100),G4,X(100)
8.             INTEGER I
9.             READ (5,10) G4
10.     10     FORMAT (E12.5)
11.            WRITE (6,20) G4
12.     20     FORMAT (' G4= ',E12.5)
13.            DO 11 I=1,61
14.            READ (5,12) X(I),G3(I)
15.     12     FORMAT (F6.2,E12.5)
16.            WRITE (6,22) X(I),G3(I)
17.     22     FORMAT (' Y= ',F6.2,' G3= ',E12.5)
18.     11     CONTINUE
19.            DO 13 I=1,61
20.            READ (5,14) G2(I)
21.     14     FORMAT (E12.5)
22.     13     CONTINUE
23.            DO 15 I=1,61
24.            READ (5,16) G1(I)
25.     16     FORMAT (E12.5)
26.            PHI(I)=G4*G3(I)+G2(I)*G1(I)
27.            WRITE (6,17) X(I),PHI(I)
28.     17     FORMAT (' Y= ',F6.2,' DEL PHI= ',E12.5)
29.            WRITE (6,27) G2(I),G1(I)
30.     27     FORMAT (' G2= ',E12.5,' G1= ',E12.5)
31.     15     CONTINUE
32.            CALL GRAPH (61,X,PHI,11,1,10.0,8.0,15.0,0.0,0.0,0.05,0.0
33.           &,'Y, CM.;','DETECTOR RESPONSE;','PLOT;','X=55.88;')
34.            STOP
35.            END
36.     //GO.SYSIN  DD  *
37.     //GO.FT14F001  DD  DSNAME=&SM,UNIT=SCRTCH,DISP=(NEW,PASS),
38.     //  SPACE=(800,(120,15)),DCB=(RECFM=VBS,LRECL=796,BLKSIZE=800)
39.     //SMPLTTR  EXEC  PLOT,PLOTTER=PRINTER
```

XI. APPENDIX B: CONSTANTS USED IN THE COMPUTER PROGRAMS

This appendix contains a list of variable names used in the computer programs and the variable's common names. The letters R and L after some of the variable names found in the program refer to the right (south) and left (north) cores, respectively.

Variable Name	Common Name, Description
PI	π
SIGAOM	Σ_{a20} (graphite)
SIGAF	Σ_{a20} (fuel)
DF1	D (fuel, group 1)
DF2	D (fuel, group 2)
A1	Total x dimension
B1	0-B1 dimension
B2	B1-B2 dimension
B3	B2-B3 or Yϕ-B3 dimension
B4	B3-B4 dimension
B5	B4-B5 dimension
Yϕ	B2-Yϕ dimension
SRM	Σ_{R1} (graphite)
SRF	Σ_{R1} (fuel)
SF	Σ_{f} (group 1)
SAM	Σ_{a1} (graphite)
SAF	Σ_{a1} (fuel)
DM1	D (graphite, group 1)
DM2	D (graphite, group 2)
Beta	β
Z	Z dimension
XO	X position of perturbation
Y	Y position of detector
X1	X position of detector

The values used for the reactor cross section data given in the programs of Appendix A are data used for program testing. The values used in the final calculations are listed in Appendix C.

XII. APPENDIX C: REACTOR DATA

This appendix lists the reactor data used for the theoretical model. The computer program LEOPARD [8] was used to generate the two-group cross sections for the calculations. Input data for the LEOPARD code is also included.

The input data required for LEOPARD are volume fractions of aluminum and water and the atom densities of U-235 and U-238. If desired, a nonlattice fraction can be included to account for the portion of the core that is not part of the repeating unit cell. The procedure used for preparing the input for LEOPARD basically followed the procedures described by Al-Ammar [5] and Salih [10].

A nonlattice fraction was calculated using the aluminum core tank, aluminum dividers, nonfuel bearing aluminum in the edges of the fuel plates, and water between these edges. The height of the material was taken as 23 inches (58.4 cm), the length of the fuel bearing portion of the fuel plates. The following volumes were used:

Aluminum in core tank	302 in^3 (4.95×10^3 cm^3)
Aluminum in dividers	115 in^3 (1.89×10^3 cm^3)
Aluminum in edges of fuel plates	33 in^3 (541 cm^3)
Edge water	152 in^3 (2.49×10^3 cm^3)

Based on a total core tank volume of 2.98×10^3 in^3 (4.89×10^4 cm^3), the nonlattice fraction was calculated as

$$\frac{4.95 \times 10^3 + 1.89 \times 10^3 + 541 + 2.49 \times 10^3}{4.89 \times 10^4} = 0.202.$$

The fraction that is aluminum is 0.748 and the fraction that is water is 0.252. The U-235 and U-238 atom densities were based on 1483 gm for the north core and 1502 gm for the south core (loading pattern B). Using the relationship

$$\text{atoms/cm}^3 = \frac{(\text{gm of fuel})(6.02 \times 10^{23})}{(235)(\text{volume of fuel plates})}$$

the following atom densities were calculated.

North core

U-235 - 1.27×10^{21} atoms/cm^3

U-238 - 8.30×10^{19} atoms/cm^3

South core

U-235 - 1.29×10^{21} atoms/cm^3

U-238 - 8.51×10^{19} atoms/cm^3

The LEOPARD input data follows:

SHEET A COLUMN

TITLE

a.	1	3
b.	0	6
c.	1	9
d.	2	12
e.	1	15
f.	1	18
g.	1	21
h.	NE	
i.	NE	
j.	NE	
k.	NE	

(Sheet A continued)

l.	NE	
m.	NE	
n.	0	42
o.	NE	
p.	NE	
q.	-2	51
r.	0	54

SHEET B North Core

Volume Fractions:

Index	Pellet	Clad	Moderator	Extra
9	1.0	1.0	0.0	0.748
18	0.00127	0.0	0.0	0.0
20	0.0000830	0.0	0.0	0.0
100	0.0	0.0	1.0	0.252
777	0.0	0.0	0.0	0.0
777	0.0	0.0	0.0	0.0

Temperatures, buckling, and peaking factor:[1]

80.	80.	80.	80.	0.002904	1.0

Radii and nonlattice factor:[1]

0.02	0.04	0.48	--	--	0.2019

Pressure:[1]

14.7

---

[1] Applies to both cores

SHEET B South Core

Volume Fractions:

Index	Pellet	Clad	Moderator	Extra
9	1.0	1.0	0.0	0.748
18	0.00129	0.0	0.0	0.0
20	0.0000851	0.0	0.0	0.0
100	0.0	0.0	1.0	0.252
777	0.0	0.0	0.0	0.0
777	0.0	0.0	0.0	0.0

SHEET B Graphite

Volume Fractions:

Index	Pellet	Clad	Moderator	Extra
4	1.0	1.0	1.0	0.0
777	0.0	0.0	0.0	0.0
777	0.0	0.0	0.0	0.0

Temperatures, buckling, and peaking factor:

Same as cores

Radii and nonlattice factor:

0.02 0.04 0.48 -- -- --

Pressure:

Same as cores

The two group output data are presented in the following tables for loading pattern B.

North Core LEOPARD Output

D_1	1.4064
D_2	0.22302
Σ_{a1}	0.19756×10^{-2}
Σ_{r1}	0.34250×10^{-1}
Σ_{a2}	0.53385×10^{-1}
$\nu\Sigma_f$	0.78021×10^{-1}

South Core LEOPARD Output

D_1	1.4064
D_2	0.22313
Σ_{a1}	0.19912×10^{-2}
Σ_{r1}	0.34238×10^{-1}
Σ_{a2}	0.53788×10^{-1}
$\nu\Sigma_f$	0.78879×10^{-1}

Graphite

D_1	1.16541
D_2	0.99152
Σ_{a1}	0.0
Σ_{r1}	0.25256×10^{-2}
Σ_{a2}	0.20127×10^{-3}

The core dimensions used were:

Core length (graphite plus fuel) - 142.24 cm
Core width - 111.76 cm
Width of core tanks - 16.11 cm
Width of internal reflector - 45.30 cm
Width of external reflectors - 32.36 cm